

Supporting Information

Croconamides: A new dual hydrogen bond donating motif for anion recognition and organocatalysis

Anne Jeppesen, Bjarne E. Nielsen, Dennis Larsen, Olivia M. Akselsen, Theis I. Sølling, Theis Brock-Nannestad and Michael Pittelkow*

Department of Chemistry, University of Copenhagen, Universitetsparken 5, DK-2100 Copenhagen, Denmark.

Table of contents

1. General	2
2. Kinetics studies.....	5
Procedure for Catalysed Tetrahydropyranylation.....	5
Screening of catalysts.....	5
Equation for Non-Linear Regression to Obtain Second-Order Rate Constants	8
3. Hammett analysis	9
4. Study of catalysis conditions.....	12
5. Binding studies	15
General.....	15
¹ H-NMR titration experiments	15
UV/Vis titration experiments	25
Study of binding stoichiometry.....	31
6. Study of hydrates of croconamides.....	32
7. Determination of p <i>K</i> _a	38
Equation for Non-Linear Regression to Obtain <i>K</i> _{eq}	41
8. Crystal structure data	43
9. Computational results.....	47
10. Synthetic procedures.....	64

1. General

Chemicals and Instruments

All chemicals were purchased from commercial suppliers and used as received unless otherwise stated. Dimethyl croconate was synthesised according to the procedure by Williams,¹ and barium croconate for this synthesis was synthesised by SunChemicals. For synthesis and kinetic studies HPLC grade solvents were used, for kinetic studies these were dried using molecular sieves (4 Å). For UV/Vis titrations spectroscopic grade solvents were used, and dimethyl sulfoxide was dried by standing over molecular sieves (4 Å) prior to use.

Melting points are uncorrected.

A Bruker Ultrashield Plus 500 spectrometer with a Cryoprobe was used to record NMR spectra of the synthesised compounds. The spectrometer operated at 500 MHz for ¹H and 126 MHz for ¹³C. For ¹⁹F and titrations a Bruker Avance 3 spectrometer with a BBFO probe was used, operating at 470 MHz for ¹⁹F, 500 MHz for ¹H and 126 MHz for ¹³C. The spectrometers operated at 20 °C and all spectra were referenced to the internal solvent residue for ¹H and ¹³C, and to trifluoroacetic acid in a sealed tube for ¹⁹F. The ¹⁹F spectrum for the Schreiner catalyst, however, was recorded on an Oxford NMR 300 spectrometer, operating at 282 MHz.

NMR chemical shifts (δ) are cited in ppm and coupling constants (J) are quoted in Hz. The following abbreviations are used when reporting multiplicities of NMR resonances: s: singlet; d: doublet; t: triplet; q: quartet; m: multiplet. MestReNova version 10.0.2 from MestreLab Research S.L. was used to process the NMR data. Standard 1D and 2D NMR techniques (COSY, ¹³C-APT, HSQC (for ¹H and ¹³C), and HMBC (for ¹H and ¹³C)) was used to assign ¹H and ¹³C resonances.

UV/Vis measurements were performed using a Perkin Elmer UV/Vis spectrometer Lambda 2.

HPLC-UV and LC-MS

HPLC analysis was carried out on a Dionex UltiMate 3000, which was coupled to an UltiMate 3000 diode array UV/Vis detector that measured absorbance of light between 190 – 800 nm.

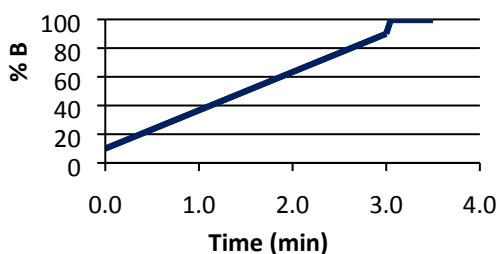
LC-MS analysis were obtained by coupling the above mentioned HPLC apparatus with a Bruker MicroTOF-QII system equipped with an ESI source with nebulizer gas at 1.2 bar, dry gas at 10 L/min, dry temperature was 200 °C, capillary at 4500 V and an endplate offset at -500 V. The ion transfer was performed with funnel 1 and funnel RF's at 200.0 Vpp and hexapole RF at 100.0 Vpp and the quadrupole ion energy was set at 5.0 eV with a low mass cutoff at 100.00 m/z. In the collision cell, collision energy was set at 8.0 eV, collision RF at 100.0 Vpp, and a transfer time of 80.0 μ s and pre-pulse storage of 1.0 μ s were used.

¹ R. F. X. Williams, *Phosphorus, Sulfur Silicon Relat. Elem.*, 1976, **2**, 141-146.

LC-MS grade solvents and additives were purchased from commercial suppliers and used as received. Water was purified on a Millipore Milli-Q Integral 5 system. The mobile phase solutions prepared were: (A) water containing 0.1 % formic acid and (B) acetonitrile containing 0.1 % formic acid. The column was conditioned to the starting eluent with at least five column volumes prior to each injection. For synthesised compounds and catalysis experiments, separations was achieved using a Dionex Acclaim RSLC 120 C18 2.2 μm 120 \AA 2.1 \times 50 mm column at 20 or 40 $^{\circ}\text{C}$. The gradient for synthesised compounds and catalysis experiments, method A, is outlined below. Method B was developed for use in experiments with catalyst **1b**.

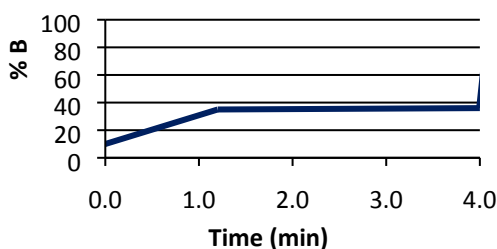
For Hammett analysis, separation was achieved using a Dionex Acclaim RSLC PolarAdvantage II (PA2) C18 2.2 μm 120 \AA 2.1 \times 50 mm column at 40 $^{\circ}\text{C}$.

Method A



Time (min)	% A	% B
0.00	90	10
3.00	10	90
3.05	0	100
3.50	0	100
Flow rate	1.200 ml/min	

Method B



Time (min)	% A	% B
0.00	90	10
1.20	65	35
4.00	64	36
4.10	0	100

4.50	0	100
Flow rate	1.200 ml/min	

2. Kinetics studies

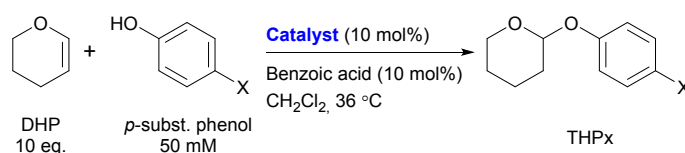
Procedure for Catalysed Tetrahydropyranylation

Freshly prepared stock solutions of the reactants and catalyst(s) were made in dichloromethane. The reactions were started by mixing reactants and catalyst(s) in screw cap glass vials of either 1.5 or 2.0 ml total volume with septa, and the reactions were followed by LC-MS. In order to determine retention times, all starting materials and products were identified by MS.

To ensure stable temperatures throughout the experiments, the samples were placed in appropriately sized holes in a temperature-controlled aluminum block, except when not briefly transferred to a thermostatically controlled auto sampler for measuring. No stirring was applied during the experiment. The time of analysis was calculated down to the minute using the time of injection registered by the apparatus. The screw caps were replaced after every injection to prevent evaporation of solvent.

Screening of catalysts

The reactions were followed by HPLC-UV at 290 nm (Scheme 1), and data were fitted to a second-order reaction model using non-linear regression in order to obtain second-order rate constants (k_2).



Scheme 1 Conditions for catalyst screening.

Under these conditions, it was noted that a significant time lag from preparation of the sample and the start of the reaction, was present. This time period, the induction time, t_i , was taken into account in the second-order function by fitting to $(t - t_i)$ instead of t . Assuming first order dependence on both the alcohol and **DHP**, the concentration of product $[P]_{t_i}$ as a function of $(t - t_i)$ can be expressed by the starting concentrations of the alcohol, $[Alc]_0$, and **DHP**, $[DHP]_0$, and k_2 :

$$[P]_{t_i} = \frac{[Alc]_0 \cdot e^{([Alc]_0 - [DHP]_0)k_2(t - t_i)} - [Alc]_0}{\frac{[Alc]_0}{[DHP]_0} \cdot e^{([Alc]_0 - [DHP]_0)k_2(t - t_i)} - 1}$$

Thus plotting the product concentration as a function of time, $[P]_{t_i}$, allows the use of non-linear regression to determine t_i and k_2 (see next section for a full elucidation of this equation).

The reaction was monitored by HPLC-UV at 290 nm. The response factor was determined to be 1.33, by dividing the area of the starting material and the area of the product, when the concentration for the two was identical.

	Catalyst	<i>p</i> -subst. phenol	$k_2 (\times 10^{-5} \text{ M}^{-1} \text{ S}^{-1})$	$t_i(\text{h})$
1	1a	-OMe	3.74 ± 0.03	1.06 ± 0.09
2	1b	-OMe	1.06 ± 0.04	10.3 ± 1.0
3	Schreiner's Catalyst	-OMe	Could not be determined	Could not be determined

For *Schreiner's* catalyst only minor amounts of product was observed, under these conditions, therefore it was not possible to obtain a value of k_2 .

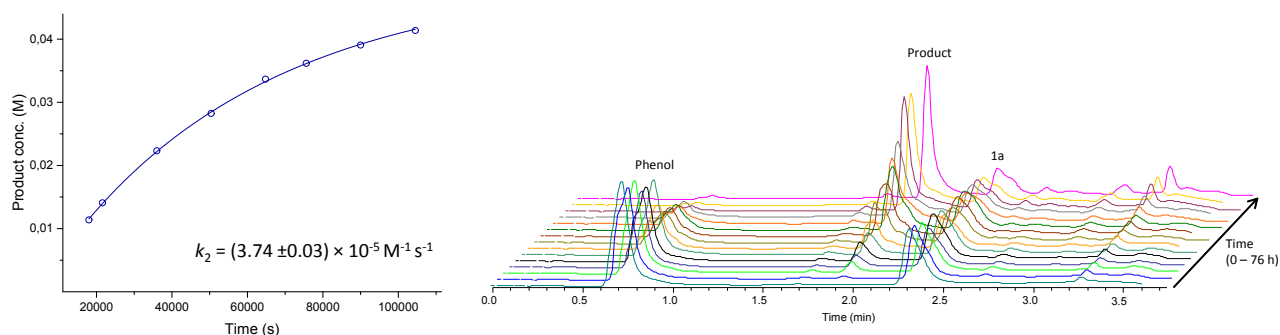


Figure 1 Plot and HPLC chromatograms for catalysis of the tetrahydropyranylation with catalyst **1a**.

For the reaction catalyzed by **1b** it was necessary to change the method as the retention time for the product of the reaction and the catalyst was identical.

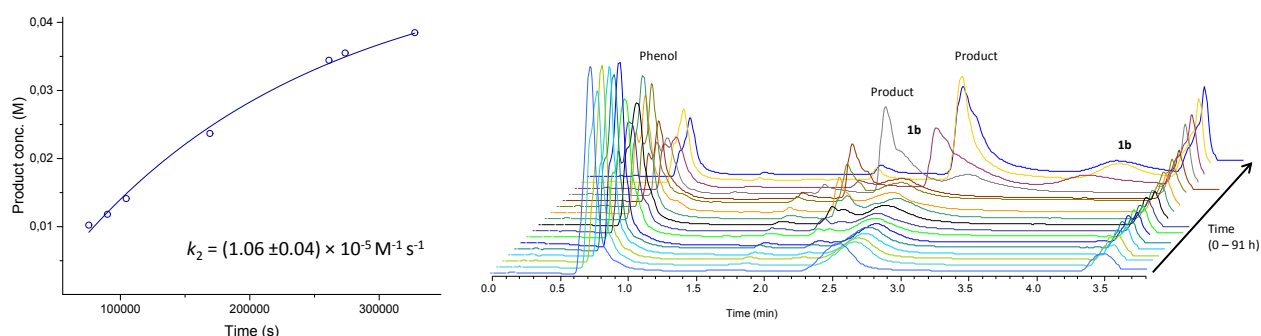


Figure 2 Plot and HPLC chromatograms for catalysis of the tetrahydropyranylation with catalyst **1b**.

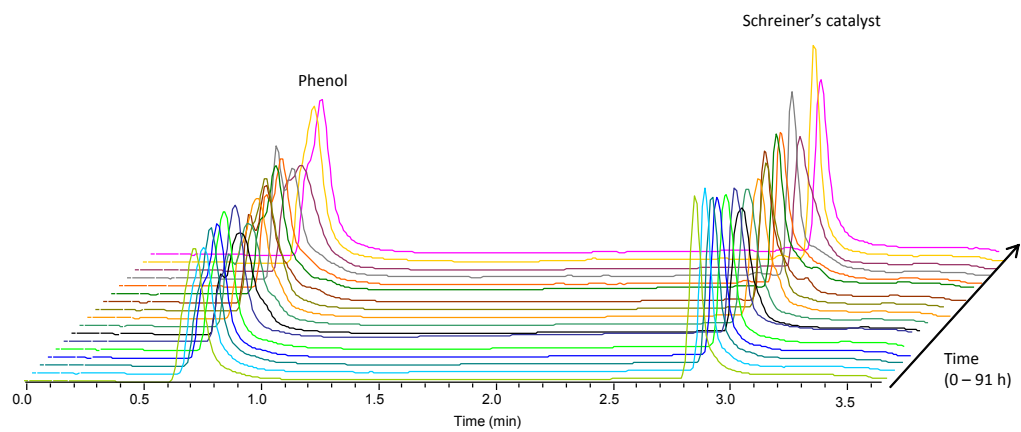


Figure 3 HPLC chromatograms for catalysis of the tetrahydropyranylation with Schreiner's catalyst.

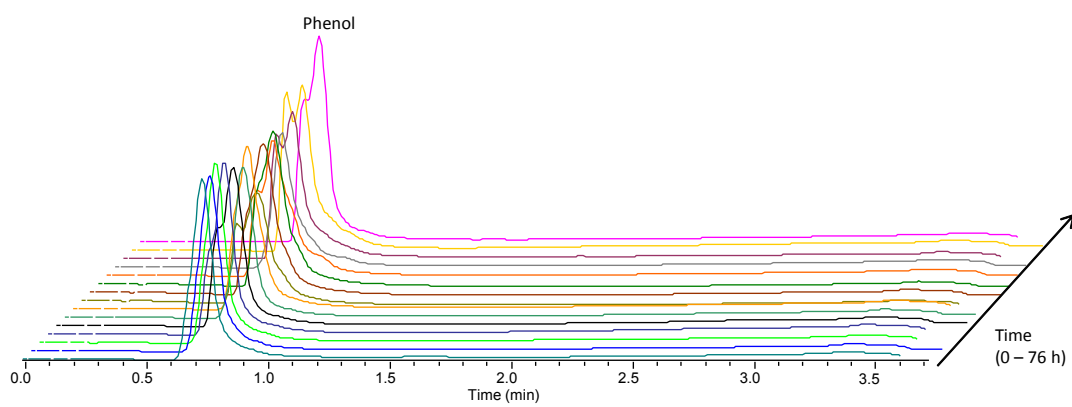
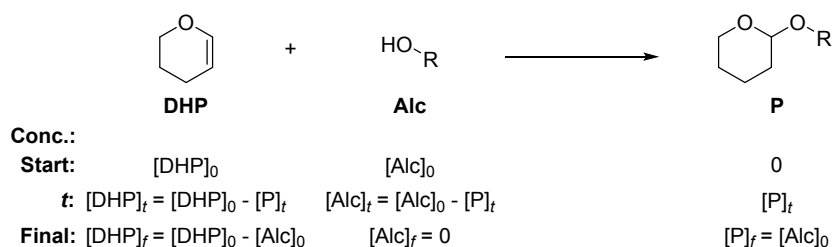


Figure 4 HPLC chromatograms for catalysis of the tetrahydropyranylation without catalyst.

Equation for Non-Linear Regression to Obtain Second-Order Rate Constants

For the reaction between **DHP** and an alcohol, the concentrations of starting materials and product as the reaction starts, during the reaction, and at the end of the reaction is expressed as follows:



The concentrations of alcohol and product is monitored by HPLC-UV, and the concentration of **DHP** can be derived from those values.

For $[Alc]_0 \neq [DHP]_0$, the integrated second order rate law (assuming first order in both $[Alc]$ and $[DHP]$) can be written as:²

$$\frac{[Alc]_t}{[DHP]_t} = \frac{[Alc]_0}{[DHP]_0} \cdot e^{([Alc]_0 - [DHP]_0)k_2 t}$$

where k_2 is the second order rate constant.

Exploiting $[DHP]_t = [DHP]_0 - [P]_t$ and $[Alc]_t = [Alc]_0 - [P]_t$, and then rearranging to isolate $[P]_t$, one arrives at:

$$[P]_t = \frac{[Alc]_0 \cdot e^{([Alc]_0 - [DHP]_0)k_2 t} - [Alc]_0}{\frac{[Alc]_0}{[DHP]_0} \cdot e^{([Alc]_0 - [DHP]_0)k_2 t} - 1}$$

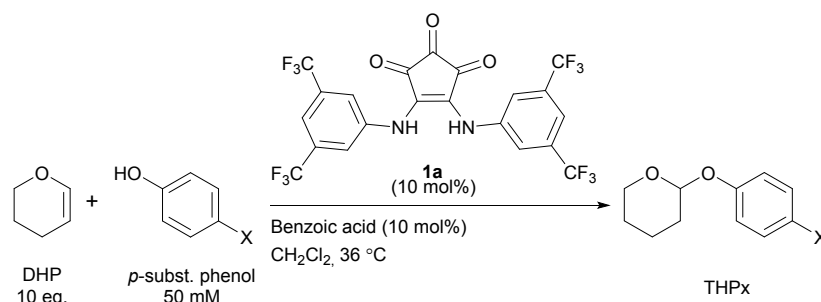
This equation assumes the reaction to start at t_0 , however as this was found not to be the case, this equation fails to give acceptable fits when fitting the observed product concentration versus t . Therefore, the data was fitted as a function of $(t - t_i)$ instead of t :

$$[P]_{t_i} = \frac{[Alc]_0 \cdot e^{([Alc]_0 - [DHP]_0)k_2(t - t_i)} - [Alc]_0}{\frac{[Alc]_0}{[DHP]_0} \cdot e^{([Alc]_0 - [DHP]_0)k_2(t - t_i)} - 1}$$

² Atkins, P. & Paula, J. D. *Atkins' physical chemistry*. 8th edn. (Oxford University Press, 2006).

3. Hammett analysis

A series of *para*-substituted phenols (x in the Scheme below), were investigated for reaction with **DHP** when catalysed by **1a**.



Scheme 2 Conditions for Hammett analysis.

The analysis was performed by preparing a series of solutions as outlined in Scheme 2.

By plotting the total area under the starting material and the product as a function of the conversion percentage, and under the assumption that the phenol is converted fully and exclusively to the desired tetrahydropyranyl ether, the response factor can be derived by reading the values at 0 and 100 % conversion respectively.

The reaction was monitored by HPLC-UV at the wavelength listed below. Product concentrations were calculated using the response factors indicated. The following fitting function described above was employed for obtaining the values of k_2 :

$$[P] = \frac{[Alc]_0 \cdot e^{([Alc]_0 - [DHP]_0)k_2(t)} - [Alc]_0}{\frac{[Alc]_0}{[DHP]_0} \cdot e^{([Alc]_0 - [DHP]_0)k_2(t)} - 1}$$

<i>p</i> -subst. phenol	Monitored at	λ_{\max}		Response factor	k_2 ($10^{-5} \text{ m}^{-1} \text{ s}^{-1}$)
		Starting material	Product		
4 -OMe	290 nm	290 nm	286 nm	1.33	3.44 ± 0.05
5 -Me	290 nm	280 nm	277 nm	4.06	3.15 ± 0.13
6 -H	272 nm	272 nm	270 nm	1.64	2.72 ± 0.06
7 -CN	255 nm	246 nm	244 nm	0.89	1.42 ± 0.02
8 -NO ₂	290 nm	316 nm	307 nm	0.78	1.264 ± 0.019

Plots of the data (blue circles) and the best fit (solid blue line) are shown below :

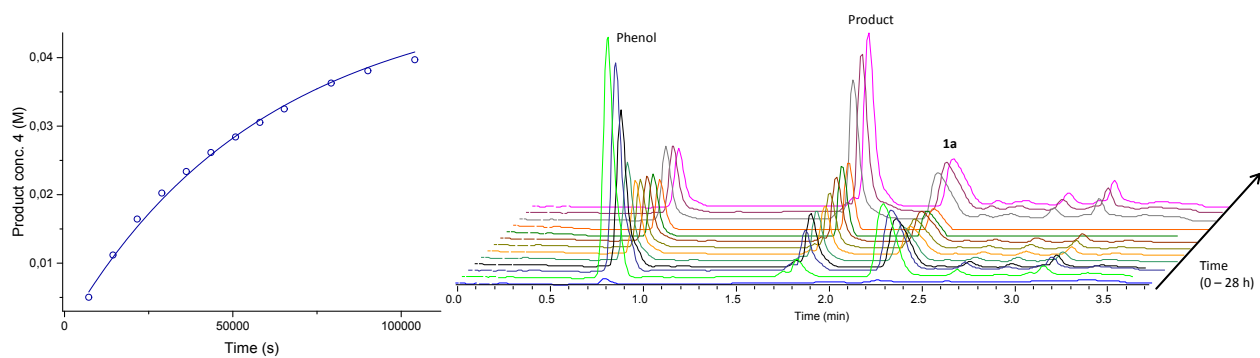


Figure 5 Plot and HPLC chromatograms for Hammett analysis of the tetrahydropyranylation with catalyst 1a and phenol 4.

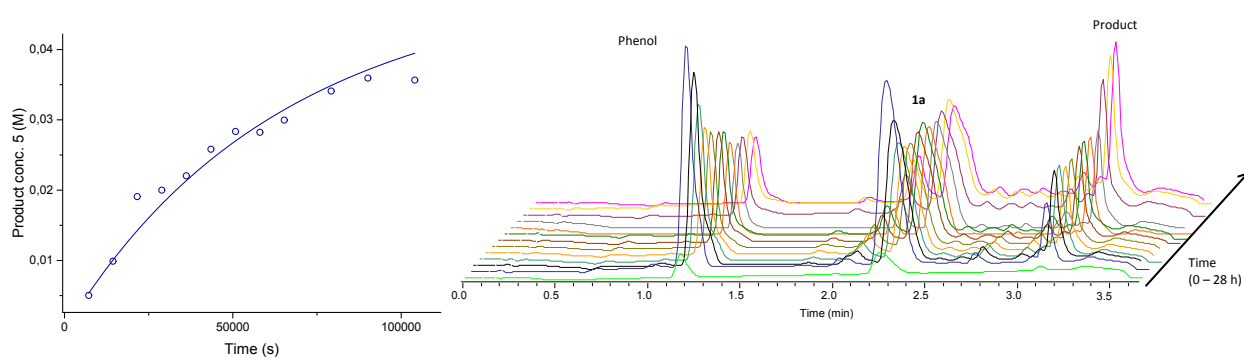


Figure 6 Plot and HPLC chromatograms for Hammett analysis of the tetrahydropyranylation with catalyst 1a and phenol 5.

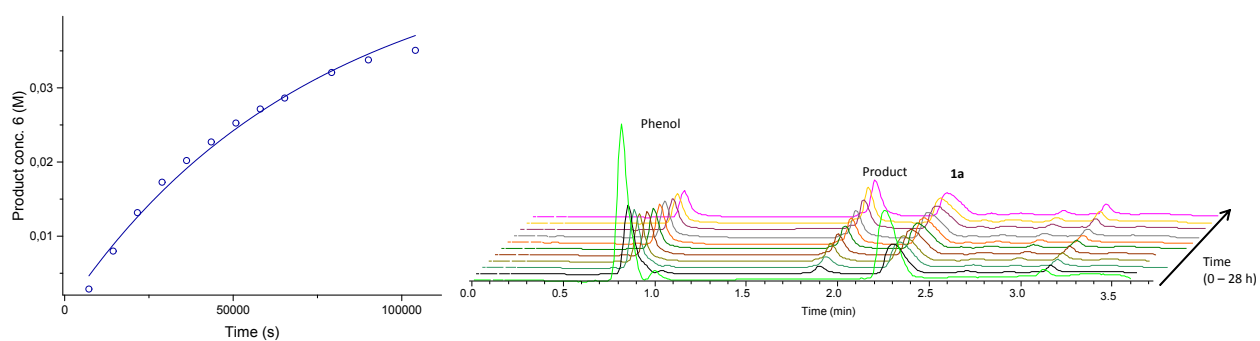


Figure 7 Plot and HPLC chromatograms for Hammett analysis of the tetrahydropyranylation with catalyst 1a and phenol 6.

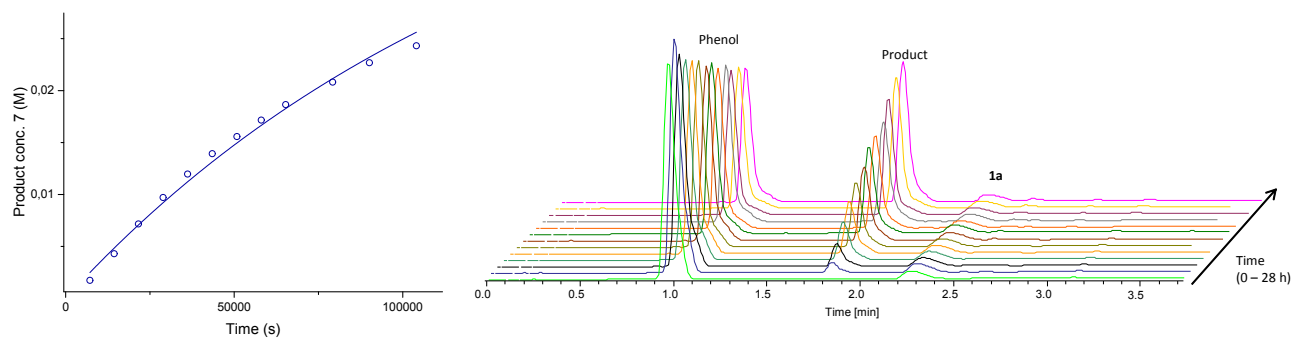


Figure 8 Plot and HPLC chromatograms for Hammett analysis of the tetrahydropyranylation with catalyst 1a and phenol 7.

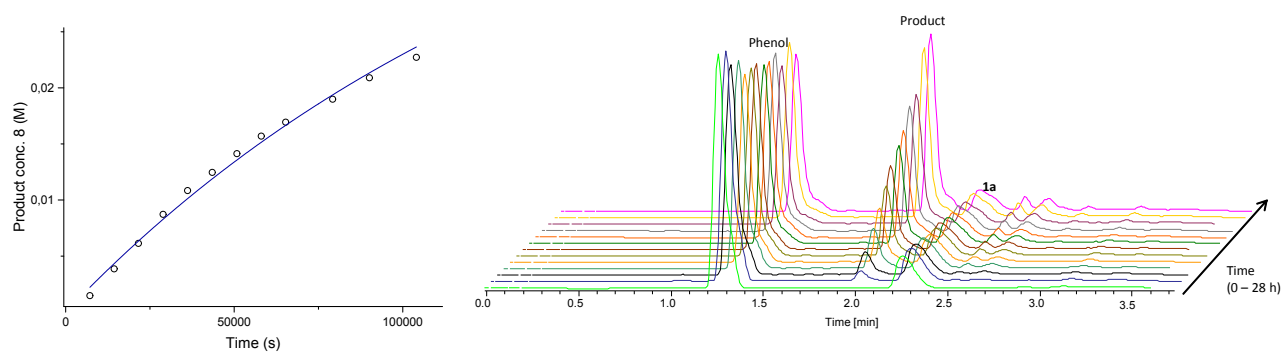


Figure 9 Plot and HPLC chromatograms for Hammett analysis of the tetrahydropyranylation with catalyst 1a and phenol 8.

4. Study of catalysis conditions

To ensure that the conditions applied in the catalysis studies does not affect the catalyst, ^1H -NMR spectra were obtained of catalyst **1a** and benzoic acid, DHP, *para*-methoxy phenol in a 1 to 1 mixture in CD_2Cl_2 . No change in chemical shift values for the catalyst was observed.

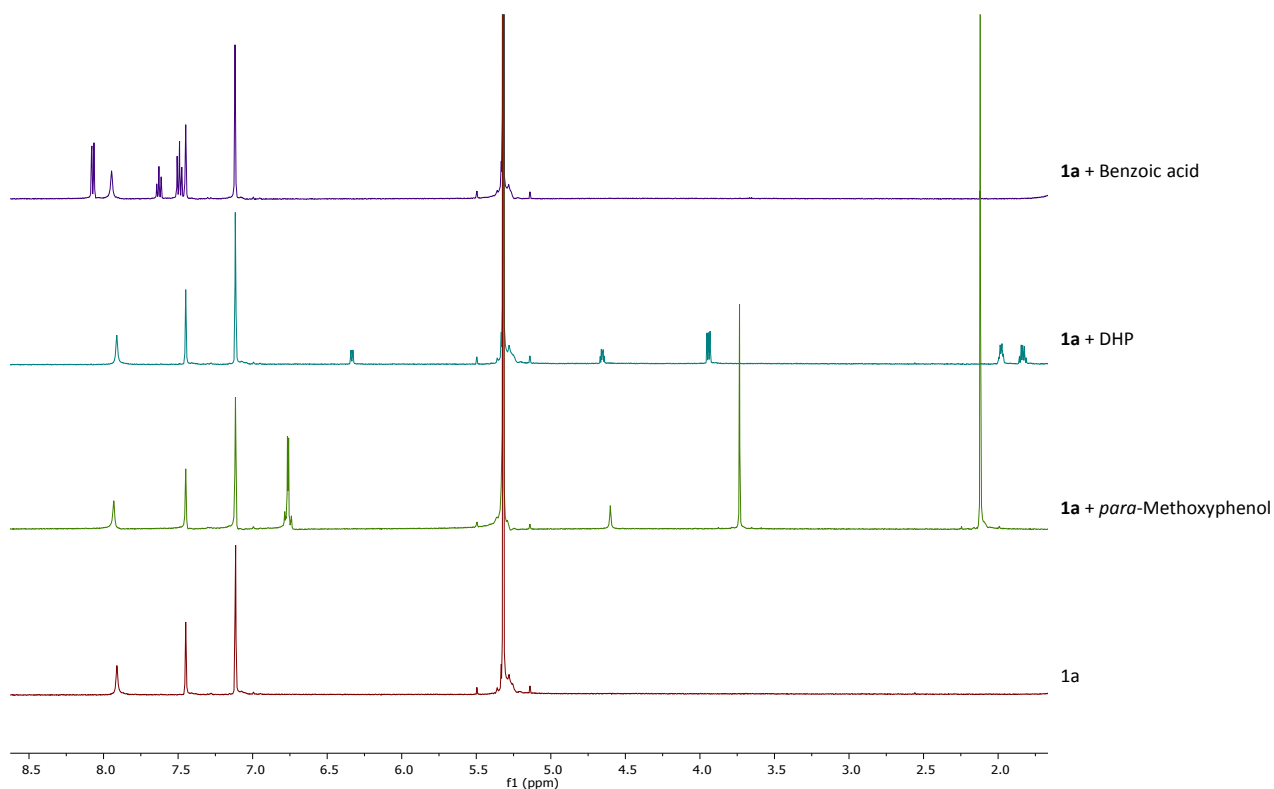


Figure 10 ^1H -NMR (500 MHz, CD_2Cl_2) of **1a** and **1a** added the conditions for the catalysis experiment.

To further elucidate this point, ^1H -NMR spectra of the pure compounds benzoic acid, DHP, *para*-methoxy phenol in CD_2Cl_2 was compared. No change in chemical shift values was observed, indicating no interference between catalyst **1a** and the conditions applied for the catalyst experiments.

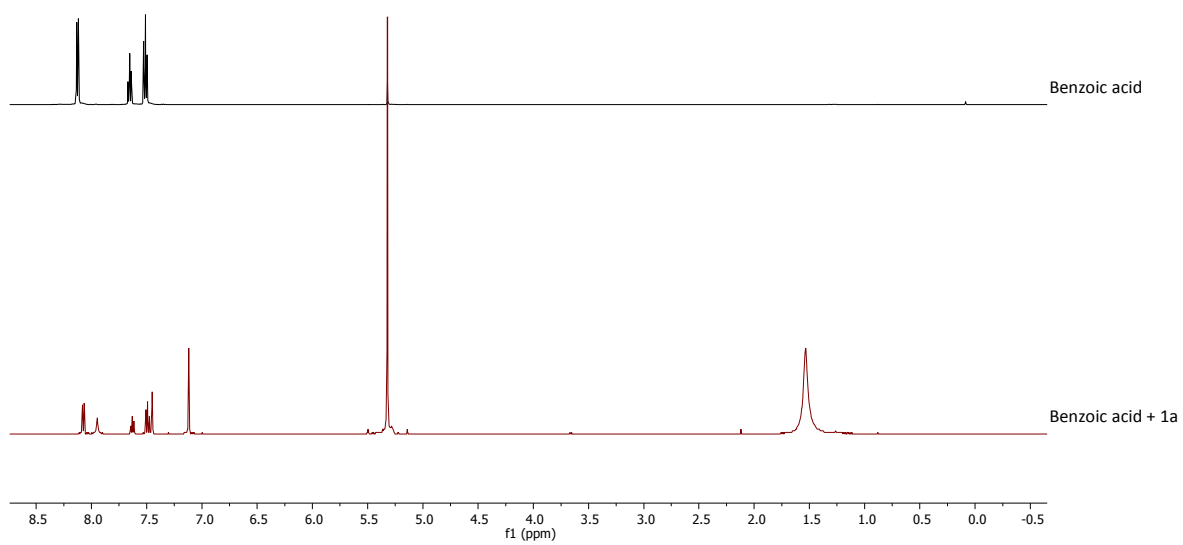


Figure 11 ¹H-NMR (500 MHz, CD₂Cl₂) of Benzoic acid and catalyst 1a.

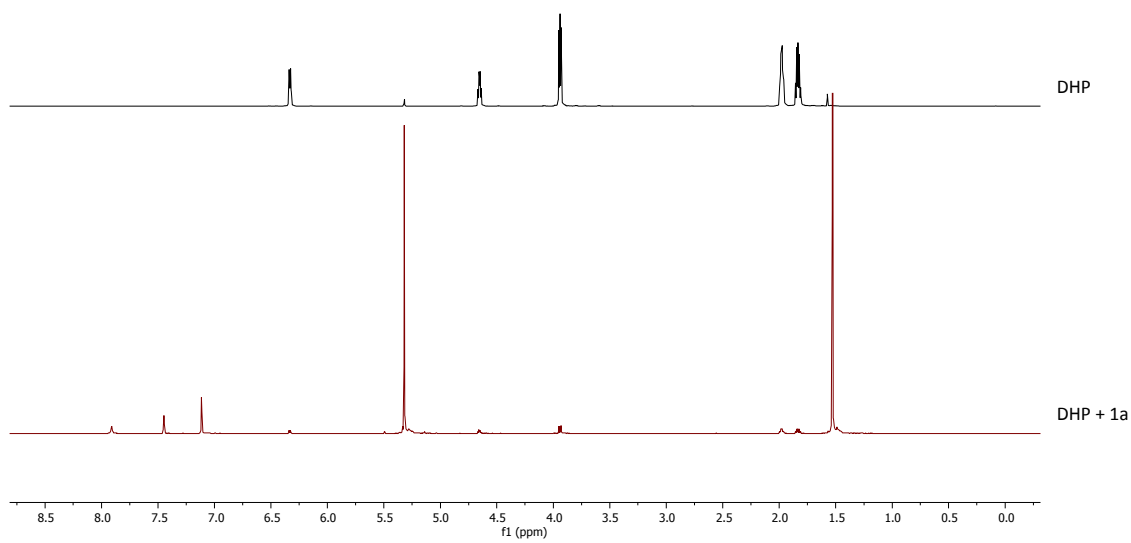


Figure 12 ¹H-NMR (500 MHz, CD₂Cl₂) of DHP and catalyst 1a.

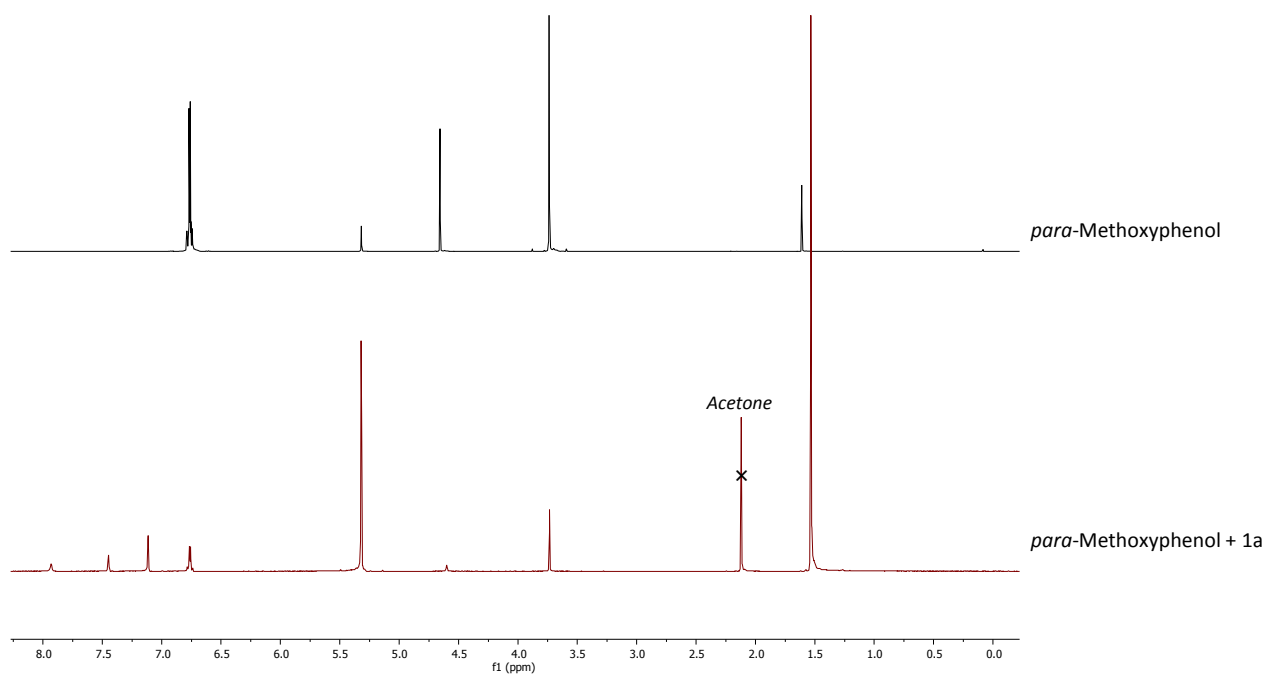


Figure 13 ¹H-NMR (500 MHz, CD₂Cl₂) of *para*-methoxyphenol and catalyst 1a.

5. Binding studies

General

A range of titrations were performed in order to determine the binding stoichiometry and the binding constants for **1a** and **1b** towards a series of tetrabutylammonium salts. Prior to use the tetrabutylammonium salts were dissolved in acetonitrile, and the mixture evaporated *in vacuo* three times or more. The resulting salt was dried overnight under high vacuum and hereafter stored in a dessicator over phosphorus pentoxide to avoid excess water.

¹H-NMR titration experiments

Continuous variation method (Job's) method

To a 1.0 mM solution of host (**1a** or **1b**), a 1.0 mM solution of guest (tetrabutylammonium salts) in CD₂Cl₂ was added in various volumes. Each sample was analysed by ¹H-NMR.

The general method for sample preparation is outlined in Table 1 below.

Table 1 General method for sample preparation.

Sample No.	V(Host) [mL]	V(Guest) [mL]
1	0.45	0.00
2	0.45	0.10
3	0.45	0.25
4	0.45	0.30
5	0.45	0.45
6	0.45	0.65
7	0.45	1.00
8	0.45	1.35
9	0.00	0.50

For the chloride titration with **1a**, the titration data is showed in Table 2.

Table 2 Titration data for chloride with **1a**.

$\chi(\text{Guest})$	$\chi(\text{Host})$	Conc total (Host+Guest)	Host(H_b) (ppm)	$\Delta\delta$ (ppm)	$\chi(\text{Host})\Delta\delta$ (ppm)
0.0000	1.00000	0.00100	7.1152	0.000	0.0000000
0.1818	0.81818	0.00100	7.2362	0.121	0.0990000
0.3571	0.64286	0.00100	7.4795	0.364	0.2341929
0.4000	0.60000	0.00100	7.5514	0.436	0.2617200
0.5000	0.50000	0.00100	7.7257	0.611	0.3052500
0.5909	0.40909	0.00100	7.7737	0.659	0.2693864
0.6897	0.31034	0.00100	7.7776	0.662	0.2055724

0.7500	0.25000	0.00100	7.7794	0.664	0.1660500
1.0000	0.00000	0.00100	0.0000	0.000	0.0000000

The above data results in a plot with maximum at 0.5, which reveals 1:1 binding stoichiometry for **1a** and TBACl (Figure 14).

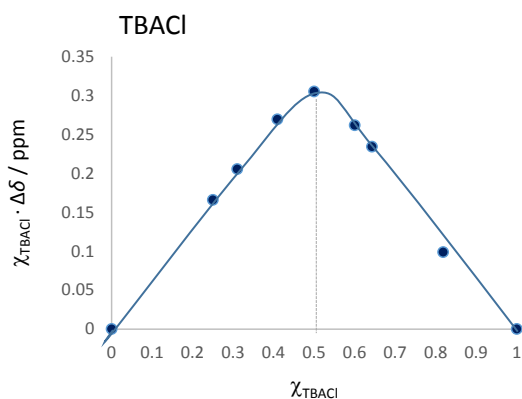


Figure 14 Job plot for chloride.

The Job plots for **1a** with bromide, iodide, hydrogensulphate, or nitrate (Figure 15):

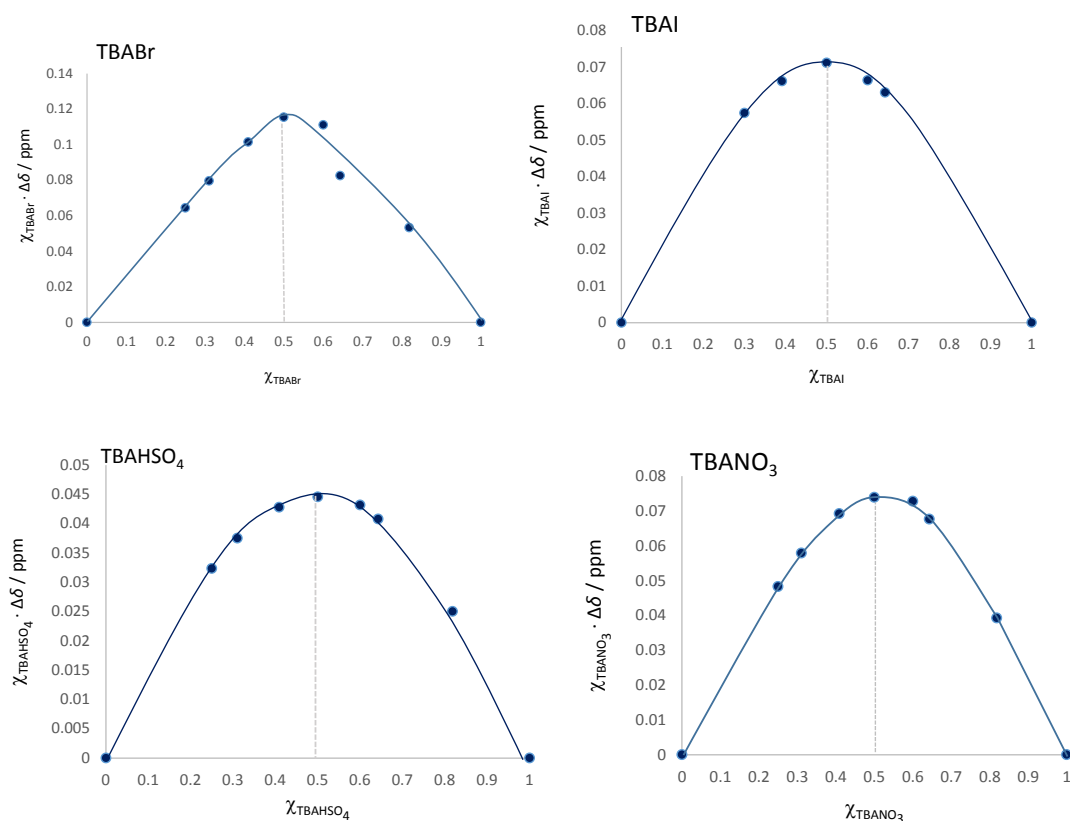


Figure 15 Job plots for binding of bromide, iodide, hydrogensulphate, and nitrate to **1a**.

The Job plot for **1b** with chloride (Figure 16):

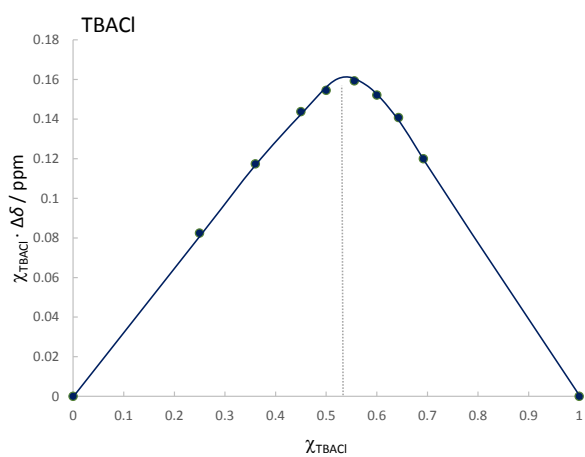


Figure 16 Job plot for binding of chloride to 1b.

¹H-NMR titrations in CD₂Cl₂

The NMR titrations were either carried out in several NMR tubes or in one single tube. For all NMR titrations, the host concentration was kept constant, and the guest added in increasing concentrations.

If several NMR tubes were used, a stock solution of host, **1a**, 1.0 mM, and guest (TBA salt), 10 mM, containing 1 mM host, were made in CD₂Cl₂. The two stock solutions were mixed in various volumes as outlined in Table 3. For the single tube procedure, see Table 4.

Table 3 General method for sample preparation in several NMR tubes.

Sample No.	Guest conc. (mM)	Vol. (μl)	Host Vol.	Guest (μl)
1	0	500		0
2	0.1	495		5
3	0.2	490		10
4	0.3	485		15
5	0.4	480		20
6	0.5	475		25
7	0.6	470		30
8	0.7	465		35
9	0.8	460		40
10	0.9	455		45
11	1.0	450		50
12	1.25	437.5		62.5
13	1.5	425		75
14	2.0	400		100
15	3.0	350		150
16	4.0	300		200
17	5.0	250		250

Table 4 General method for performing ¹H-NMR titrations in a single NMR tube.

Sample No.	V(Host) [mL]	V(Guest) [mL]	V(G) added [mL]	V(total) [mL]	conc (Host) [M]	conc (Guest) [M]
1	0.5	0	0	0.5	1.0000E-03	0.000000E+00
2	0.5	0.00505	0.00505	0.50505	1.0000E-03	9.999010E-05
3	0.5	0.0103	0.00525	0.5103	1.0000E-03	2.018421E-04
4	0.5	0.0158	0.0055	0.5158	1.0000E-03	3.063203E-04
5	0.5	0.0215	0.0057	0.5215	1.0000E-03	4.122723E-04
6	0.5	0.028	0.0065	0.528	1.0000E-03	5.303030E-04
7	0.5	0.034	0.006	0.534	1.0000E-03	6.367041E-04
8	0.5	0.04	0.006	0.54	1.0000E-03	7.407407E-04
9	0.5	0.047	0.007	0.547	1.0000E-03	8.592322E-04

10	0.5	0.054	0.007	0.554	1.0000E-03	9.747292E-04
11	0.5	0.061	0.007	0.561	1.0000E-03	1.087344E-03
12	0.5	0.07	0.009	0.57	1.0000E-03	1.228070E-03
13	0.5	0.078	0.008	0.578	1.0000E-03	1.349481E-03
14	0.5	0.14	0.062	0.64	1.0000E-03	2.187500E-03
15	0.5	0.275	0.135	0.775	1.0000E-03	3.548387E-03
16	0.5	0.79	0.515	1.29	1.0000E-03	6.124031E-03

The position of the chemical shifts of the host was monitored for each $^1\text{H-NMR}$, and the difference in chemical shift was plotted against the guest concentration. OriginPro 2015 was used to handle the equation below³. Using OriginPro to fit to this equation by non-linear regression it allowed for determination of the binding constant K_a (blue solid line in the plots below):

$$\Delta\delta = \frac{\delta_{\Delta HG}}{2H_0} \left(\left(G_0 + H_0 + \frac{1}{K_a} \right) - \sqrt{\left(\left(G_0 + H_0 + \frac{1}{K_a} \right)^2 - 4H_0G_0 \right)} \right)$$

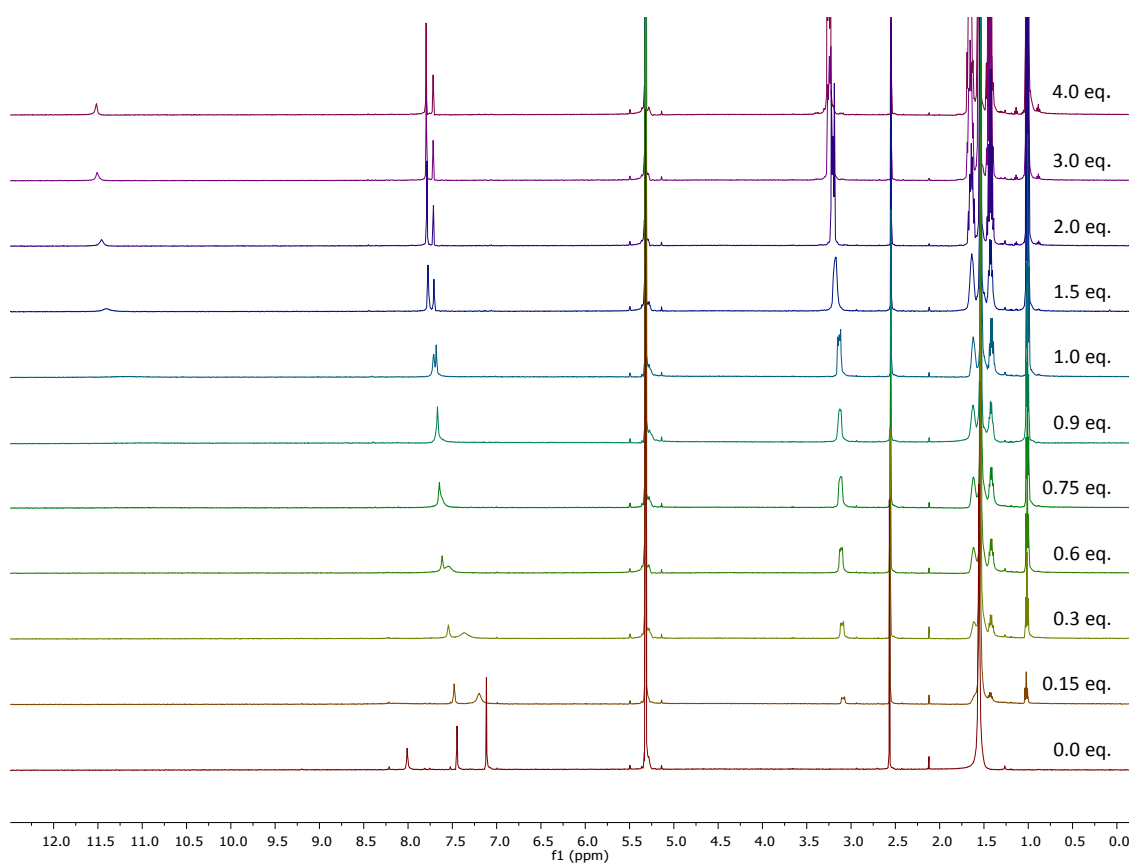


Figure 17 $^1\text{H-NMR}$ (500 MHz, CD_2Cl_2) titration experiments for 1a and TBABr.

³ P. Thordarson, *Chemical Society Reviews*, 2011, **40**, 1305-1323.

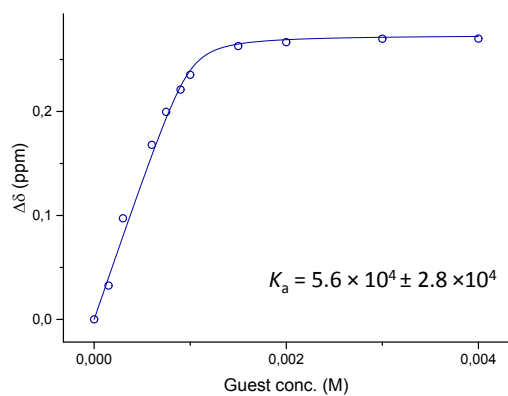


Figure 18 Plot for ^1H -NMR titration of 1a with TBABr following proton H_a with the fitted curve.

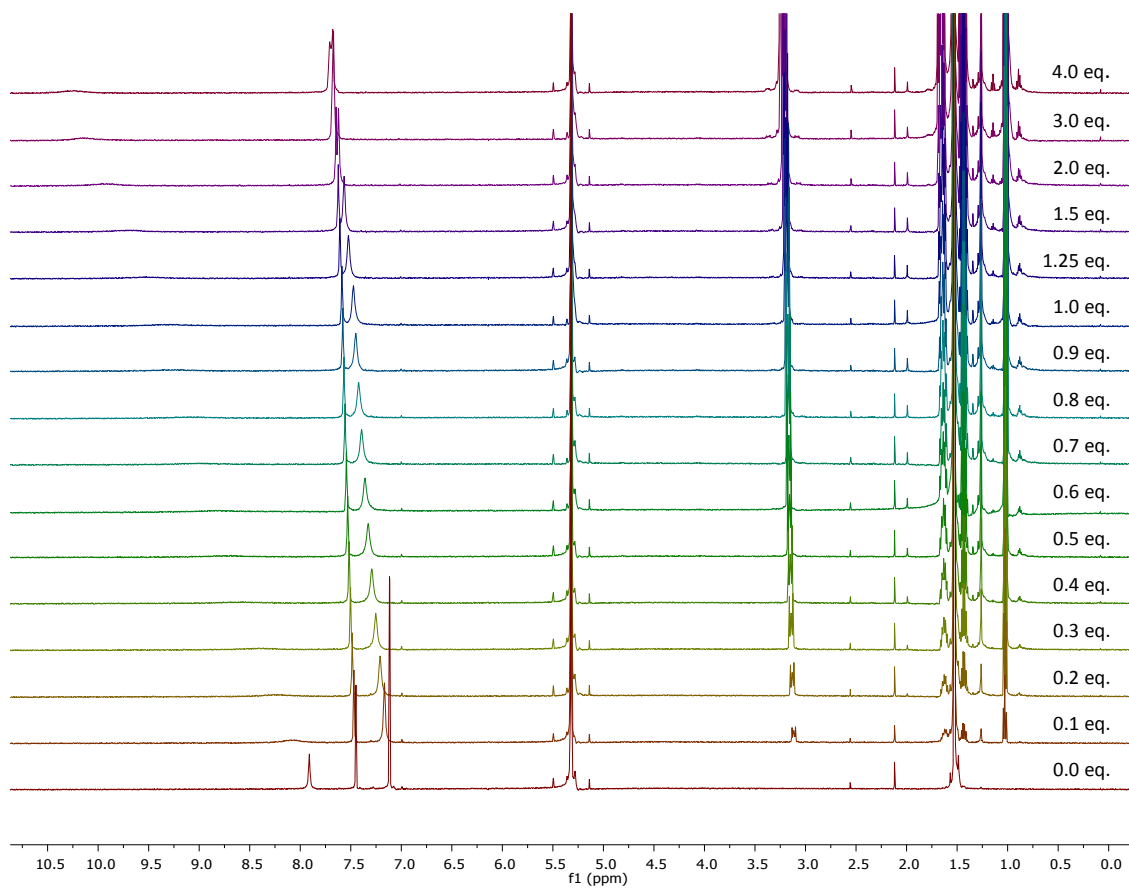


Figure 19 ^1H -NMR (500 MHz, CD_2Cl_2) titration experiments for 1a and TBAl.

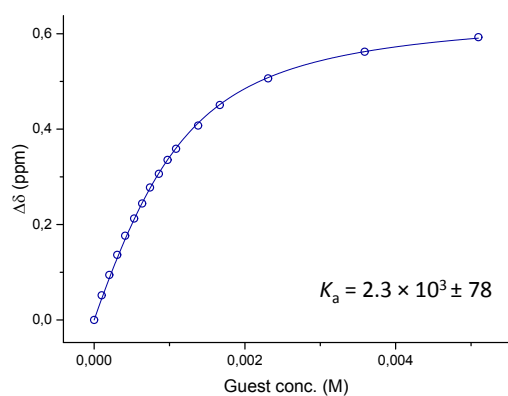


Figure 20 Plot for $^1\text{H-NMR}$ titration of 1a with TBAI following proton H_b with the fitted curve.

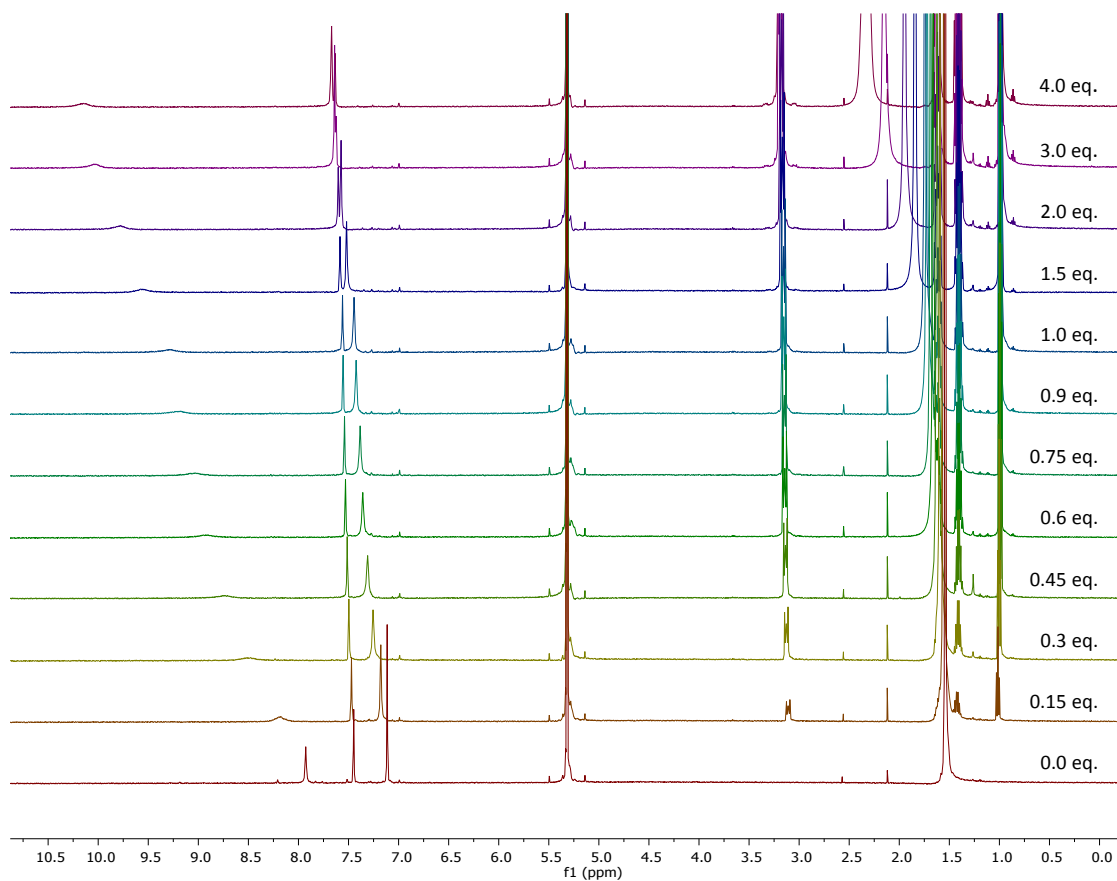


Figure 21 $^1\text{H-NMR}$ (500 MHz, CD_2Cl_2) titration experiments for 1a and TBAHSO₄.

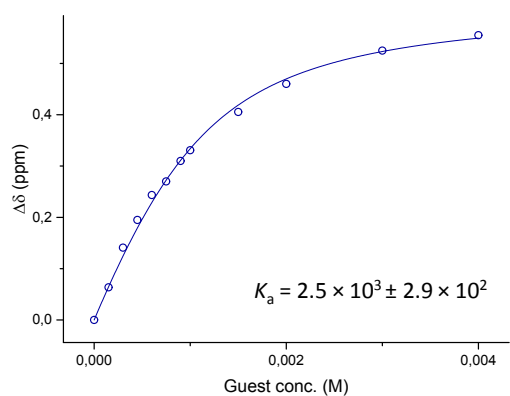


Figure 22 Plot for $^1\text{H-NMR}$ titration of 1a with TBAHSO_4 following proton H_b with the fitted curve.

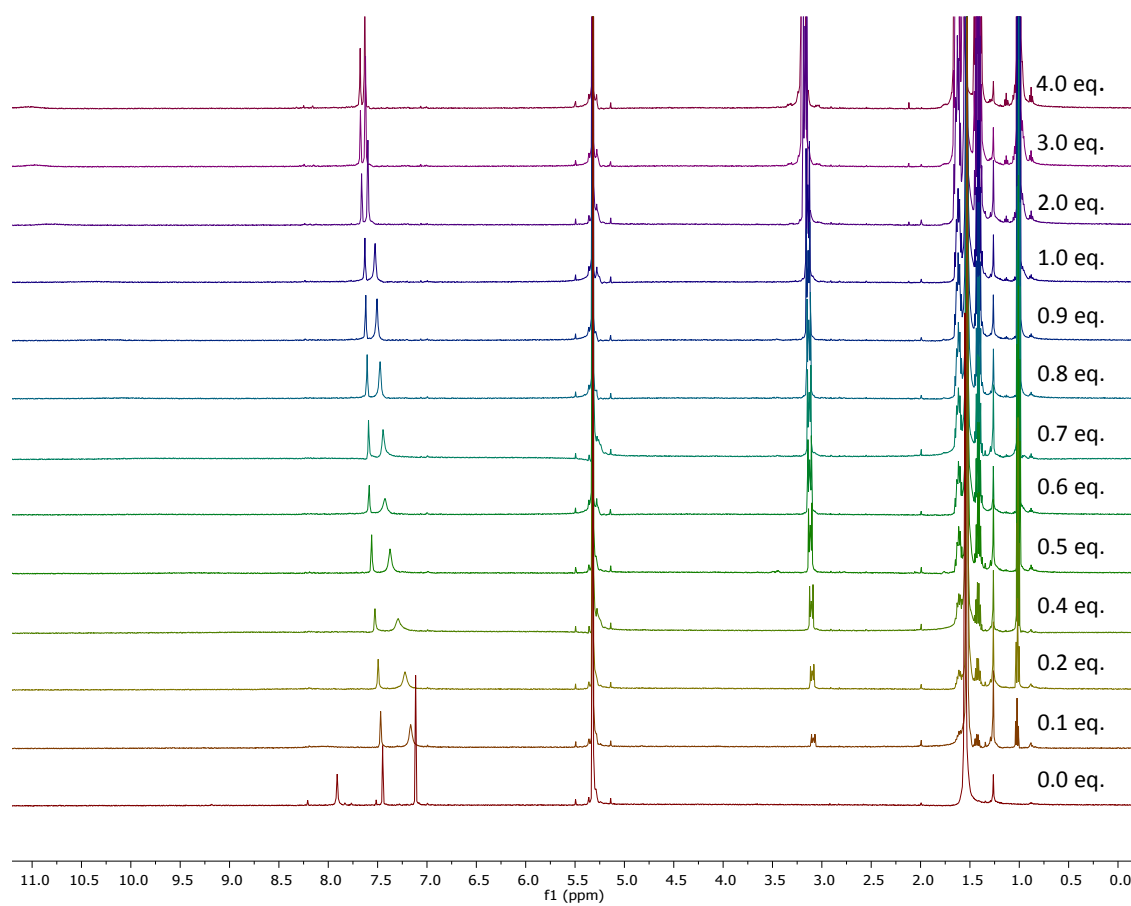


Figure 23 $^1\text{H-NMR}$ (500 MHz, CD_2Cl_2) titration experiments for 1a and TBANO_3 .

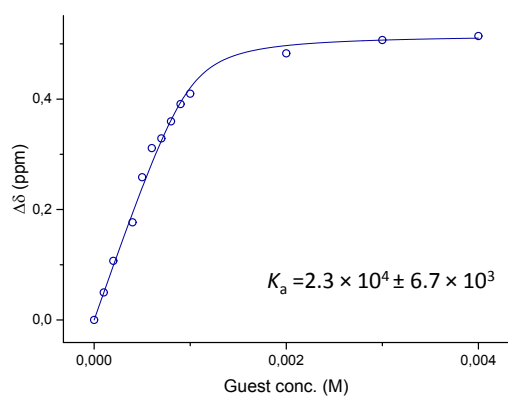


Figure 24 Plot for $^1\text{H-NMR}$ titration of 1a with TBANO_3 following proton H_b with the fitted curve.

$^1\text{H-NMR}$ titrations in $\text{DMSO-}d_6$

The experiments were performed as outlined above, with the exception of the stock solution of guest, which was adjusted to 500 mM (still with 1.0 mM host concentration).

The experiments were performed in several NMR tubes, as outlined in Table 5.

Table 5 General method for $^1\text{H-NMR}$ titrations in $\text{DMSO-}d_6$ in several NMR tubes

Sample No.	Guest conc. (mM)	Vol. Host (μl)	Vol. Guest (μl)
1	0	500	0
2	50	450	50
3	100	400	100
4	150	350	150
5	200	300	200
6	250	250	250
7	300	200	300
8	350	150	350
9	400	100	400
10	450	50	450
11	500	0	500

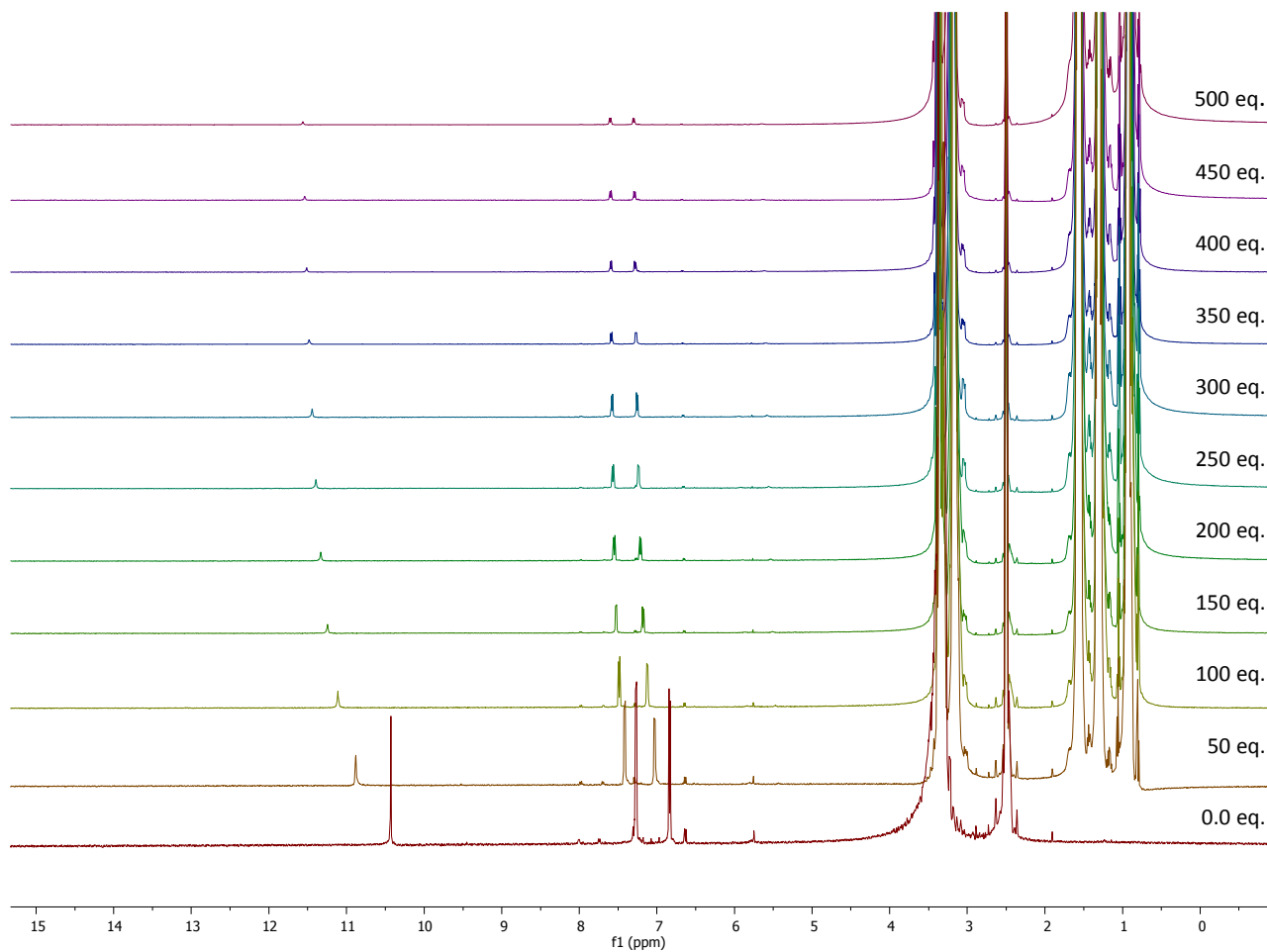


Figure 25 $^1\text{H-NMR}$ (500 MHz, DMSO-d_6) titration experiments for **1b** and TBACl.

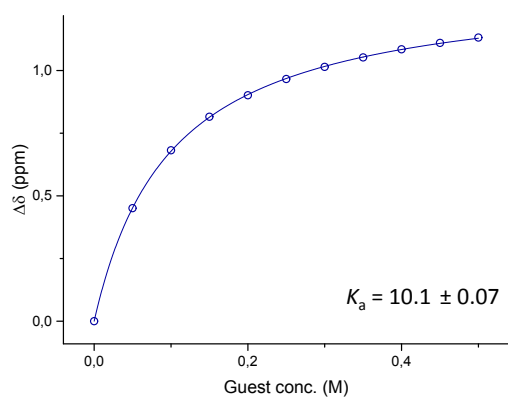


Figure 26 Plot for $^1\text{H-NMR}$ titration of **1b** with TBACl, following the amide proton, with the fitted curve.

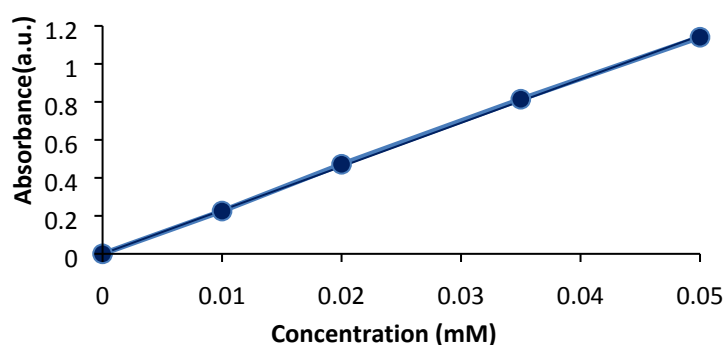
UV/Vis titration experiments

In general UV/Vis experiments were performed in the same cuvette which was positioned equally in the spectrophotometer for each measurement and experiment. A blank spectrum of pure dichloromethane was recorded for use as reference.

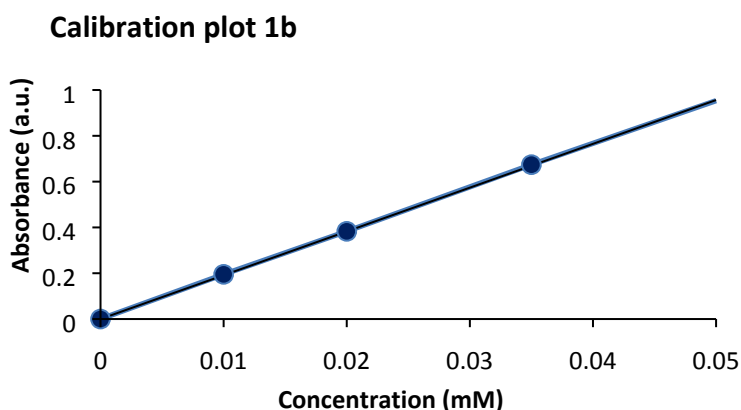
To ensure no aggregation of the compounds (**1a** and **1b**) interfered with the experiments, a calibration curve was performed in dichloromethane by plotting the concentration of host and the intensity of absorption. A straight line was obtained for both compounds indicating no aggregation.

ConC (mM)	Absorbance (a.u)
0	0
0.01	0.2252
0.02	0.4715
0.035	0.814
0.05	1.1403

Calibration plot 1a



ConC (mM)	Absorbance (a.u)
0	0
0.01	0.1951
0.02	0.3829
0.035	0.674
0.05	0.9534



For UV/Vis titration experiments, a stock solution of host (0.01 mM) was made, and from this a stock solution of guest (0.15 mM) was made. The titration experiments were performed in a single cuvette, and the guest was added to the host in increasing volumes (Table 6).

Table 6 General method for performing UV/Vis titrations in one cuvette.

No.	V(H) [mL]	V(G) [mL]	V(G) tilsat [mL]	V(total) [mL]	conc [M]	(H) [M]	conc [M]	(G)
1	2	0	0	2.00	9.9240E-06	0.000000E+00		
2	2	0.02	0.02	2.02	9.9240E-06	1.485149E-06		
3	2	0.04	0.02	2.04	9.9240E-06	2.941176E-06		
4	2	0.06	0.02	2.06	9.9240E-06	4.368932E-06		
5	2	0.08	0.02	2.08	9.9240E-06	5.769231E-06		
6	2	0.10	0.02	2.10	9.9240E-06	7.142857E-06		
7	2	0.12	0.02	2.12	9.9240E-06	8.490566E-06		
8	2	0.14	0.02	2.14	9.9240E-06	9.813084E-06		
9	2	0.16	0.02	2.16	9.9240E-06	1.111111E-05		
10	2	0.18	0.02	2.18	9.9240E-06	1.238532E-05		
11	2	0.20	0.02	2.20	9.9240E-06	1.363636E-05		
12	2	0.25	0.05	2.25	9.9240E-06	1.666667E-05		
13	2	0.30	0.05	2.30	9.9240E-06	1.956522E-05		
14	2	0.35	0.05	2.35	9.9240E-06	2.234043E-05		
15	2	0.40	0.05	2.40	9.9240E-06	2.500000E-05		

Each absorbance spectrum of **1a** or **1b** was monitored, and the difference in absorbance at a certain wavelength was plotted against the concentration of guest. OriginPro 2015 was used to handle the equation below². Using OriginPro to fit to this equation by non-linear regression it allowed for determination of the binding constant K_a (blue solid line in Figure 28 and Figure 30):

$$\Delta Abs = \varepsilon_{HG} \frac{1}{2} \left(\left(G_0 + H_0 + \frac{1}{K_a} \right) - \sqrt{\left(\left(G_0 + H_0 + \frac{1}{K_a} \right)^2 - 4H_0G_0 \right)} \right)$$

At 382 and 381 nm the spectrometer changed lamps, which led to an artifact in the absorbance spectra. Therefore, these datapoints were omitted.

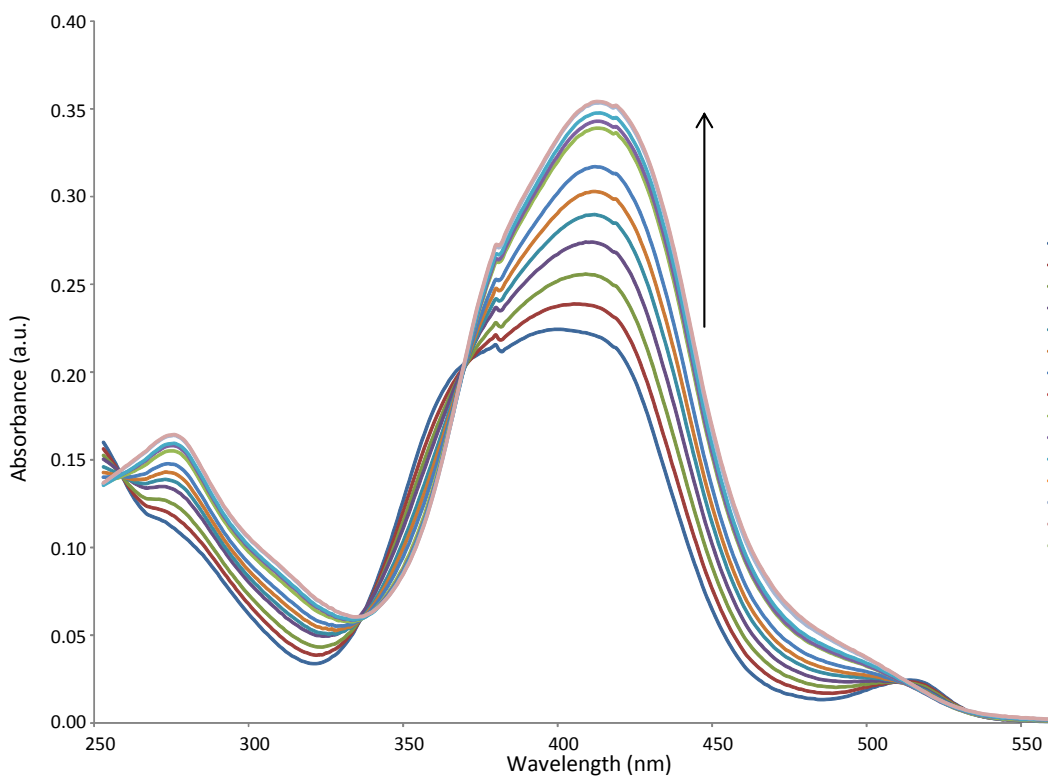


Figure 27 UV/Vis titration of 1a with TBACl. Black arrow indicates the increasing absorbance as guest concentration is increased.

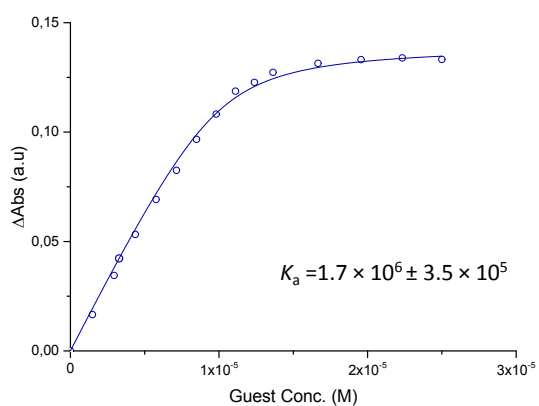


Figure 28 Plot for UV/Vis titration of 1a with TBACl at 413 nm with the fitted curve.

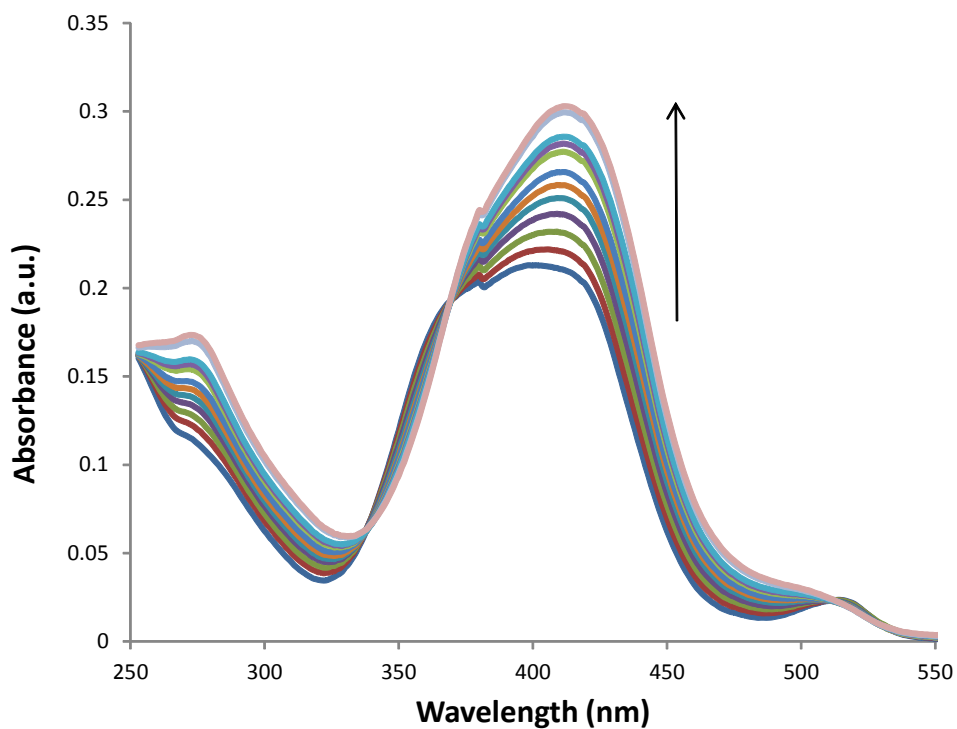


Figure 29 UV/Vis titration of 1a with TBABr. Black arrow indicates the increasing absorbance as guest concentration is increased.

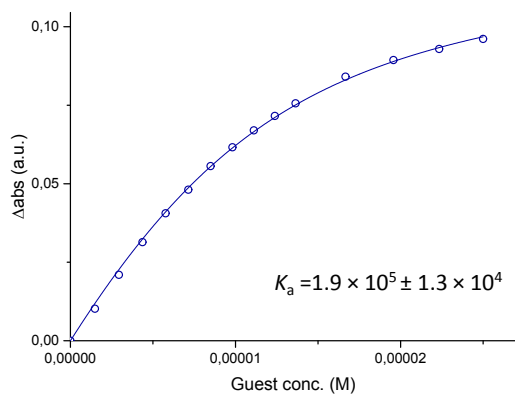


Figure 30 Plot for UV/Vis titration of 1a with TBABr at 412 nm with the fitted curve.

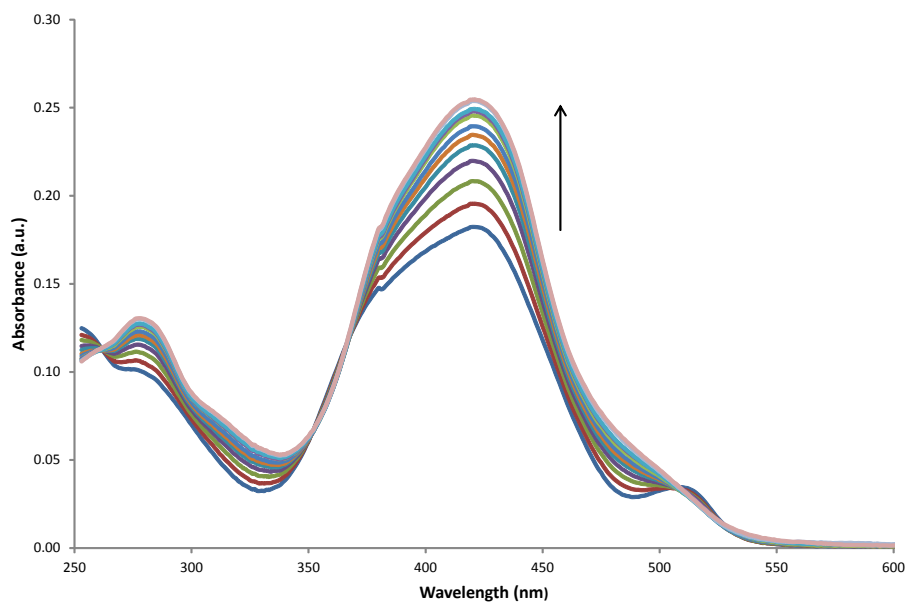


Figure 31 UV/Vis titration of 1b with TBACl. Black arrow indicates the increasing absorbance as guest concentration is increased.

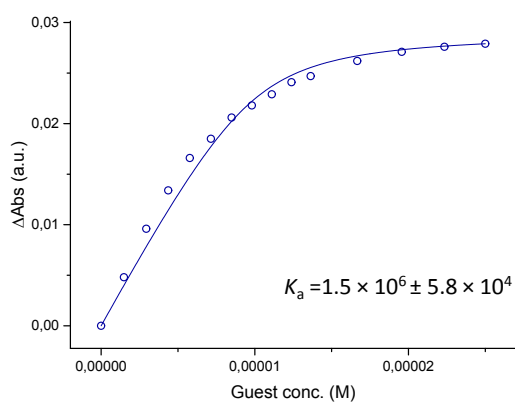
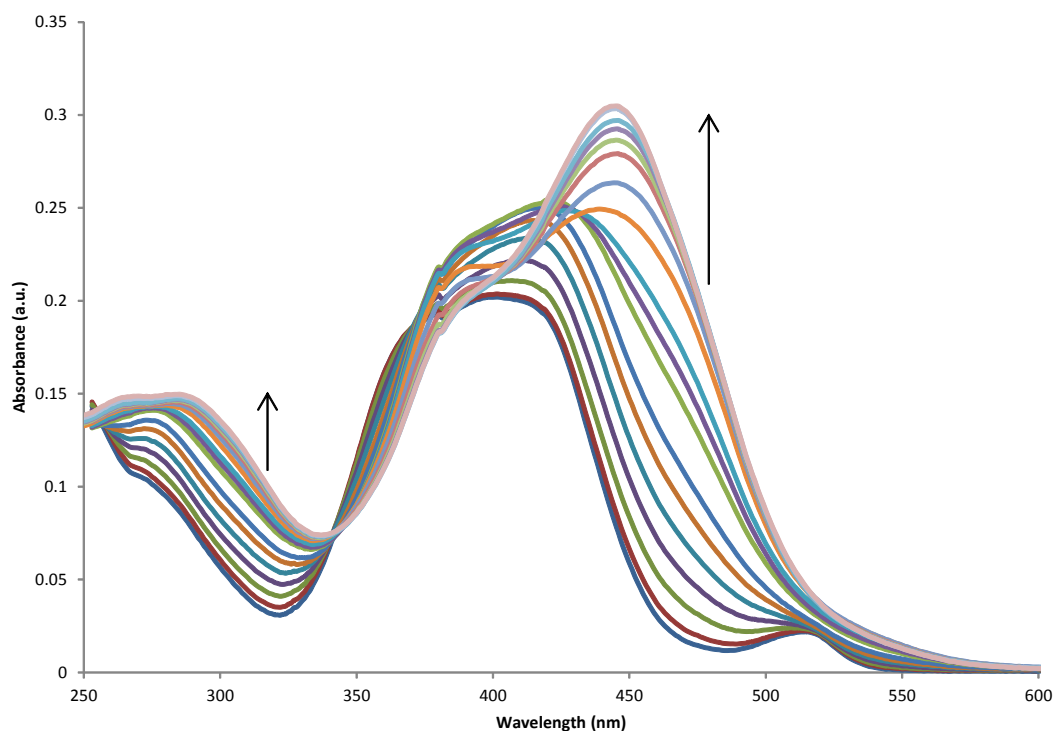


Figure 32 Plot for UV/Vis titration of 1b with TBACl at 275 nm with the fitted curve.

UV/Vis titration with tetrabutyl acetate

The procedure described above for titration was used, and the absorbance spectra obtained are shown below for addition of tetrabutyl acetate ($0 - 3.68 \times 10^{-5}$ M). The spectra shows an increase in absorption throughout the titration around 275 nm. An increase in absorbance is observed at 400 nm up on till 1 equivalent of guest. Over 1 equivalent, the absorbance is decreasing at this wavelength, and a new absorption band at 450 nm emerges, which continuous to increase throughout the titration.



Study of binding stoichiometry

In order of supporting the results from the Job's plot method described above, the above titrations were fitted to a 1:2 binding stoichiometry as well. This allowed us to analyse the residuals of the different fits which could further indicate the binding stoichiometry. All binding constants obtained are shown in the table below.

		1:1 binding	1:2 binding		Solvent	Method of titration	Method of fitting
	Anion	K_a (M^{-1})	K_1 (M^{-1})	K_2 (M^{-1})			
1a	Chloride	$1.7 \times 10^6 \pm 3.5 \times 10^5$	Fit failed		CH_2Cl_2	UV/Vis	OriginPro
			$6.6 \times 10^8 \pm 4.1 \times 10^9$	$1.4 \times 10^7 \pm 8.9 \times 10^7$			BindFit
	Bromide	$1.9 \times 10^5 \pm 1.3 \times 10^4$	$37.1 \pm 3.2 \times 10^4$	$2.1 \times 10^7 \pm 1.8 \times 10^{10}$	CH_2Cl_2	UV/Vis	OriginPro
			Fit failed				BindFit
	Iodide	$2.3 \times 10^3 \pm 78$			CD_2Cl_2	NMR	OriginPro
			$2.3 \times 10^3 \pm 87$	-41 ± -74			BindFit
Nitrate	$2.3 \times 10^4 \pm 6.7 \times 10^3$			CD_2Cl_2	NMR	OriginPro	
		$2.2 \times 10^4 \pm 1.8 \times 10^4$	$3.1 \times 10^2 \pm 1.3 \times 10^3$			BindFit	
Hydrogen sulphate	$2.5 \times 10^3 \pm 2.9 \times 10^2$			CD_2Cl_2	NMR	OriginPro	
1b	Chloride	$1.5 \times 10^6 \pm 5.8 \times 10^4$	$3.1 \times 10^3 \pm 3.9 \times 10^2$	$-1.1 \times 10^2 \pm -44$	CH_2Cl_2	UV/Vis	OriginPro
			$46.8 \pm 3.3 \times 10^3$	$2.9 \times 10^8 \pm 2.1 \times 10^{10}$			BindFit
	Chloride	10.1 ± 0.07	$1.0 \times 10^2 \pm 6$	$5.4 \times 10^7 \pm 4.4 \times 10^6$	DMSO	NMR	OriginPro
		8.93 ± 0.08	-1.56 ± -0.3			BindFit	

From the above, it is evident that the binding stoichiometry for the croconamides are leaning towards 1:1. When fitting to a 1:2 binding model a greater error on the fit arises. Also, 'Fit failed' in the Table above is an expression for the fit not being able to converge to the applied data.

For UV/Vis titrations where the fitting was performed using OriginPro, each absorbance spectrum of **1a** or **1b** was monitored, and the difference in absorbance at a certain wavelength was plotted against the concentration of guest. OriginPro 2015 was used to handle the equation below². Using OriginPro to fit to this equation by non-linear regression it allowed for determination of the binding constant K_a (blue solid line in the plots below):

$$\Delta Abs = \frac{\varepsilon_{\Delta HG}[H_0]K_1[G] + \varepsilon_{\Delta HG2}[H_0]K_1K_2[G]^2}{1 + K_1[G] + K_1K_2[G]^2}$$

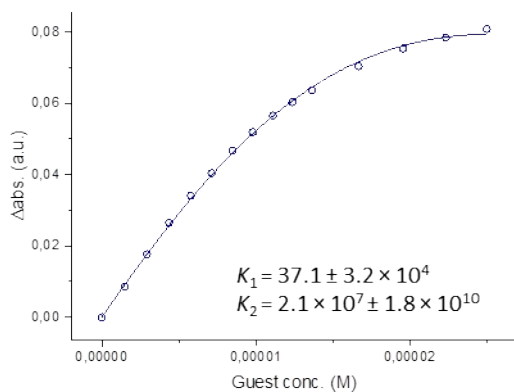


Figure 33 Plot for UV/Vis titration of 1a with TBACl at 413 nm with the fitted curve to a 1:2 binding model.

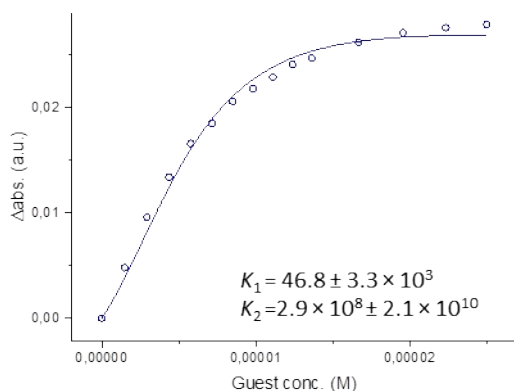
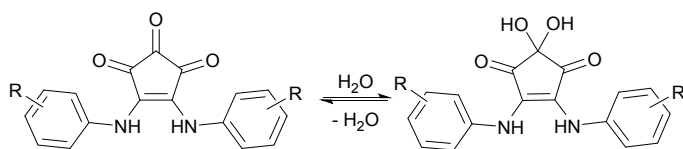


Figure 34 Plot for UV/Vis titration of 1b with TBACl at 275 nm with the fitted curve to a 1:2 binding model.

For the association constants, depicted in the Table above, obtained with BindFit, the data titration data was uploaded to www.supramolecular.org, and a guess of the binding constants was provided. The program then performs a non-linear regression on this data using the exact binding equation implemented via a Python program located on the server of www.supramolecular.org. This yields the binding constants. If necessary, another guess of the value of the binding constants can be provided, based on the first result of the calculation.

6. Study of hydrates of croconamides

Croconamides **1a** and **1b** were investigated in dry DMSO and DMSO in the presence of water using $^1\text{H-NM}$, and UV/Vis (Scheme 3), to investigate the possible addition of water to and formation of a hydrate species.



Scheme 3 Addition of water to croconamides.

$^1\text{H-NMR}$ experiments

The $^1\text{H-NMR}$ experiments were performed in $\text{DMSO-}d_6$ with 0.5 vol. % D_2O or H_2O , and for the dry experiments a new bottle of $\text{DMSO-}d_6$ was opened immediately before use. The start concentration of croconamide was 8.9 mM for **1a** and 11.7 mM for **1b**.

For the samples containing water, a second set of signals emerged in the $^1\text{H-NMR}$ spectrum after a few hours. The $^1\text{H-NMR}$ spectra is shown below.

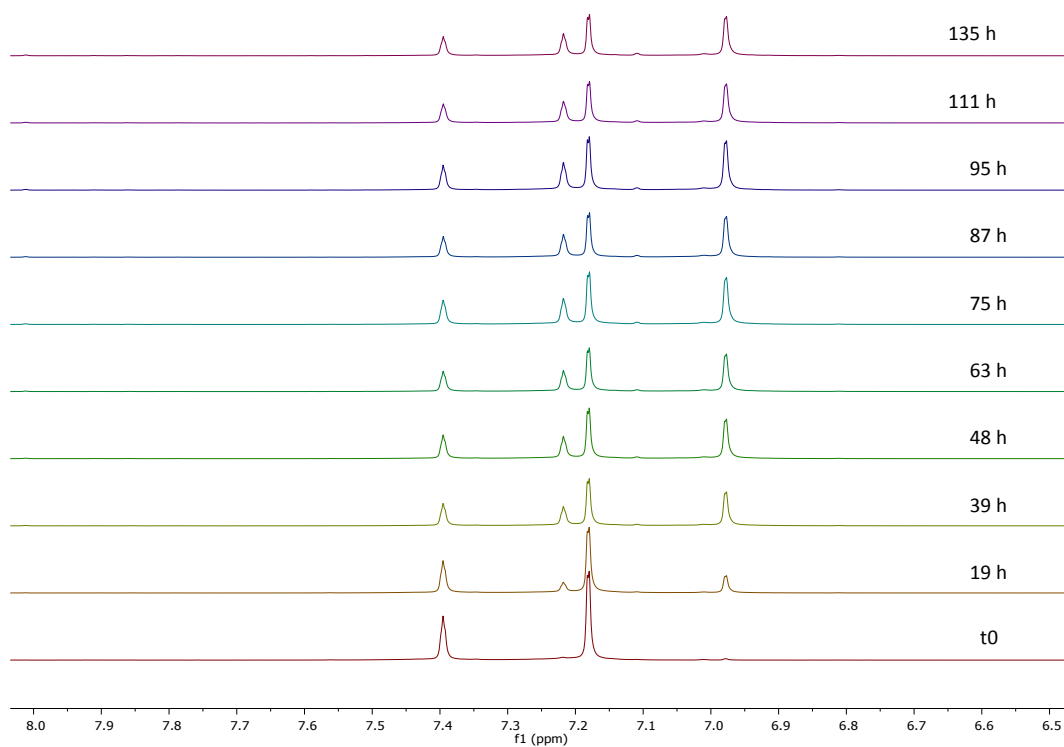


Figure 35 $^1\text{H-NMR}$ (500 MHz, $\text{DMSO-}d_6$, 0.5 vol. % D_2O) of **1a**.

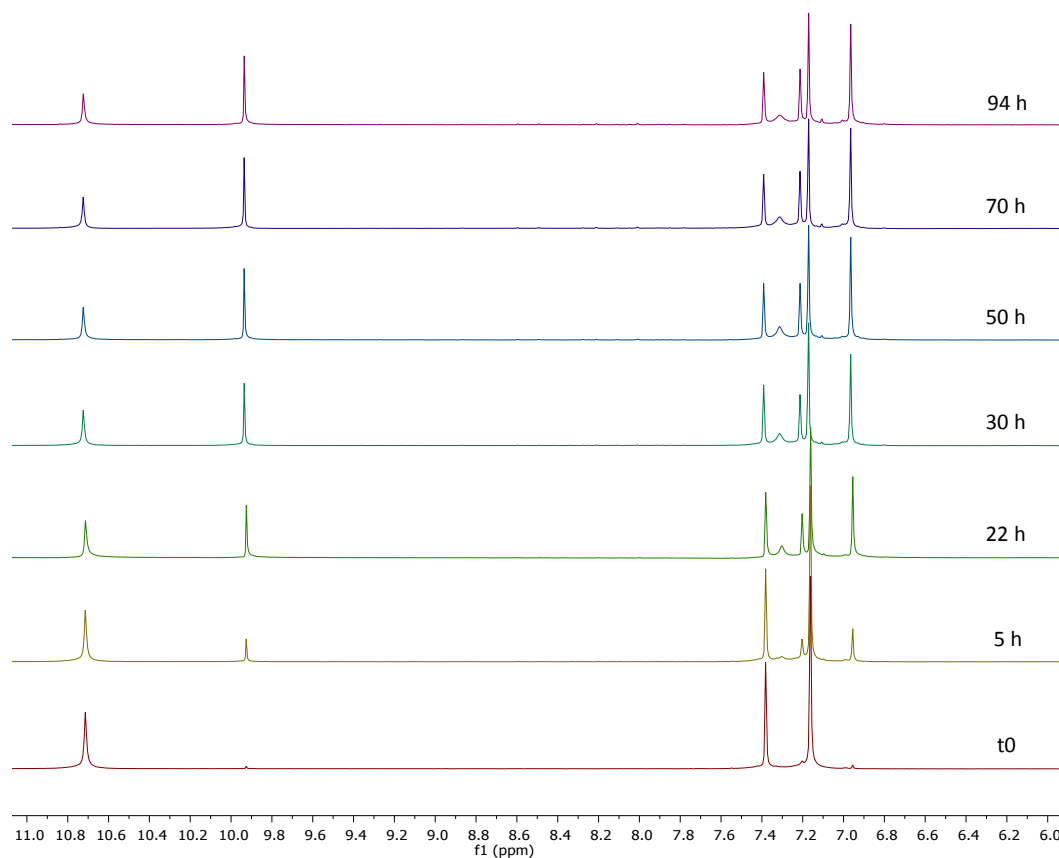


Figure 36 $^1\text{H-NMR}$ (500 MHz, $\text{DMSO-}d_6$, 0.5 vol. % H_2O) of 1a.

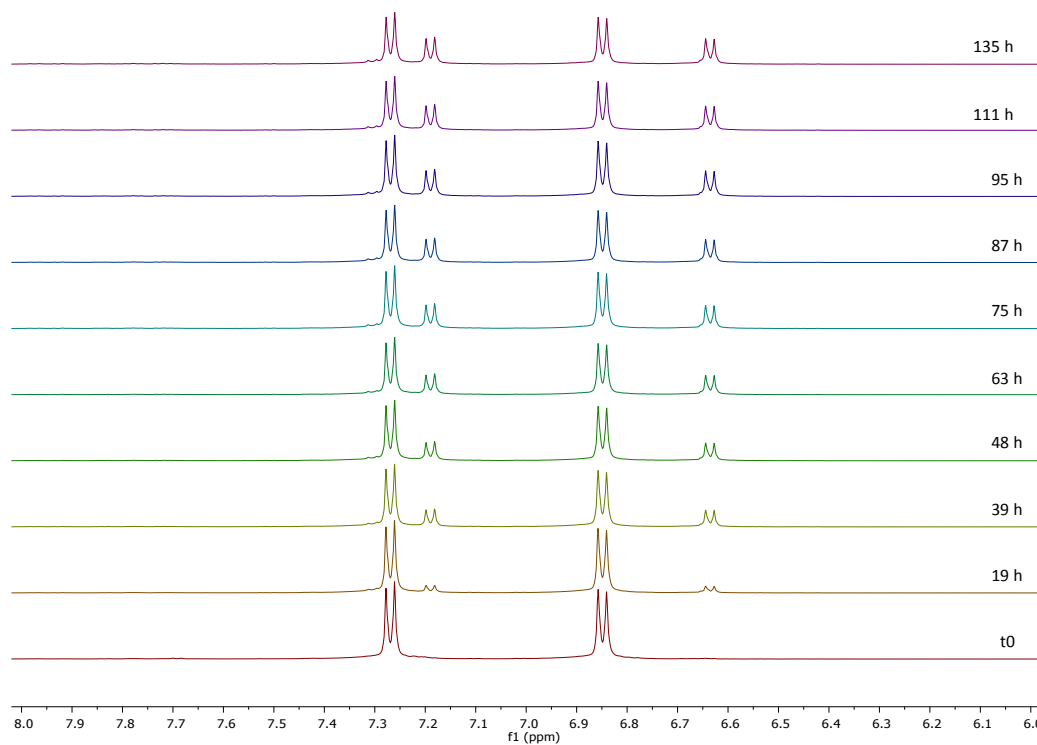


Figure 37 $^1\text{H-NMR}$ (500 MHz, $\text{DMSO-}d_6$, 0.5 vol. % D_2O) of 1b.

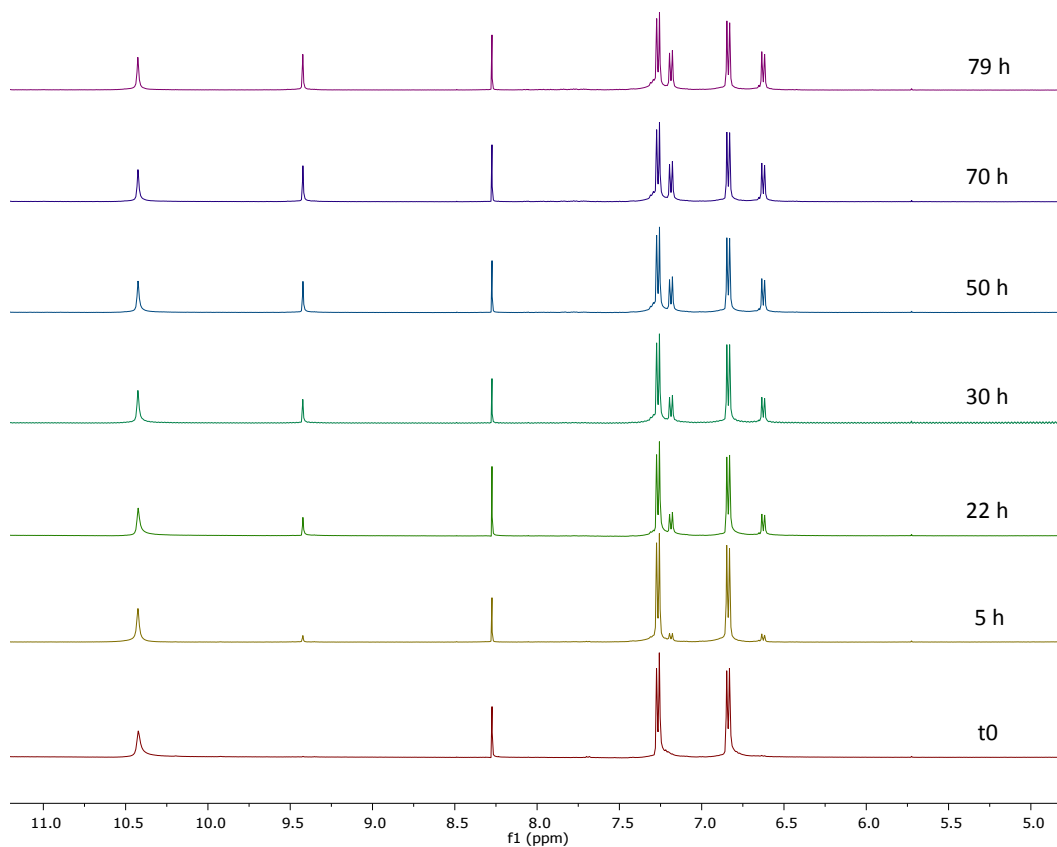
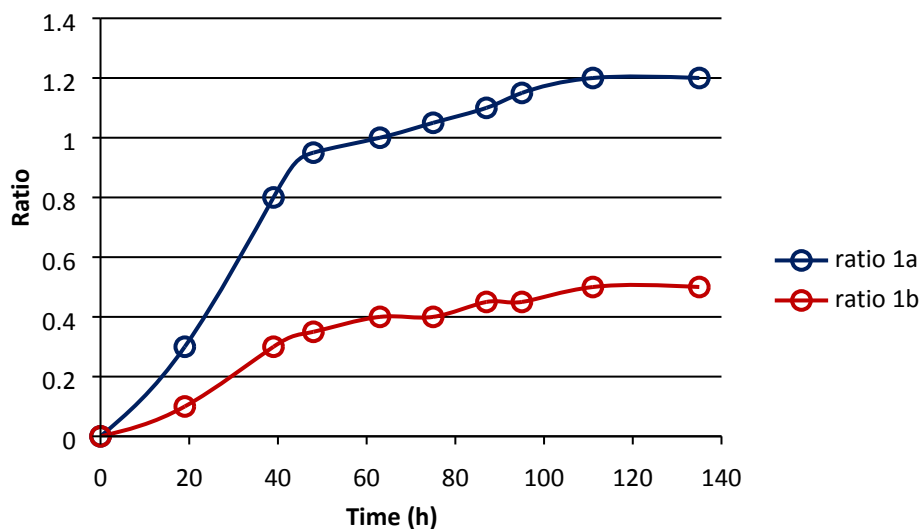


Figure 38 ¹H-NMR (500 MHz, DMSO-*d*₆, 0.5 vol. % H₂O) of **1b**.

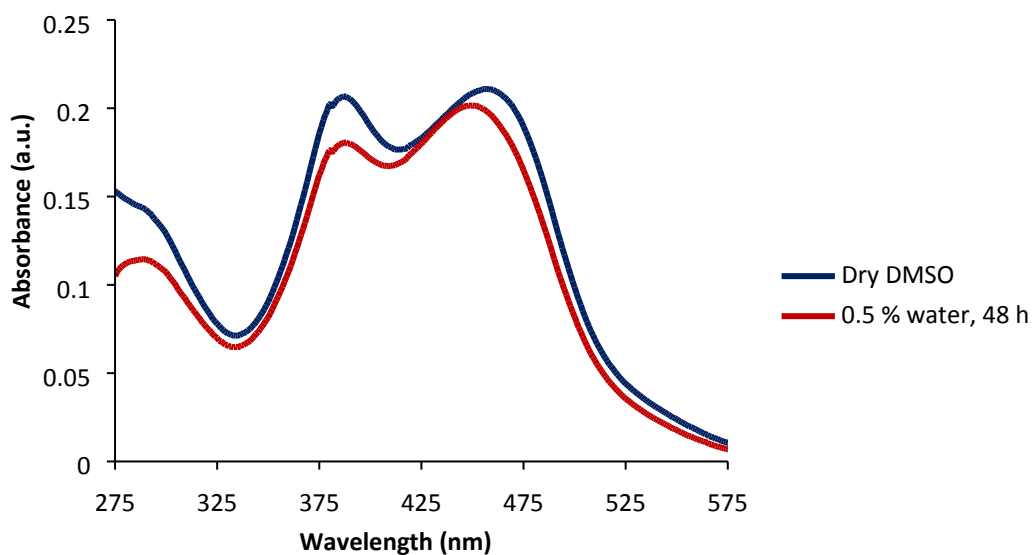
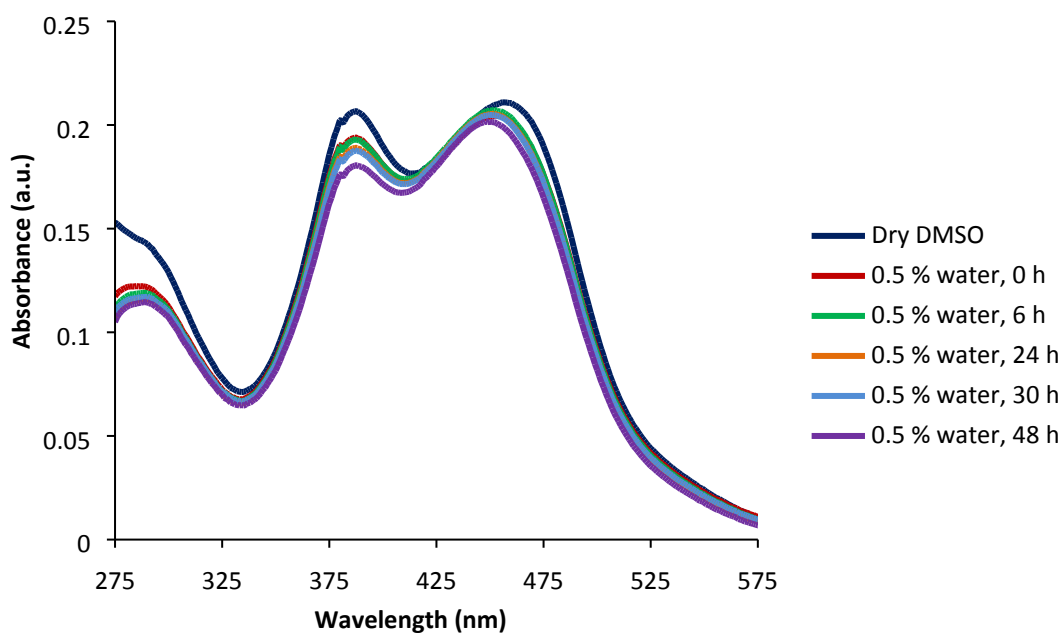
For the spectra obtained with D₂O added, the integral of one proton of croconamide was compared to its hydrate. This was plotted against the time of the experiment. The experiments implies that formation of hydrate proceeds faster for **1a** than for **1b**, and after approximately 48 hours, the hydrate formation reaches a plateau.



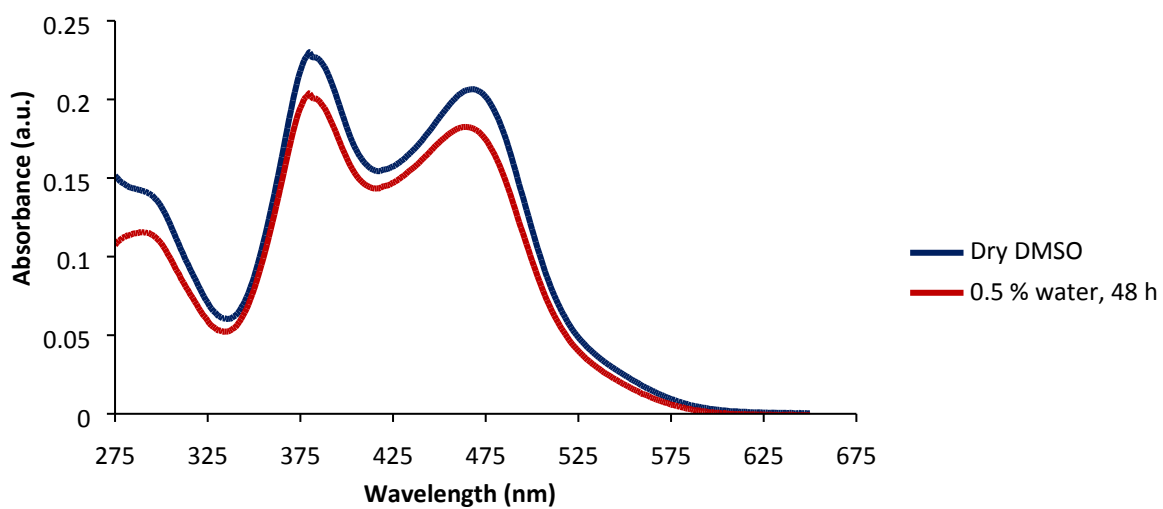
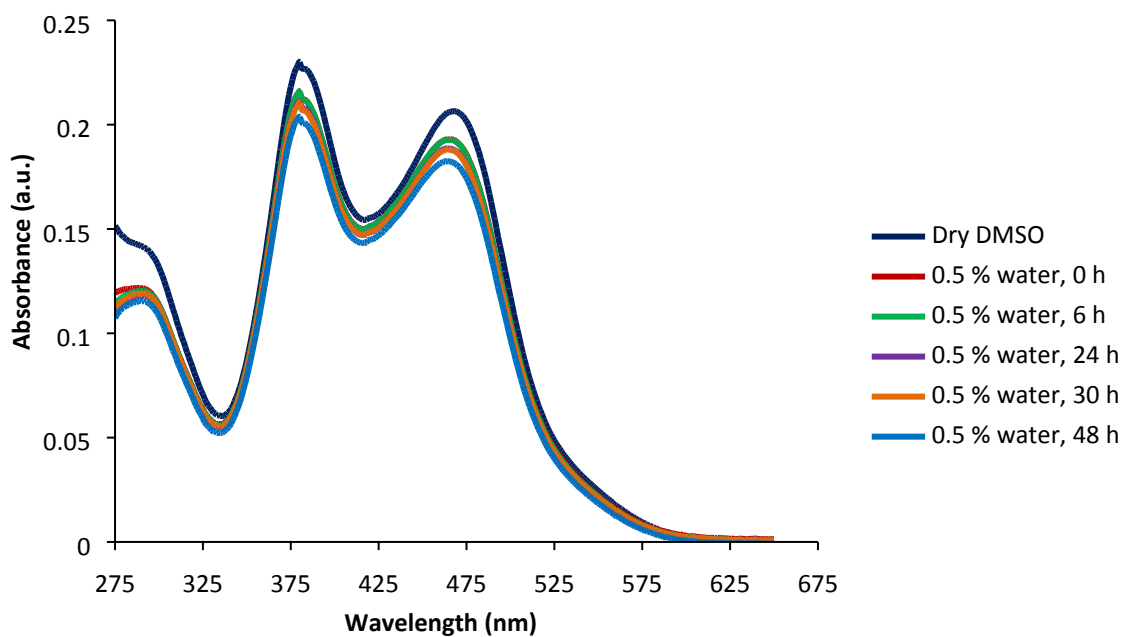
UV/Vis experiments

For the UV/Vis experiments, the absorbance spectra were monitored upon the addition of 0.5 vol. % water and compared to a spectrum in dry DMSO (0 % water). This dry DMSO was spectroscopic grade, and dried over molecular sieves prior to use.

The absorbance spectra for **1a** are shown below:



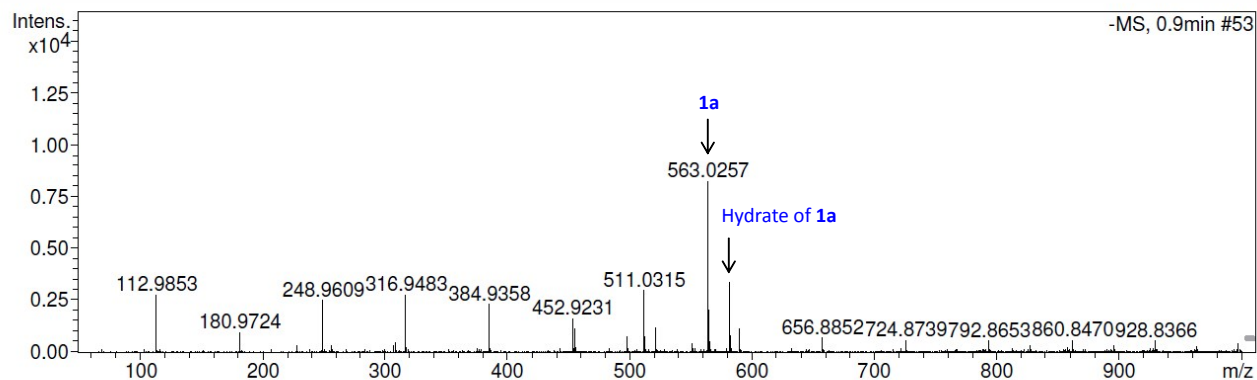
The absorbance spectra for **1b** are shown below:



The presence of hydrates was confirmed using direct inlet on the LC/MS apparatus described above. HRMS analyses are shown below for the hydrate of **1a** and **1b**.

Acquisition Parameter

Source Type	ESI	Ion Polarity	Negative	Set Nebulizer	2.0 Bar
Focus	Not active	Set Capillary	3500 V	Set Dry Heater	240 °C
Scan Begin	50 m/z	Set End Plate Offset	-500 V	Set Dry Gas	10.0 l/min
Scan End	1000 m/z	Set Collision Cell RF	100.0 Vpp	Set Divert Valve	Waste

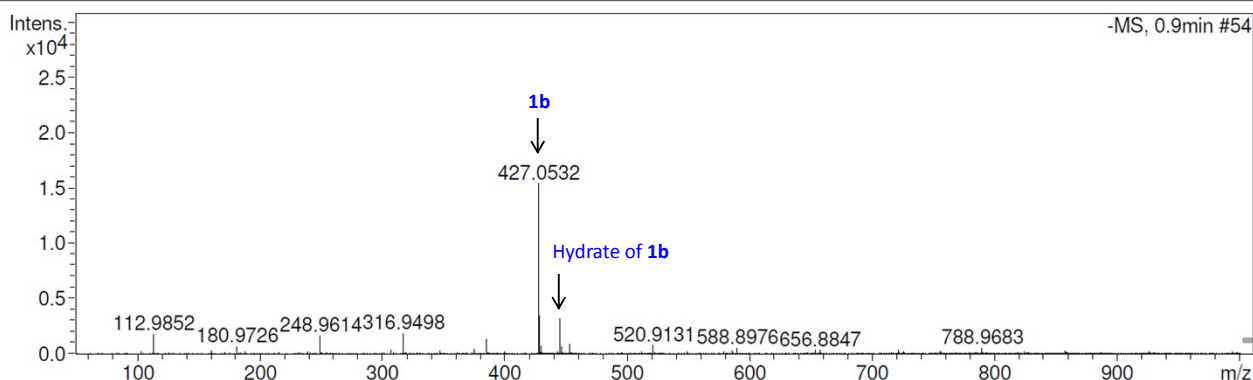


Meas. m/z	#	Formula	Score	m/z	err [mDa]	err [ppm]	mSig ma	rdb	e ⁻ Conf	N-R ule
581.0377	1	C ₂₁ H ₉ F ₁₂ N ₂ O ₄	100.00	581.0376	-0.1	-0.1	9.3	12.5	even	ok

Figure 39 HRMS analysis of the hydrate of 1a.

Acquisition Parameter

Source Type	ESI	Ion Polarity	Negative	Set Nebulizer	2.0 Bar
Focus	Not active	Set Capillary	3500 V	Set Dry Heater	240 °C
Scan Begin	50 m/z	Set End Plate Offset	-500 V	Set Dry Gas	10.0 l/min
Scan End	1000 m/z	Set Collision Cell RF	100.0 Vpp	Set Divert Valve	Waste

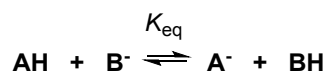


Meas. m/z	#	Formula	Score	m/z	err [mDa]	err [ppm]	mSig ma	rdb	e ⁻ Conf	N-R ule
445.0621	1	C ₁₉ H ₁₁ F ₆ N ₂ O ₄	100.00	445.0628	0.7	1.6	8.4	12.5	even	ok

Figure 40 HRMS analysis of the hydrate of 1b.

7. Determination of pK_a

The pK_a values of **1a** and **1b** were determined using a modification of the overlapping indicator method.⁴ In this modification, catalyst **1a** or **1b** functioned as the indicator, while benzoate was used as the base (B in the scheme below). Deprotonation of the catalyst (AH in the general scheme below) results in a slight change of color.



Note that it follows that $K_{\text{eq}} = K_{\text{a(AH)}} \cdot K_{\text{a(BH)}}^{-1}$.

The change in absorbance at 445 nm was used as indication of deprotonisation for **1a**, and 447 nm for **1b**, as tetrabutylammonium benzoate was added in 0.07 – 4.29 eq.

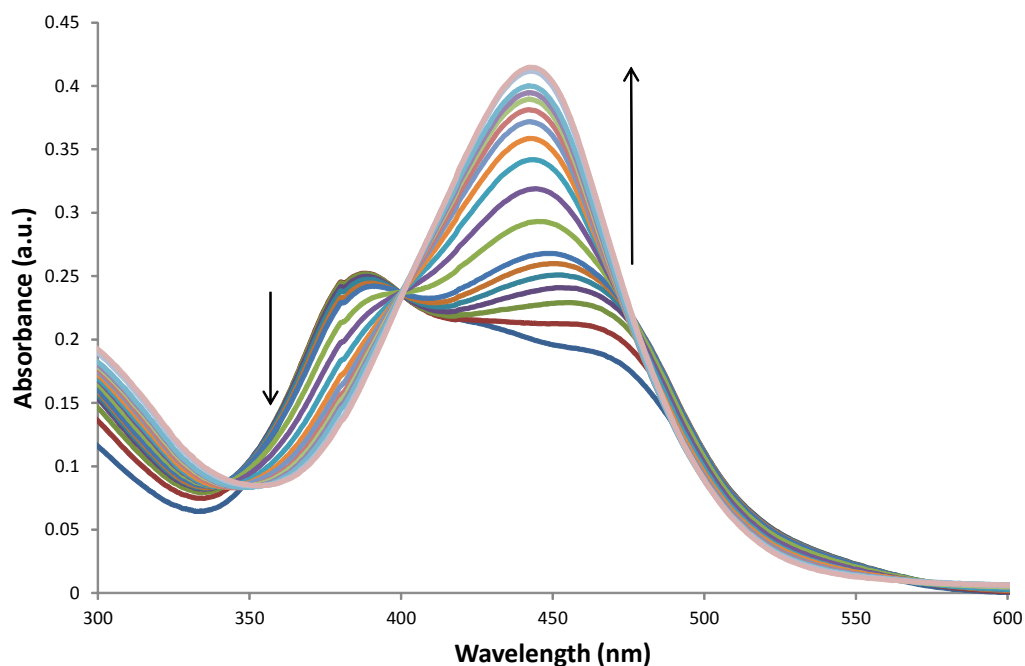


Figure 41 UV/Vis titration of **1a** with TBA benzoate. Black arrows indicates the increasing or decreasing absorbance as guest concentration is increased (0.07 – 4.29 eq.).

⁴ Matthews, W. S. *et al.* Equilibrium acidities of carbon acids. Vi. Establishment of an absolute scale of acidities in dimethyl sulfoxide solution. *J. Am. Chem. Soc.* **97**, 7006-7014 (1975).

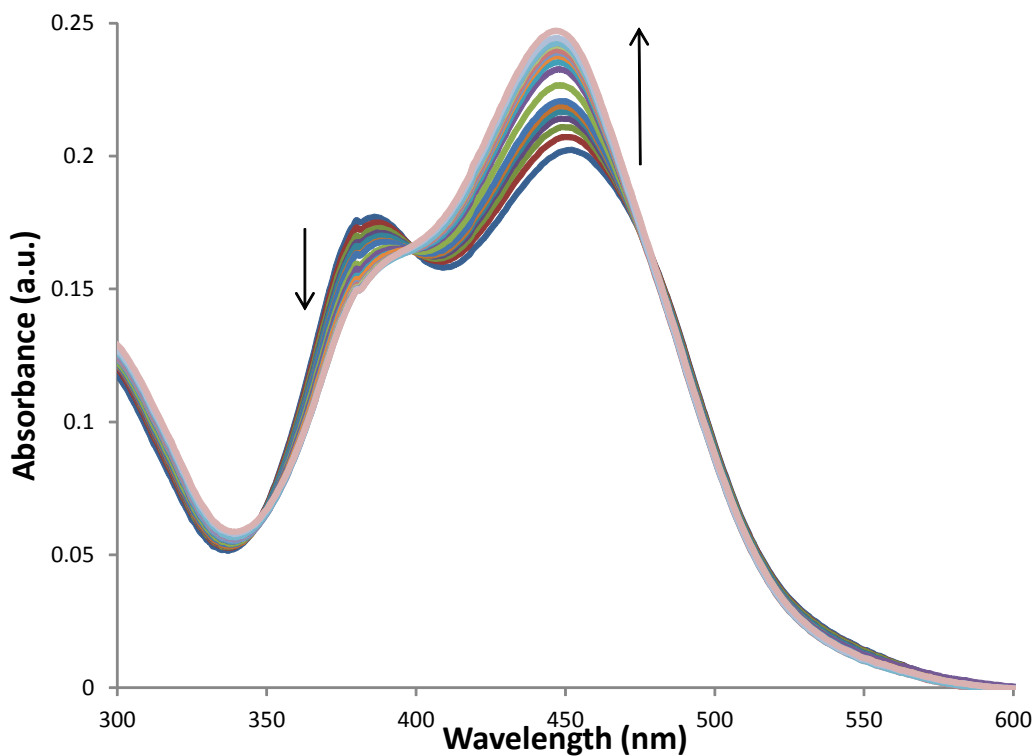


Figure 42 UV/Vis titration of 1b with TBAbenzoate. Black arrows indicates the increasing or decreasing absorbance as guest concentration is increased (0.07 – 4.29 eq.).

A titration curve can be obtained from the absorbance spectra above, from which K_{eq} can be determined.

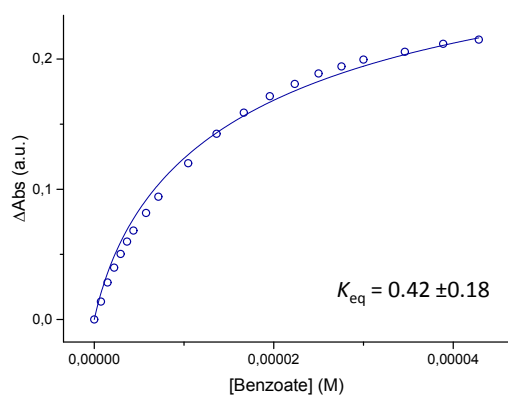


Figure 43 Plot for UV/Vis titration of 1a with TBAbenzoate at 445 nm with the fitted curve.

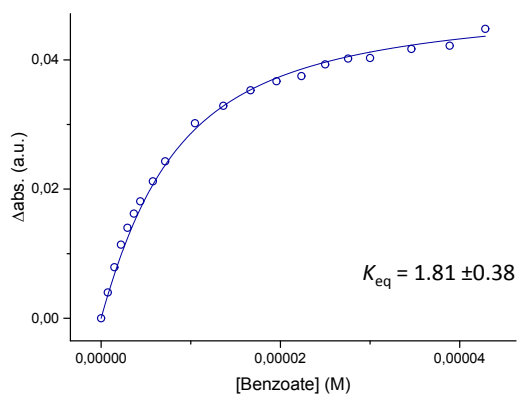


Figure 44 Plot for UV/Vis titration of **1b** with TBA benzoate at 447 nm with the fitted curve.

The pK_a value of AH (**1a** and **1b**) is given by:

$$pK_{a(AH)} = pK_{a(BH)} - \log(K_{eq})$$

The pK_a value of benzoic acid in DMSO is 11.1,⁵ and so the following values are calculated (error based on propagation of error on K_{eq} when assuming no error on $pK_{a(BH)}$ literature values):

1a: $pK_a = 11.5 \pm 0.2$

1b: $pK_a = 10.8 \pm 0.1$

⁵ Bordwell, F. G. Equilibrium acidities in dimethyl sulfoxide solution. *Acc. Chem. Res.* **21**, 456-463 (1988).

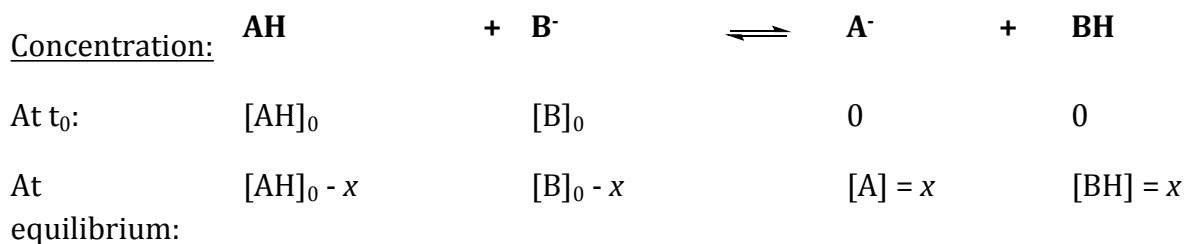
Equation for Non-Linear Regression to Obtain K_{eq}

K_{eq} was determined by non-linear regression to the following equation:

$$\Delta Abs = \frac{Abs_{max}([AH]_0 + [B]_0 - \sqrt{([AH]_0 + [B]_0)^2 - 4(1 - K_{eq}^{-1})[AH]_0 \cdot [B]_0})}{2[AH]_0 - 2[AH]_0 \cdot K_{eq}^{-1}}$$

Abs is the measured absorbance (at a wavelength of 445 or 447 nm in this case). Since the measured compounds does not have zero absorbance at zero concentration of base, the absorbance for pure catalyst (**1a** or **1b**) at 445 or 447 nm, respectively is used to obtain the difference in absorbance (ΔAbs), which is plotted as a function of added base ($[B]_0$), while the concentration of acid (**1a** or **1b**), $[AH]_0$, is maintained constant (0.010 mM in this experiment). The maximum absorbance, Abs_{max} , and K_{eq} is found by fitting to the equation above (blue solid line, Figure 41 and Figure 42).

Consider the following reaction:



When this reaction is monitored by the UV/Vis absorbance of **A⁻**, it follows from Lambert-Beer's law that

$$x = \frac{Abs}{Abs_{max}}[AH]_0$$

if monitored at a wavelength where only **A⁻** absorbs.

The equilibrium constant for the reaction is given by:

$$K_{eq} = \frac{[A][BH]}{[AH][B]} = \frac{x^2}{([AH]_0 - x)([B]_0 - x)}$$

This is rewritten to:

$$0 = (1 - K_{eq}^{-1})x^2 - ([AH]_0 + [B]_0)x + [AH]_0[B]_0$$

This quadratic equation has two (non-complex) solutions:

$$x = \frac{[AH]_0 + [B]_0 + \sqrt{([AH]_0 + [B]_0)^2 - 4(1 - K_{eq}^{-1})[AH]_0[B]_0}}{2(1 - K_{eq}^{-1})} \quad (\text{Eq. 1})$$

and

$$x = \frac{[AH]_0 + [B]_0 - \sqrt{([AH]_0 + [B]_0)^2 - 4(1 - K_{eq}^{-1})[AH]_0[B]_0}}{2(1 - K_{eq}^{-1})} \quad (\text{Eq. 2})$$

To identify the proper solution (within non-imaginary numbers), we utilise the real-life criteria:

$$0 < x \leq [AH]_0$$

$$[B]_0 > 0$$

$$K_{eq} > 0$$

The final criterion specifies that there must be a (non-complex) solution also for $0 < K_{eq} < 1$, since this is a subset of $K_{eq} > 0$. Any K_{eq} between 0 and 1 results in a negative denominator in both Eq.'s 1 and 2. Since $[AH]_0 + [B]_0$ is larger than zero (based on the real-life criteria), Eq. 1 cannot give a value of $x > 0$ for $0 < K_{eq} < 1$. Thus, only Eq. 2 can give (non-complex) solutions for all $K_{eq} > 0$, and therefore is the only equation that meets all of the real-life criteria.

Substituting $x = \frac{Abs}{Abs_{max}}[AH]_0$ and rearranging, one arrives at the final equation

$$Abs = \frac{Abs_{max}([AH]_0 + [B]_0 - \sqrt{([AH]_0 + [B]_0)^2 - 4(1 - K_{eq}^{-1})[AH]_0 \cdot [B]_0})}{2[AH]_0 - 2[AH]_0 \cdot K_{eq}^{-1}}$$

which describes the relationship between absorbance, Abs , and starting concentration of base, $[B]_0$, and makes it possible to identify *via* non-linear regression the equilibrium constant, K_{eq} , provided that the starting concentration of acid, $[AH]_0$, is kept constant.

In this case, since the measured compounds do not show zero absorbance at zero concentration of base, it is the ΔAbs that is plotted.

8. Crystal structure data

All single-crystal X-ray diffraction data were collected at 123(2) K on a Bruker D8 Venture instruments equipped with a I μ S microfocus source, a KAPPA goniometer, a nitrogen cryosystem cooling apparatus and a PHOTON 100 detector with Mo- K_{α} radiation. The structure was solved using Direct Methods (SHELXS)⁶ in Olex2⁷ and refined with the XL⁵ refinement package using Least Squares minimization.

1a

C₂₁H₈F₁₂N₂O₃; M = 564.29; Monoclinic; a = 20.0339(13) Å, b = 8.4046(7) Å, c = 13.8902(10) Å, $\alpha = 90^{\circ}$, $\beta = 122.816(2)^{\circ}$, $\gamma = 90^{\circ}$; V = 2082.5(3) Å³; T = 123.15 K; space group P2₁/n; Z = 4; $\mu(\text{Mo-}K_{\alpha}) = 0.07 \text{ mm}^{-1}$; 45150 reflections measured, 4089 independent reflections ($R_{int} = 0.0952$). The final R_1 value was 0.0466 [$F^2 > 2\sigma(F^2)$]. The final R_1 value was 0.0570 (all data). The final $wR(F^2)$ (all data) value was 0.1254. The goodness of fit on F^2 was 1.053

An electronic version of the refined structure has been deposited with the Cambridge Structural Database: CCDC-1522925.

⁶ Sheldrick, G.M. (2008). Acta Cryst. A64, 112-122.

⁷ Dolomanov, O.V., Bourhis, L.J., Gildea, R.J, Howard, J.A.K. & Puschmann, H. (2009), J. Appl. Cryst. 42, 339-341.

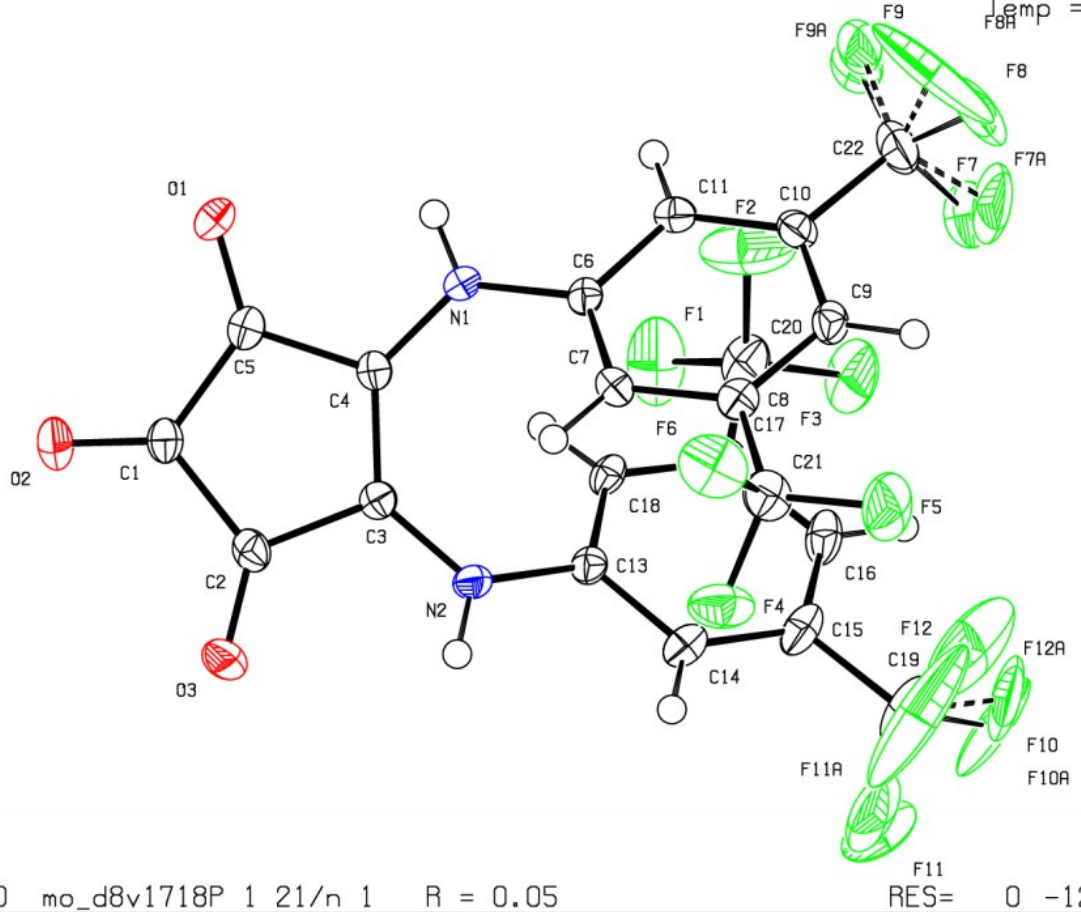
9 Y

PLATON-Dec 5 12:44:28 2016 - (70316)

Z -110 mo_d8v1718P 1 21/n 1 R = 0.05

NOMOVE FORCED

Prob = 50
Temp = 123

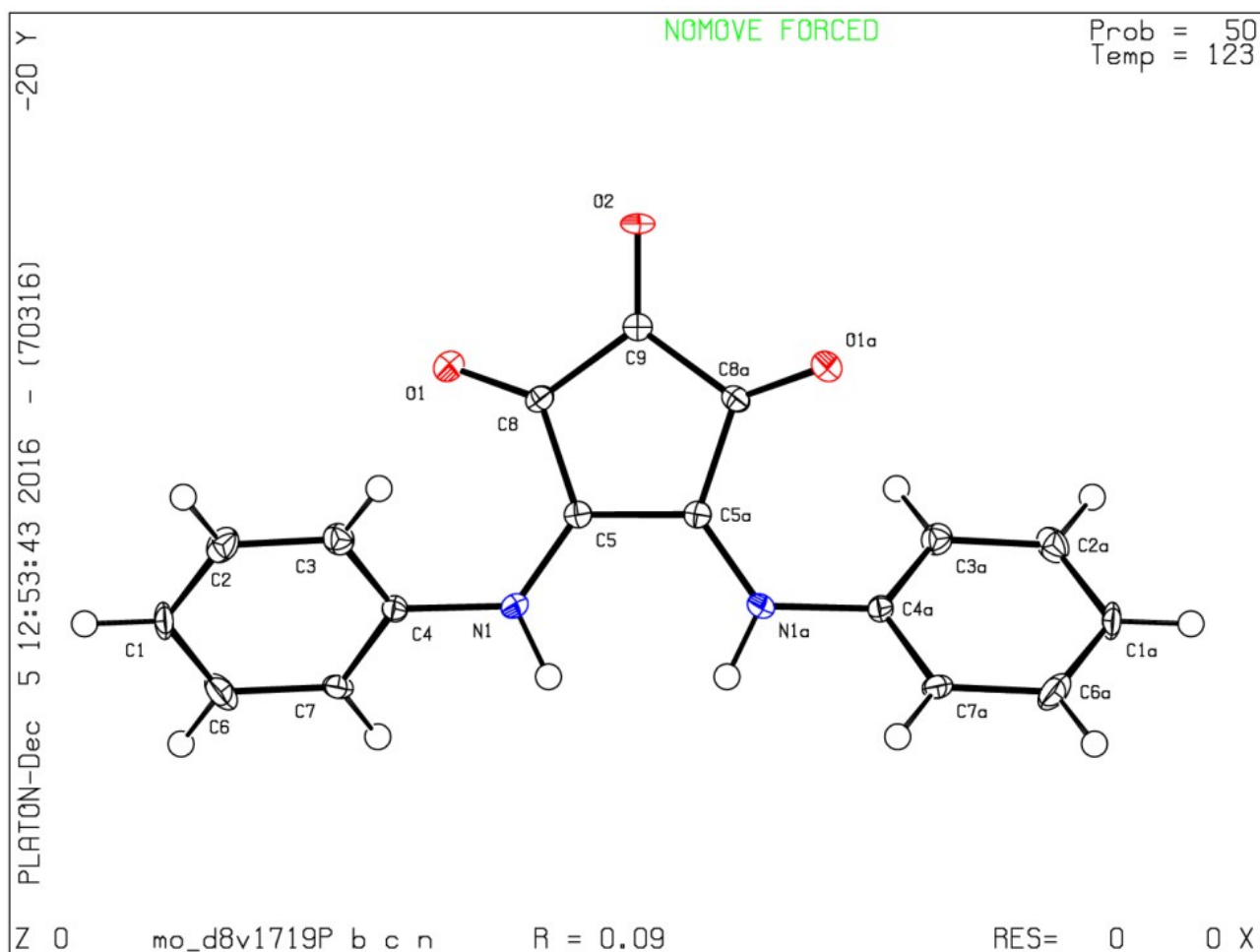


F11
RES= 0 -126 X

1c

$C_{17}H_{12}N_2O_3$; $M = 292.29$; Orthorhombic; $a = 25.356(3) \text{ \AA}$, $b = 6.9395(9) \text{ \AA}$, $c = 7.4967(11) \text{ \AA}$, $\alpha = 90^\circ$, $\beta = 90^\circ$, $\gamma = 90^\circ$; $V = 1319.1(3) \text{ \AA}^3$; $T = 123.15 \text{ K}$; space group $Pbcn$; $Z = 4$; $\mu(Mo-K\alpha) = 0.07 \text{ mm}^{-1}$; 29177 reflections measured, 1446 independent reflections ($R_{int} = 0.1283$). The final R_1 value was 0.0898 [$F^2 > 2\sigma(F^2)$]. The final R_1 value was 0.1037 (all data). The final $wR(F^2)$ (all data) value was 0.2207. The goodness of fit on F^2 was 1.092.

An electronic version of the refined structure has been deposited with the Cambridge Structural Database: CCDC-1522926.



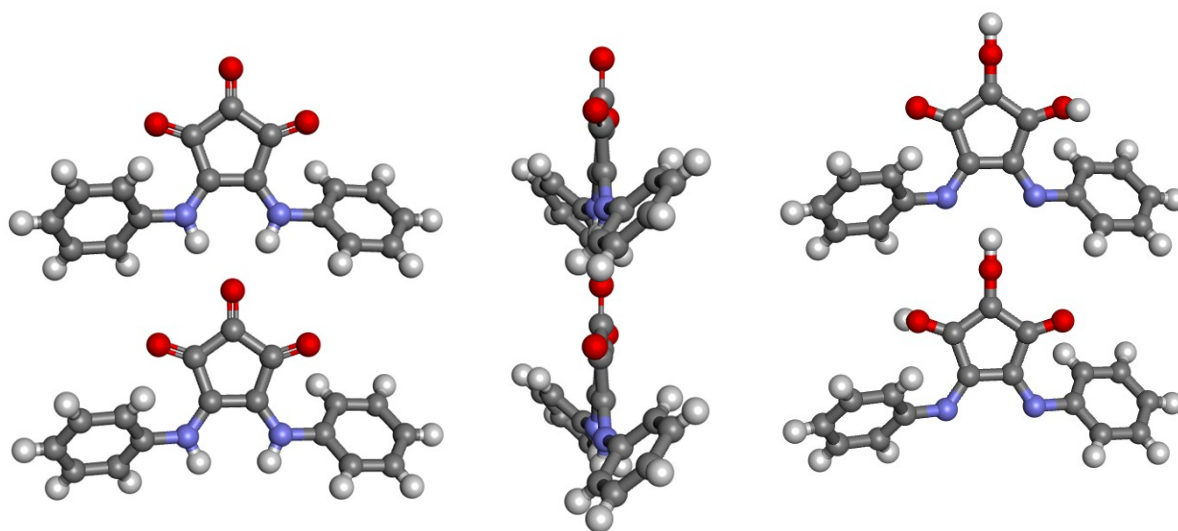


Figure 45 Crystal structures of 1c. Left: frontview, middle: sideview, right: frontview of tautomer.

9. Computational results

Complexation energies are calculated at the B3LYP/MiDiX level with the GAUSSIAN 09, suite of programs⁸ The vibrational frequencies were calculated to ensure that the optimized geometries are true minima (0 imaginary frequencies) and the energies are given as the sum of the electronic energy and the zero point vibrational energy contribution. Additional calculations were carried out for assessment with a fourth generation composite method referred to as G4MP2⁹ with the GAUSSIAN 09, suite of programs.⁷ G4MP2 theory is approximating a large basis set CCSD(T) single point calculation on a B3LYP/6-31G(2df,p) geometry and is incorporating a so-called higher level correction that is derived by a fit to the experimental values in the G3/05 test set with 454 experimental values.¹⁰ The average absolute derivation from the experimental test set values is 1.04 kcal mol⁻¹, which places the G4MP2 results well within chemical accuracy of 10 kJ mol⁻¹. The transition structures for the reactions reported in this work have been confirmed in each case by the calculation of vibrational frequencies (one imaginary frequency) and an intrinsic reaction coordinate analysis. Relative free energies stated within the text correspond to G4MP2 values at 298.15 K. The calculated total energies are available in Table 7. B3LYP/MidiX optimised geometries in the form of cartesian coordinates are shown in the tables below.

⁸ M.J. Frisch, G.W. Trucks, H.B. Schlegel, G.E. Scuseria, M.A. Robb, J.R. Cheeseman, G. Scalmani, V. Barone, B. Mennucci, G.A. Petersson, H. Nakatsuji, M. Caricato, X. Li, H.P. Hratchian, A.F. Izmaylov, J. Bloino, G. Zheng, J.L. Sonnenberg, M. Hada, M. Ehara, K. Toyota, R. Fukuda, J. Hasegawa, M. Ishida, T. Nakajima, Y. Honda, O. Kitao, H. Nakai, T. Vreven, J. J. A. Montgomery, J.E. Peralta, F. Ogliaro, M. Bearpark, E.B. J. J. Heyd, K.N. Kudin, V.N. Staroverov, R. Kobayashi, J. Normand, K. Raghavachari, A. Rendell, J.C. Burant, S.S. Iyengar, J. Tomasi, M. Cossi, N. Rega, J.M. Millam, M. Klene, J.E. Knox, J.B. Cross, V. Bakken, C. Adamo, J. Jaramillo, R. Gomperts, R.E. Stratmann, O. Yazyev, A.J. Austin, R. Cammi, C. Pomelli, J.W. Ochterski, R.L. Martin, K. Morokuma, V.G. Zakrzewski, G.A. Voth, P. Salvador, J.J. Dannenberg, S. Dapprich, A.D. Daniels, O. Farkas, J.B. Foresman, J.V. Ortiz, J. Cioslowski, D.J. Fox, Gaussian 09, Revision A.02, Gaussian, Inc., Wallingford CT, 2009.

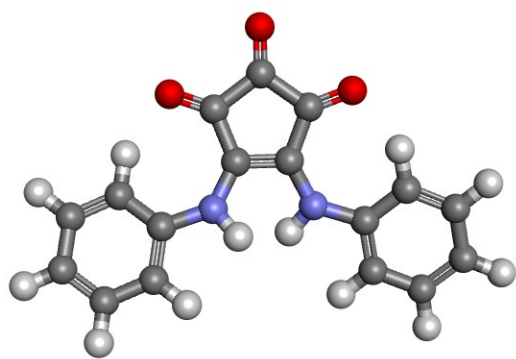
⁹ L.A. Curtiss, P.C. Redfern, K. Raghavachari, *Journal of Chemical Physics*, 2007, 127, 124105.

¹⁰ L. A. Curtiss, P. C. Redfern, and K. Raghavachari, *Gaussian-4 Theory*, *Journal of Chemical Physics*, 2007, 126, 084108.

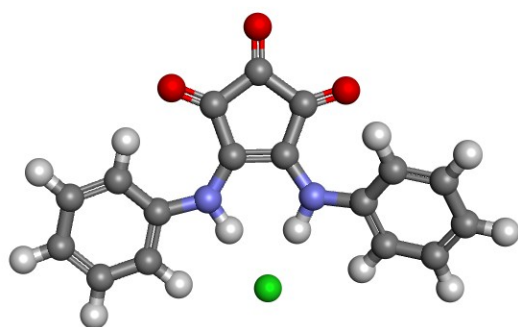
Table 7 Total energies (Hartrees)

Complex	Energy (kcal/mol) (B3LYP)/MidiX + ZPE	Energy (kcal/mol) (G4MP2)
Cl ⁻	-458,05431	-459.837448
Br ⁻	-2562,04968	-2572.976072
I ⁻	-6890,20560	
Croconamide	-984,1917469	-988.821587
Squaramide	-871,52159	
Thiourea	-1004,835813	
Complex		
Croconamide·Cl ⁻	-1442,354764	-1448.738813
Croconamide·Br ⁻	-3546,332309	-3561.868244
Croconamide·I ⁻	-7874,459476	
Squaramide·Cl ⁻	-1329,68750	
Squaramide·Br ⁻	-3433,66596	
Squaramide·I ⁻	-7761,79372	
Thiourea·Cl ⁻	-1462,992120	
Thiourea·Br ⁻	-3566,971794	
Thiourea·I ⁻	-7895,102736	

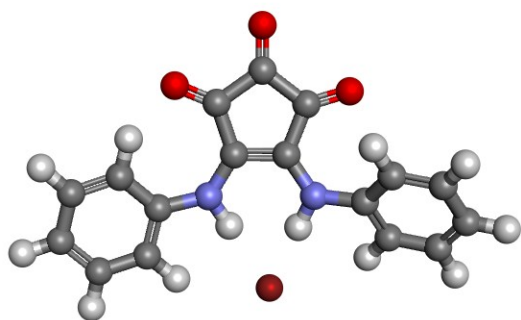
B3LYP/MidiX coordinates are shown in the tables below with the structure of each complex:



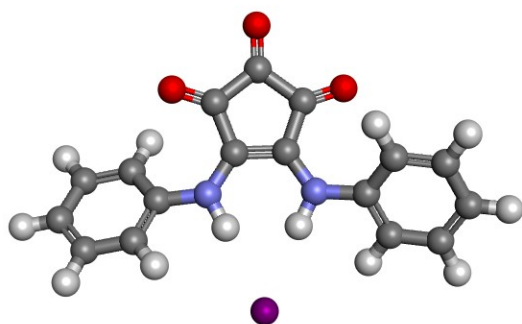
Croconamide	x	y	z
C	-10.2615	1.347115	2.259566
C	-9.66119	0.546083	1.161822
C	-9.31377	1.377677	0.070734
C	-9.4158	2.810046	0.451714
C	-10.067	2.805272	1.836846
O	-10.3748	3.78472	2.485396
O	-9.1087	3.827922	-0.16178
O	-10.7795	0.999362	3.316696
N	-8.94949	0.77507	-1.10821
N	-9.41235	-0.7999	1.050847
C	-8.35142	1.229097	-2.30948
C	-9.79502	-1.94274	1.7954
C	-8.20807	0.273106	-3.33121
C	-7.60038	0.614471	-4.53426
C	-7.12213	1.911014	-4.73671
C	-7.2707	2.858842	-3.72304
C	-7.88119	2.532282	-2.51345
C	-9.25179	-3.16934	1.372603
C	-9.59628	-4.35154	2.018265
C	-10.4901	-4.33128	3.091317
C	-11.0232	-3.11194	3.512005
C	-10.6841	-1.9185	2.877052
H	-9.35721	-0.16403	-1.20504
H	-8.64574	-0.99916	0.395019
H	-8.57414	-0.74181	-3.17673
H	-7.49893	-0.13598	-5.31507
H	-6.64479	2.179173	-5.6759
H	-6.91424	3.875605	-3.87291
H	-8.04624	3.274587	-1.74097
H	-8.55832	-3.19204	0.532063
H	-9.16594	-5.29158	1.680245
H	-10.7623	-5.2549	3.595984
H	-11.7103	-3.08079	4.354776
H	-11.0533	-0.96209	3.229113



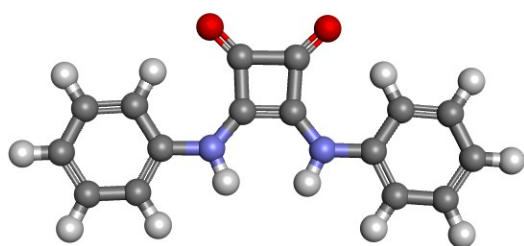
Croconamide·Cl ⁻	x	y	z
C	-11.6296	-3.55693	8.148214
C	-11.1773	-4.48012	7.070092
C	-11.6343	-3.96864	5.809693
C	-12.5661	-2.83476	6.011188
C	-12.5489	-2.54076	7.492009
O	-13.1792	-1.67192	8.079796
O	-13.232	-2.23769	5.160915
O	-11.3616	-3.51609	9.354719
N	-11.3214	-4.529	4.616585
N	-10.4625	-5.63849	7.139894
C	-11.4726	-4.01549	3.313202
C	-9.80196	-6.31555	8.188928
C	-11.4684	-4.97046	2.27475
C	-11.5528	-4.56763	0.946821
C	-11.6393	-3.2116	0.620057
C	-11.6167	-2.26407	1.645808
C	-11.5204	-2.65016	2.980507
C	-9.24008	-7.56491	7.839441
C	-8.54175	-8.30702	8.783575
C	-8.38354	-7.83436	10.09004
C	-8.94282	-6.60263	10.43415
C	-9.64575	-5.842	9.501554
H	-10.9561	-5.52845	4.600802
H	-10.4168	-6.21365	6.253037
H	-11.3623	-6.0188	2.547501
H	-11.5485	-5.32135	0.160875
H	-11.7127	-2.89678	-0.4194
H	-11.6675	-1.20282	1.406901
H	-11.5059	-1.90171	3.75957
H	-9.37309	-7.91997	6.818932
H	-8.11673	-9.26686	8.493312
H	-7.83551	-8.41908	10.82707
H	-8.83526	-6.22018	11.44862
H	-10.1071	-4.89645	9.763794
Cl	-10.3574	-7.36986	4.609175



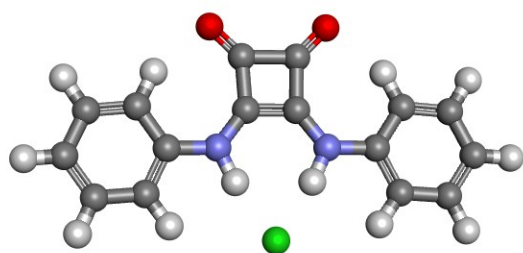
Croconamide·Br ⁻	x	y	z
C	-9.62737	0.990856	2.341379
C	-9.32808	0.261839	1.085577
C	-8.95912	1.167656	0.041625
C	-9.19142	2.560025	0.519335
C	-9.57104	2.458498	1.989382
O	-9.75456	3.407586	2.738881
O	-9.14082	3.646358	-0.06801
O	-9.87399	0.512541	3.450246
N	-8.47144	0.705505	-1.14728
N	-9.3063	-1.08702	0.967417
C	-8.17306	1.325195	-2.38193
C	-9.90547	-2.04125	1.817197
C	-7.61768	0.483815	-3.37123
C	-7.31616	0.986757	-4.63103
C	-7.55558	2.328521	-4.94134
C	-8.09974	3.159658	-3.96101
C	-8.41019	2.674093	-2.69219
C	-9.31242	-3.31699	1.858129
C	-9.88092	-4.33126	2.622568
C	-11.0451	-4.09787	3.358271
C	-11.6476	-2.83864	3.298449
C	-11.0978	-1.81898	2.526695
H	-8.20688	-0.31261	-1.16805
H	-8.72024	-1.53341	0.203228
H	-7.42822	-0.55959	-3.12141
H	-6.88777	0.319642	-5.37767
H	-7.31832	2.718946	-5.92956
H	-8.28728	4.210206	-4.18018
H	-8.80384	3.319624	-1.9152
H	-8.42157	-3.48942	1.257442
H	-9.40795	-5.31179	2.642392
H	-11.4846	-4.88945	3.962511
H	-12.565	-2.64722	3.852788
H	-11.5867	-0.85504	2.474679
Br	-7.43384	-2.46694	-1.25315



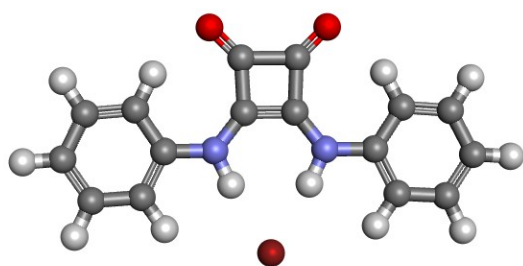
Croconamide-I ⁻	x	y	z
C	-9.59667	0.941631	2.350143
C	-9.25516	0.232204	1.092816
C	-8.90352	1.148451	0.058734
C	-9.13476	2.536076	0.554143
C	-9.53721	2.415323	2.01871
O	-9.73041	3.354495	2.776542
O	-9.07649	3.629418	-0.01673
O	-9.87229	0.443156	3.441254
N	-8.42252	0.703298	-1.14172
N	-9.20209	-1.11894	0.98544
C	-8.17217	1.33268	-2.38382
C	-9.8644	-2.0536	1.814051
C	-7.63548	0.510857	-3.3976
C	-7.38936	1.028588	-4.66373
C	-7.66687	2.366905	-4.95442
C	-8.19	3.180256	-3.94822
C	-8.44463	2.679008	-2.67332
C	-9.25903	-3.30674	2.005677
C	-9.90221	-4.28669	2.757383
C	-11.1501	-4.03579	3.331339
C	-11.7601	-2.79554	3.124781
C	-11.1347	-1.81386	2.362751
H	-8.15471	-0.30379	-1.16968
H	-8.56146	-1.56454	0.279275
H	-7.40609	-0.52909	-3.17018
H	-6.97344	0.375257	-5.42889
H	-7.47329	2.768852	-5.94734
H	-8.40442	4.228736	-4.1511
H	-8.81679	3.313706	-1.87752
H	-8.29644	-3.49817	1.537127
H	-9.42038	-5.25303	2.894943
H	-11.6478	-4.80036	3.924856
H	-12.7399	-2.59203	3.553383
H	-11.6283	-0.86589	2.184598
I	-7.0147	-2.731	-1.25473



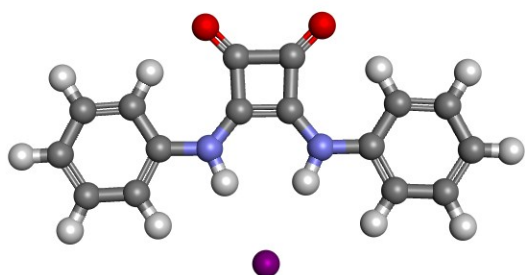
Squaramide	x	y	z
C	4.248816	17.33562	-17.8012
C	5.352078	16.76463	-16.9301
C	4.935231	17.49054	-15.7978
C	3.784962	18.14365	-16.5411
O	2.897342	18.93495	-16.2921
O	3.876682	17.22866	-18.9528
N	5.464047	17.50713	-14.5487
N	6.387962	15.89814	-17.0583
C	5.056388	18.23015	-13.4042
C	6.817112	15.16333	-18.1873
C	5.79609	18.05513	-12.2238
C	5.439953	18.74166	-11.0668
C	4.345619	19.60855	-11.0716
C	3.613403	19.77876	-12.2486
C	3.956406	19.09921	-13.4154
C	7.935953	14.32875	-18.0362
C	8.402406	13.58219	-19.1141
C	7.761783	13.65763	-20.3522
C	6.649251	14.48952	-20.4967
C	6.169438	15.24349	-19.428
H	6.283979	16.91167	-14.3899
H	6.958454	15.73838	-16.221
H	6.651164	17.37954	-12.2151
H	6.021052	18.59751	-10.1586
H	4.06716	20.14501	-10.1679
H	2.758642	20.45149	-12.2649
H	3.384798	19.23327	-14.3308
H	8.439435	14.26645	-17.0717
H	9.270236	12.93926	-18.9843
H	8.125921	13.07454	-21.1944
H	6.141599	14.5568	-21.4565
H	5.30302	15.89061	-19.5429



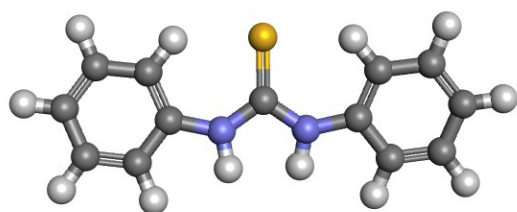
Squaramide·Cl ⁻	x	y	z
C	4.209341	17.3158	-17.7621
C	5.32503	16.74721	-16.9223
C	4.915094	17.47525	-15.7695
C	3.759909	18.1133	-16.5001
O	2.860713	18.90422	-16.2399
O	3.813876	17.21276	-18.9176
N	5.472988	17.47759	-14.5427
N	6.363193	15.89671	-17.0458
C	5.080428	18.18735	-13.4031
C	6.776433	15.17597	-18.1711
C	5.855732	17.99776	-12.2407
C	5.528348	18.66859	-11.0679
C	4.43167	19.53584	-11.0252
C	3.666081	19.72069	-12.1798
C	3.976573	19.0584	-13.3654
C	7.909384	14.35132	-18.0141
C	8.380941	13.60385	-19.0872
C	7.741666	13.65926	-20.3301
C	6.619047	14.478	-20.481
C	6.129953	15.23522	-19.4189
H	6.331469	16.85485	-14.4181
H	6.953942	15.74949	-16.1684
H	6.705736	17.31925	-12.2915
H	6.135845	18.51283	-10.1773
H	4.178307	20.05949	-10.105
H	2.809136	20.39325	-12.161
H	3.382766	19.19968	-14.2672
H	8.394799	14.32007	-17.04
H	9.25714	12.971	-18.9519
H	8.113797	13.07249	-21.1682
H	6.111219	14.53087	-21.4435
H	5.255614	15.87433	-19.5323
Cl	7.87229	15.64932	-14.4434



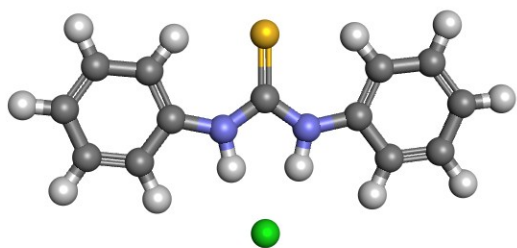
Squaramide·Br ⁻	x	y	z
C	4.220017	17.31568	-17.7608
C	5.334217	16.7447	-16.9182
C	4.922276	17.47183	-15.7671
C	3.768739	18.11115	-16.5005
O	2.869015	18.90202	-16.2447
O	3.825547	17.21554	-18.9161
N	5.472434	17.47702	-14.536
N	6.3713	15.89239	-17.0461
C	5.072291	18.19136	-13.3979
C	6.782413	15.17233	-18.1766
C	5.837278	18.00884	-12.2283
C	5.497739	18.68567	-11.0623
C	4.39958	19.55121	-11.0343
C	3.644443	19.72868	-12.1965
C	3.967203	19.06029	-13.3756
C	7.912753	14.34346	-18.0289
C	8.37643	13.60048	-19.1087
C	7.731672	13.66507	-20.3481
C	6.611468	14.48832	-20.4892
C	6.130211	15.2412	-19.4202
H	6.32478	16.86171	-14.3992
H	6.962298	15.73764	-16.1798
H	6.689197	17.33136	-12.2672
H	6.097639	18.53525	-10.1658
H	4.136957	20.07935	-10.1193
H	2.78627	20.39972	-12.1898
H	3.380423	19.19684	-14.2825
H	8.403079	14.30465	-17.0571
H	9.250957	12.96412	-18.9805
H	8.097816	13.08175	-21.1911
H	6.09894	14.54875	-21.4486
H	5.257619	15.88333	-19.5276
Br	8.085459	15.53032	-14.2874



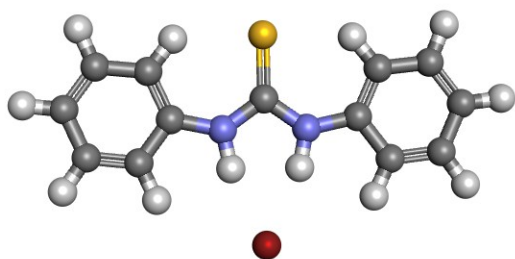
Squaramide·I ⁻	x	y	z
C	4.242246	17.30733	-17.7446
C	5.35754	16.73326	-16.9023
C	4.946749	17.46169	-15.7519
C	3.792941	18.10132	-16.4885
O	2.892009	18.8916	-16.2399
O	3.843394	17.21263	-18.8979
N	5.486121	17.47969	-14.5143
N	6.389587	15.8746	-17.0468
C	5.06942	18.20273	-13.3823
C	6.787721	15.16065	-18.1913
C	5.817681	18.03605	-12.201
C	5.457786	18.72308	-11.0467
C	4.355514	19.58277	-11.043
C	3.61661	19.7442	-12.2174
C	3.960247	19.0654	-13.3847
C	7.912675	14.32261	-18.0676
C	8.357977	13.58963	-19.1624
C	7.699348	13.67413	-20.3925
C	6.583922	14.50683	-20.5096
C	6.121442	15.2496	-19.4252
H	6.333248	16.87958	-14.3612
H	6.983564	15.70467	-16.1988
H	6.674078	17.36356	-12.2129
H	6.046039	18.58374	-10.141
H	4.077135	20.11864	-10.1374
H	2.754918	20.41035	-12.2309
H	3.384265	19.19149	-14.2994
H	8.41931	14.26294	-17.1055
H	9.229178	12.946	-19.0512
H	8.051086	13.09879	-21.247
H	6.059636	14.58348	-21.4613
H	5.25206	15.89777	-19.5168
I	8.363013	15.36122	-14.0788



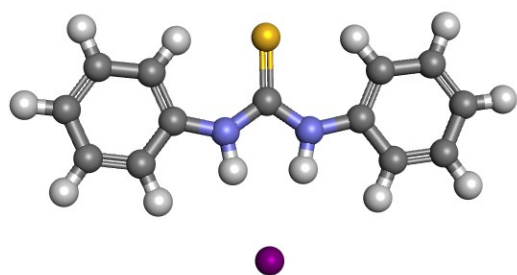
Thiourea	x	y	z
C	-4.96657	13.99937	4.434524
N	-5.25657	14.86482	5.471668
N	-4.95624	12.69689	4.895165
C	-5.49229	16.2599	5.52592
C	-4.61681	11.46274	4.289678
C	-5.50448	17.11899	4.417541
C	-5.76611	18.47612	4.600125
C	-6.01373	19.00114	5.868087
C	-5.99806	18.14651	6.972971
C	-5.7411	16.79114	6.805316
C	-4.15196	11.3107	2.975349
C	-3.83478	10.03941	2.499099
C	-3.97386	8.909477	3.304462
C	-4.44039	9.059917	4.61256
C	-4.75801	10.32149	5.101182
S	-4.66987	14.46322	2.844651
H	-5.2837	14.43955	6.403946
H	-5.28233	12.56914	5.858532
H	-5.29602	16.69656	3.445467
H	-5.77167	19.12892	3.729856
H	-6.21465	20.06189	5.997096
H	-6.18759	18.53601	7.97085
H	-5.73346	16.13124	7.673152
H	-4.06477	12.19567	2.362117
H	-3.47568	9.938815	1.477108
H	-3.72475	7.923304	2.92026
H	-4.55719	8.191261	5.256912
H	-5.119	10.42956	6.124251



Thiourea·Cl ⁻	x	y	z
C	-4.93631	14.02431	4.401669
N	-5.23018	14.88119	5.43591
N	-4.81335	12.74958	4.901775
C	-5.45563	16.25995	5.487801
C	-4.52641	11.52051	4.30052
C	-5.42774	17.14703	4.395967
C	-5.6727	18.50461	4.596495
C	-5.94798	19.01169	5.867123
C	-5.97634	18.13139	6.954626
C	-5.73481	16.77589	6.774129
C	-4.28015	11.30344	2.932297
C	-4.00567	10.01707	2.470619
C	-3.96865	8.926938	3.341043
C	-4.21333	9.140276	4.702299
C	-4.48844	10.41462	5.180478
S	-4.7542	14.46975	2.766135
H	-5.301	14.40471	6.384113
H	-4.96465	12.68189	5.952385
H	-5.21184	16.72735	3.422596
H	-5.64635	19.17465	3.737547
H	-6.13758	20.07416	6.011336
H	-6.18933	18.50581	7.955202
H	-5.75537	16.08508	7.61559
H	-4.31521	12.16579	2.280127
H	-3.81773	9.870592	1.407292
H	-3.75304	7.926723	2.968644
H	-4.18949	8.303492	5.39939
H	-4.67967	10.58814	6.238318
Cl	-5.32246	13.07898	7.871905

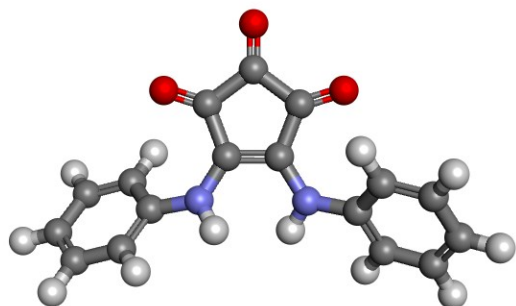


Thiourea·Br ⁻	x	y	z
C	-4.94877	14.01954	4.395624
N	-5.18934	14.89419	5.428195
N	-4.83779	12.7462	4.900966
C	-5.38106	16.28113	5.474139
C	-4.59935	11.50282	4.301274
C	-5.36696	17.15401	4.371533
C	-5.57324	18.51934	4.564122
C	-5.79556	19.04604	5.836911
C	-5.80987	18.17882	6.934992
C	-5.60634	16.81608	6.762643
C	-4.4049	11.27187	2.927702
C	-4.17598	9.976043	2.467067
C	-4.13468	8.891935	3.344474
C	-4.32797	9.120117	4.711452
C	-4.55725	10.4038	5.188712
S	-4.8103	14.44553	2.752391
H	-5.24182	14.43926	6.380501
H	-4.9539	12.68254	5.949333
H	-5.19251	16.71972	3.39647
H	-5.55859	19.17912	3.697141
H	-5.95541	20.11419	5.97472
H	-5.98158	18.56853	7.937499
H	-5.61575	16.13346	7.611733
H	-4.44184	12.1295	2.269751
H	-4.02768	9.817825	1.399284
H	-3.95508	7.884428	2.972781
H	-4.2998	8.288364	5.414142
H	-4.7088	10.59087	6.251282
Br	-5.2635	13.05034	8.136499

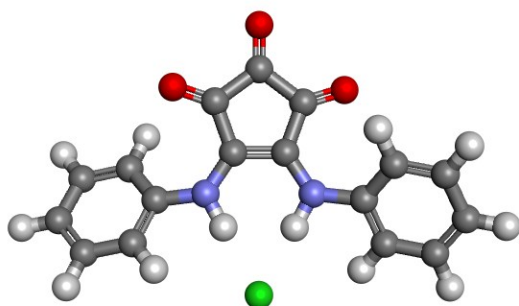


Thiourea·I ⁻	x	y	z
C	-4.98221	14.01296	4.406918
N	-5.20683	14.89142	5.441035
N	-4.78693	12.74729	4.908527
C	-5.45784	16.274	5.478061
C	-4.52345	11.51042	4.294965
C	-5.53979	17.1239	4.361406
C	-5.79567	18.48277	4.539742
C	-5.97416	19.02478	5.812572
C	-5.89289	18.18021	6.924525
C	-5.63873	16.82395	6.765915
C	-4.39521	11.29039	2.912536
C	-4.13228	10.00733	2.434593
C	-3.992	8.925649	3.304078
C	-4.11939	9.143192	4.679877
C	-4.38123	10.41459	5.174003
S	-4.95134	14.42872	2.757843
H	-5.19035	14.4609	6.395306
H	-4.84026	12.67458	5.951695
H	-5.39781	16.6803	3.385856
H	-5.85522	19.12408	3.661147
H	-6.17347	20.08746	5.939751
H	-6.02881	18.58087	7.927896
H	-5.57518	16.16489	7.631046
H	-4.50796	12.14434	2.259305
H	-4.03657	9.858393	1.359693
H	-3.78675	7.928075	2.919501
H	-4.01384	8.313951	5.377717
H	-4.48071	10.58557	6.245317
I	-5.05875	12.98066	8.502506

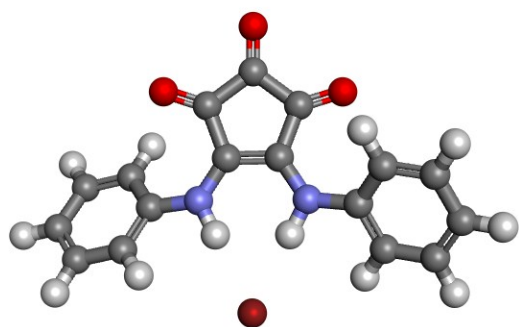
G4MP2 coordinates for the complexes with structures are shown in the tables below:



Croconamide	x	y	z
C	-9.96418	1.120514	2.168554
C	-9.53371	0.313496	1.010483
C	-9.2918	1.125027	-0.10113
C	-9.56252	2.541589	0.211475
C	-9.99402	2.562794	1.673997
O	-10.2998	3.53271	2.31554
O	-9.52334	3.494169	-0.53651
O	-10.1864	0.747697	3.299948
N	-8.94802	0.60544	-1.31239
N	-9.29114	-1.02668	0.991592
C	-8.38272	1.229014	-2.44625
C	-9.73108	-2.04669	1.863439
C	-8.65712	0.674478	-3.70049
C	-8.07775	1.21116	-4.84412
C	-7.22482	2.307692	-4.74903
C	-6.94936	2.853418	-3.49686
C	-7.51145	2.316797	-2.34463
C	-8.92386	-3.18044	2.000963
C	-9.33772	-4.24083	2.798377
C	-10.556	-4.17887	3.469774
C	-11.36	-3.04997	3.325292
C	-10.9635	-1.98927	2.519522
H	-9.25206	-0.3465	-1.4697
H	-8.59324	-1.32414	0.322383
H	-9.33552	-0.17056	-3.77733
H	-8.30132	0.772979	-5.81079
H	-6.77591	2.730469	-5.64066
H	-6.28059	3.702826	-3.40965
H	-7.2807	2.741995	-1.37817
H	-7.96562	-3.22258	1.490822
H	-8.70063	-5.11294	2.898363
H	-10.8781	-5.00313	4.095993
H	-12.3144	-2.99363	3.837361
H	-11.6015	-1.1242	2.406519



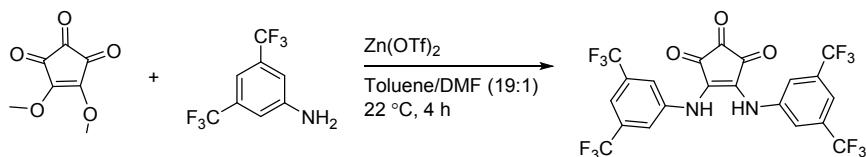
Croconamide·Cl ⁻	x	y	z
C	-9.86518	1.090197	2.128001
C	-9.54315	0.236616	0.969761
C	-9.26684	1.056445	-0.15725
C	-9.71588	2.433571	0.118091
C	-10.0412	2.487901	1.589642
O	-10.3791	3.466922	2.218928
O	-9.84791	3.352309	-0.67452
O	-9.9389	0.765256	3.302198
N	-8.78531	0.587114	-1.32498
N	-9.39935	-1.10318	0.974598
C	-8.24928	1.281443	-2.42613
C	-9.84528	-2.05723	1.908808
C	-8.24716	0.602426	-3.65432
C	-7.69039	1.193069	-4.78114
C	-7.12467	2.464604	-4.70785
C	-7.1081	3.128642	-3.48347
C	-7.65284	2.545873	-2.34458
C	-9.18486	-3.29554	1.903278
C	-9.59391	-4.31226	2.756185
C	-10.6655	-4.11869	3.625966
C	-11.3338	-2.89658	3.615331
C	-10.9419	-1.8727	2.759992
H	-8.70213	-0.44583	-1.43571
H	-8.97202	-1.5484	0.134794
H	-8.66817	-0.3959	-3.6975
H	-7.69954	0.651756	-5.72221
H	-6.6933	2.927264	-5.58976
H	-6.65698	4.113138	-3.40492
H	-7.62138	3.07329	-1.40348
H	-8.36721	-3.44571	1.207071
H	-9.06928	-5.26259	2.737421
H	-10.9821	-4.91236	4.29509
H	-12.1808	-2.73429	4.274961
H	-11.4789	-0.93653	2.760899
Cl	-8.32568	-2.4802	-1.60427



Croconamide·Br ⁻	x	y	z
C	-9.8612	1.070229	2.118152
C	-9.53344	0.219145	0.959085
C	-9.26636	1.037942	-0.16798
C	-9.71239	2.416157	0.109121
C	-10.039	2.468982	1.581206
O	-10.3786	3.44645	2.210894
O	-9.84231	3.334787	-0.68277
O	-9.93603	0.742424	3.29068
N	-8.79441	0.575421	-1.3432
N	-9.37997	-1.12027	0.973442
C	-8.25946	1.284841	-2.43742
C	-9.83255	-2.06564	1.915938
C	-8.29916	0.646419	-3.68533
C	-7.74445	1.257833	-4.80241
C	-7.14189	2.50981	-4.6979
C	-7.08525	3.133455	-3.45352
C	-7.62667	2.528345	-2.32494
C	-9.14669	-3.28776	1.965198
C	-9.56498	-4.29086	2.830183
C	-10.6693	-4.09696	3.657409
C	-11.3617	-2.88993	3.592444
C	-10.9609	-1.88128	2.723596
H	-8.71921	-0.4507	-1.46626
H	-8.94402	-1.56797	0.146858
H	-8.751	-0.33663	-3.75535
H	-7.78476	0.747917	-5.75989
H	-6.7124	2.98864	-5.57201
H	-6.60496	4.10175	-3.35155
H	-7.56099	3.020902	-1.36643
H	-8.30102	-3.43954	1.303947
H	-9.02137	-5.23018	2.854005
H	-10.993	-4.8797	4.335921
H	-12.234	-2.72869	4.218367
H	-11.5183	-0.95782	2.677348
Br	-8.25637	-2.66765	-1.72792

10. Synthetic procedures

4,5-Bis((3,5-bis(trifluoromethyl)phenyl)amino)cyclopent-4-ene-1,2,3-trione (**1a**)



Dimethylcroconate (500 mg, 2.94 mmol) and Zn(OTf)₂ (214 mg, 0.587 mmol) was suspended in toluene/DMF (19:1, 10 ml) and 3,5-bis(trifluoromethyl)aniline (1.35 g, 0.9 ml, 5.9 mmol) was added. The flask was fitted with a stopper and the reaction was stirred at room temperature for four hours. The reaction mixture was evaporated to dryness, redissolved in ethylacetate and evaporated on Celite (25 g) for purification using dry column vacuum chromatography. A column of 4 cm in diameter charged with 4 cm silica gel, a gradient of 2.5 % ethyl acetate in heptane was used. The gradient was held constant from 10 % ethyl acetate in heptane, and all fractions were 50 ml. Fraction 13 to 37 was evaporated, and the isolated material was recrystallised from dichloromethane to yield **1a** as an orange solid (503 mg, 30 %), decompose above 250°C. ¹H NMR (500 MHz, DMSO-*d*₆) δ 10.72 (s, 2H), 7.39 (s, 2H), 7.19 – 7.16 (m, 4H). ¹³C NMR (126 MHz, DMSO-*d*₆) δ 186.54, 181.27, 142.42, 139.12, 129.86 (q, *J* = 33.2 Hz), 122.77 (q, *J* = 273.0 Hz), 121.19, 116.12. ¹⁹F NMR (470 MHz, DMSO-*d*₆) δ -60.52. LC-HRMS: *m/z* = 563.0276 [M-H⁺] (Calculated 563.0271).

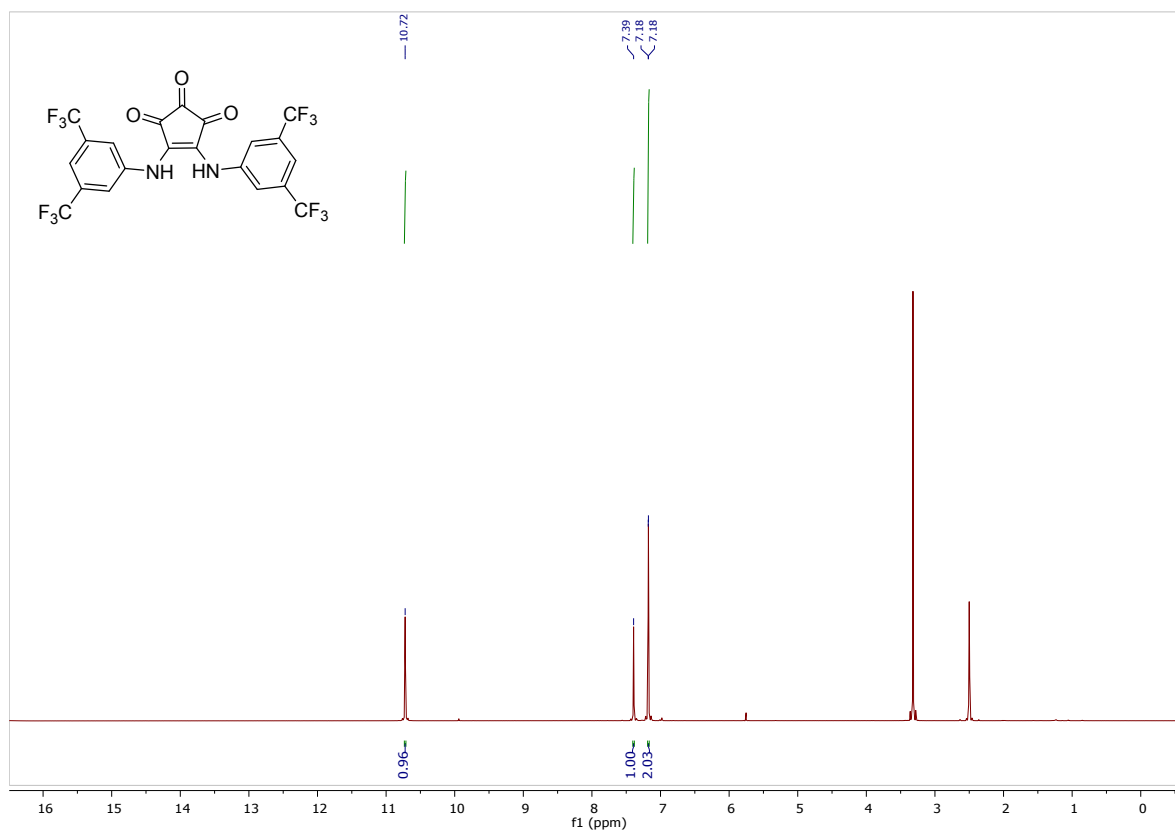


Figure 46 ¹H NMR of 1a (500 MHz, DMSO-*d*₆).

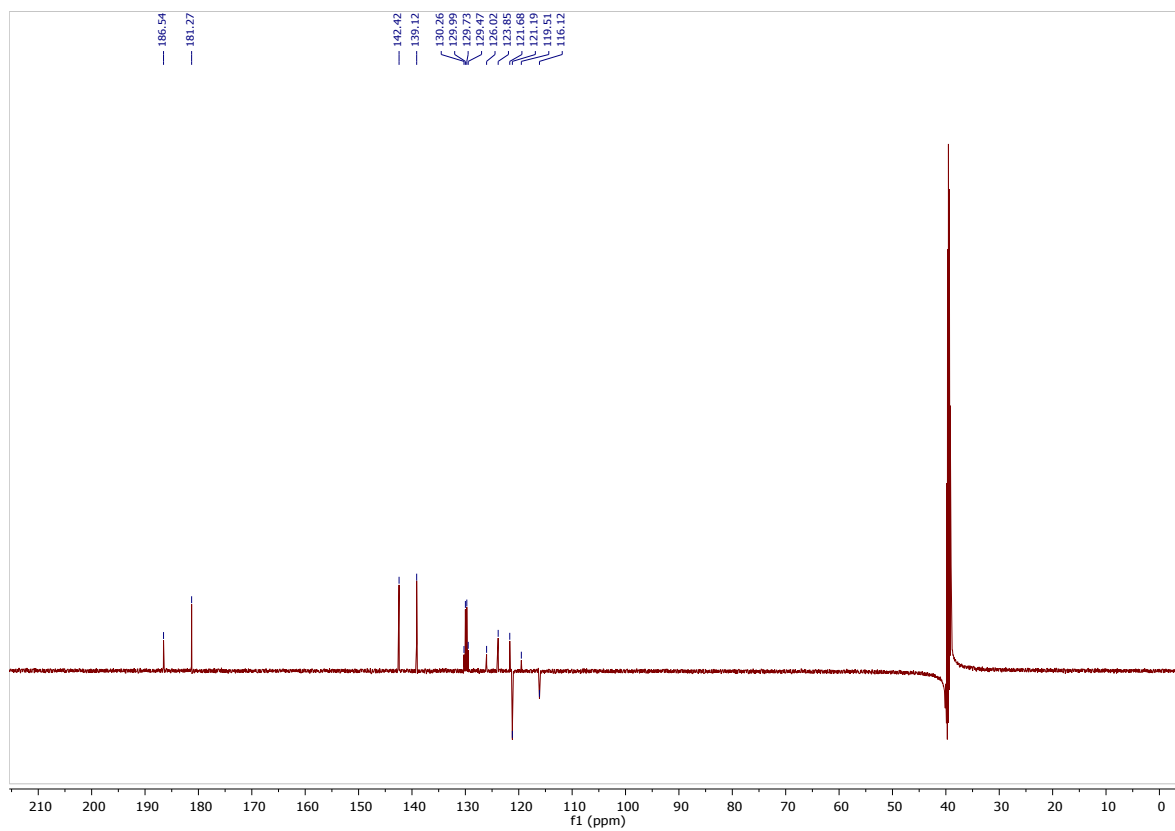


Figure 47 ¹³C NMR (APT) of 1a (126 MHz, DMSO-*d*₆).

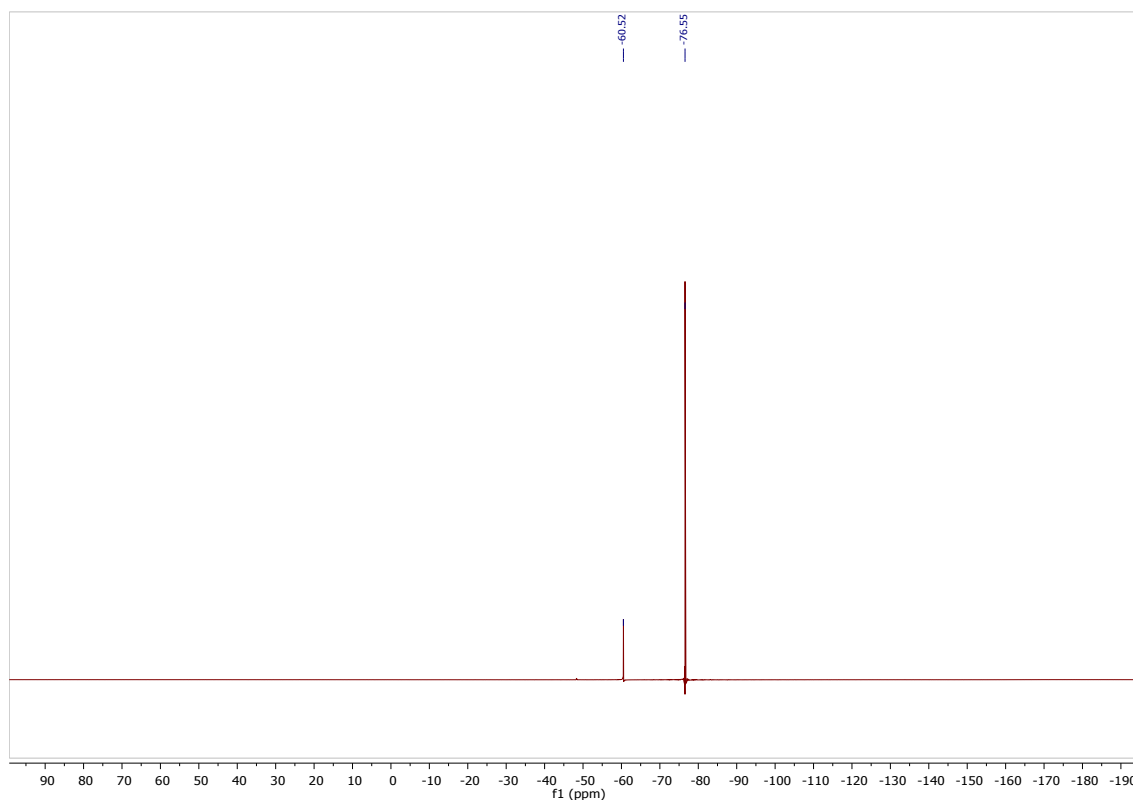
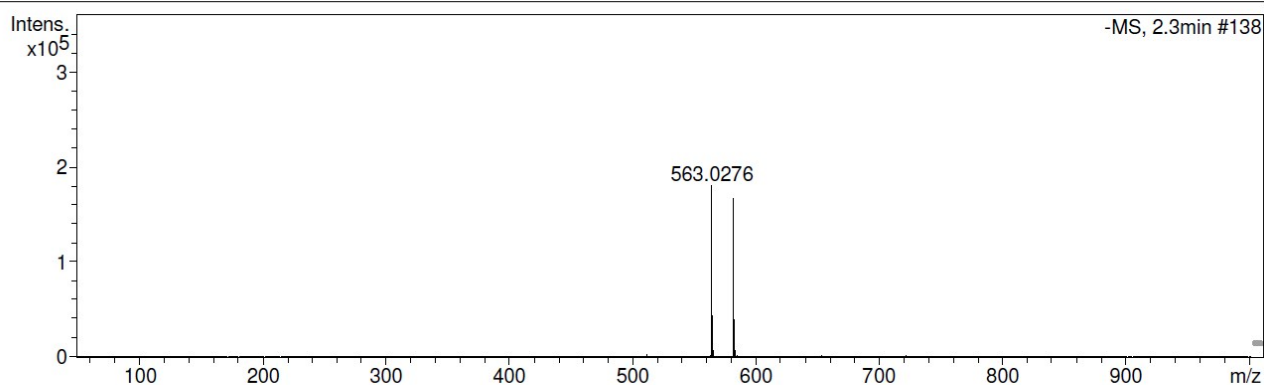


Figure 48 ^{19}F NMR of 1a (470 MHz, $\text{DMSO-}d_6$).

Acquisition Parameter

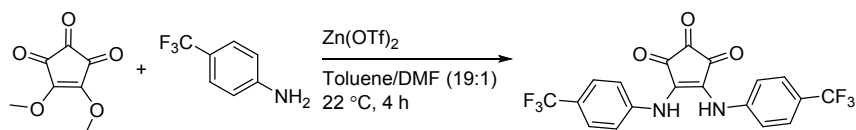
Source Type	ESI	Ion Polarity	Negative	Set Nebulizer	2.0 Bar
Focus	Not active	Set Capillary	3500 V	Set Dry Heater	240 °C
Scan Begin	50 m/z	Set End Plate Offset	-500 V	Set Dry Gas	10.0 l/min
Scan End	1000 m/z	Set Collision Cell RF	100.0 Vpp	Set Divert Valve	Waste



Meas. m/z	#	Formula	Score	m/z	err [mDa]	err [ppm]	mSigma	rdb	e ⁻ Conf	N-R ule
563.0276	1	C ₂₁ H ₇ F ₁₂ N ₂ O ₃	100.00	563.0271	-0.5	-0.9	3.5	13.5	even	ok

Figure 49 LC-HRMS (ESI) of 1a.

4,5-Bis((4-(trifluoromethyl)phenyl)amino)cyclopent-4-ene-1,2,3-trione (**1b**)



Dimethylcroconate (200 mg, 1.18 mmol) and $\text{Zn}(\text{OTf})_2$ (85 mg, 0.236 mmol) was suspended in toluene/DMF (19:1, 10 ml) and 4-(trifluoromethyl)aniline (400 mg, 2.5 mmol) was added. The flask was fitted with a stopper and the reaction was stirred at room temperature for four hours. The reaction mixture was evaporated to dryness, redissolved in ethylacetate and evaporated on Celite (20 g) for purification using dry column vacuum chromatography. A column of 4 cm in diameter charged with 4 cm silica gel, a gradient of 5 % ethyl acetate in heptane was used. Fraction 10 to 13 were evaporated, and the isolated material was recrystallised from chloroform to yield **1b** as an orange solid (85 mg, 17 %), decompose above 260 °C. ^1H NMR (500 MHz, $\text{DMSO}-d_6$) δ 10.43 (s, 2H), 7.27 (d, $J = 8.5$ Hz, 4H), 6.84 (d, $J = 8.5$ Hz, 4H). ^{13}C NMR (126 MHz, $\text{DMSO}-d_6$) δ 186.09, 180.93, 143.76, 141.14, 124.13 (q , $J = 271.2$), 124.88, 123.73 (q , $J = 32.2$), 121.77. ^{19}F NMR (470 MHz, $\text{DMSO}-d_6$) δ -59.04. LC-HRMS: $m/z = 427.0525$ [$\text{M}-\text{H}^+$] (Calculated 425.0523).

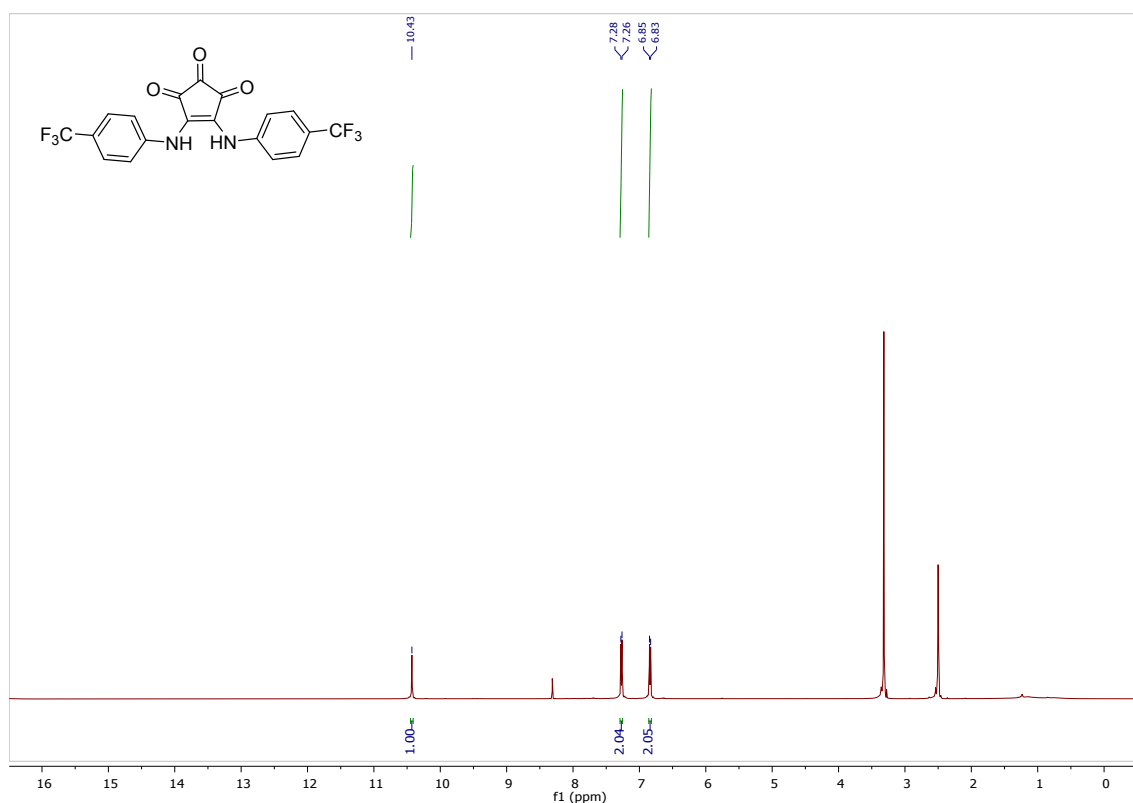


Figure 50 ^1H NMR of **1b** (500 MHz, $\text{DMSO}-d_6$).

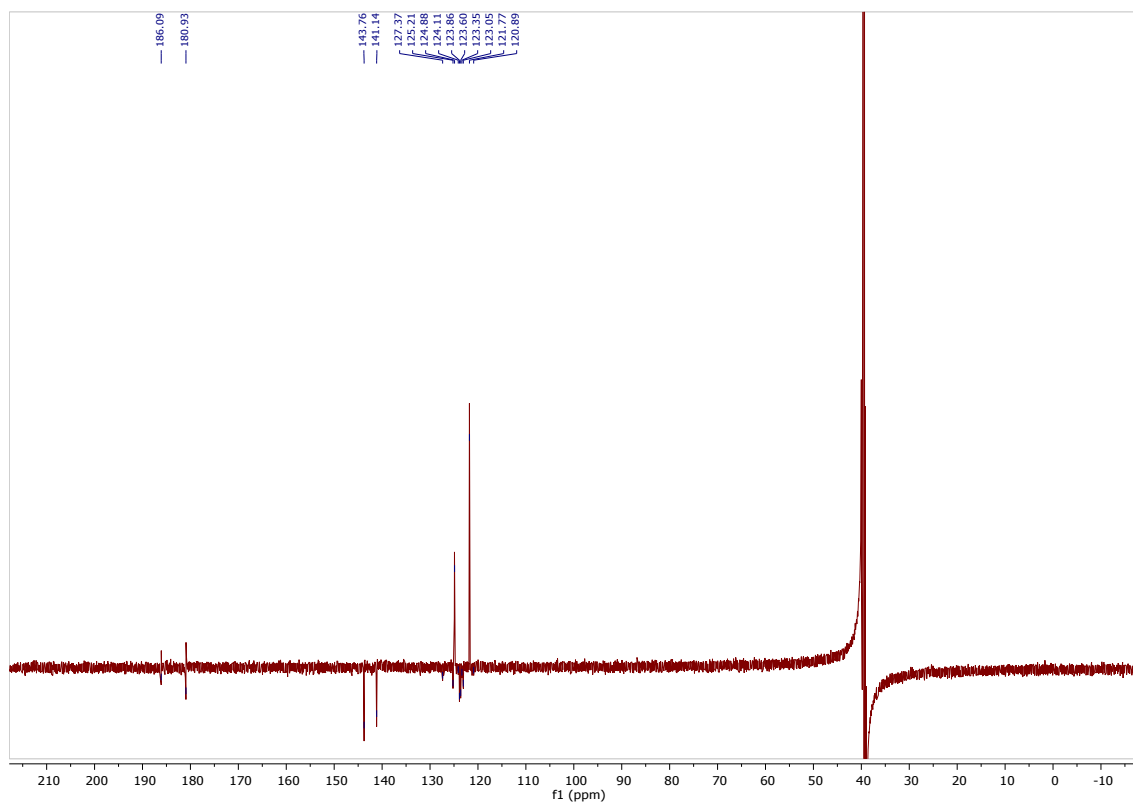


Figure 51 ^{13}C NMR (APT) of 1b (126 MHz, $\text{DMSO-}d_6$).

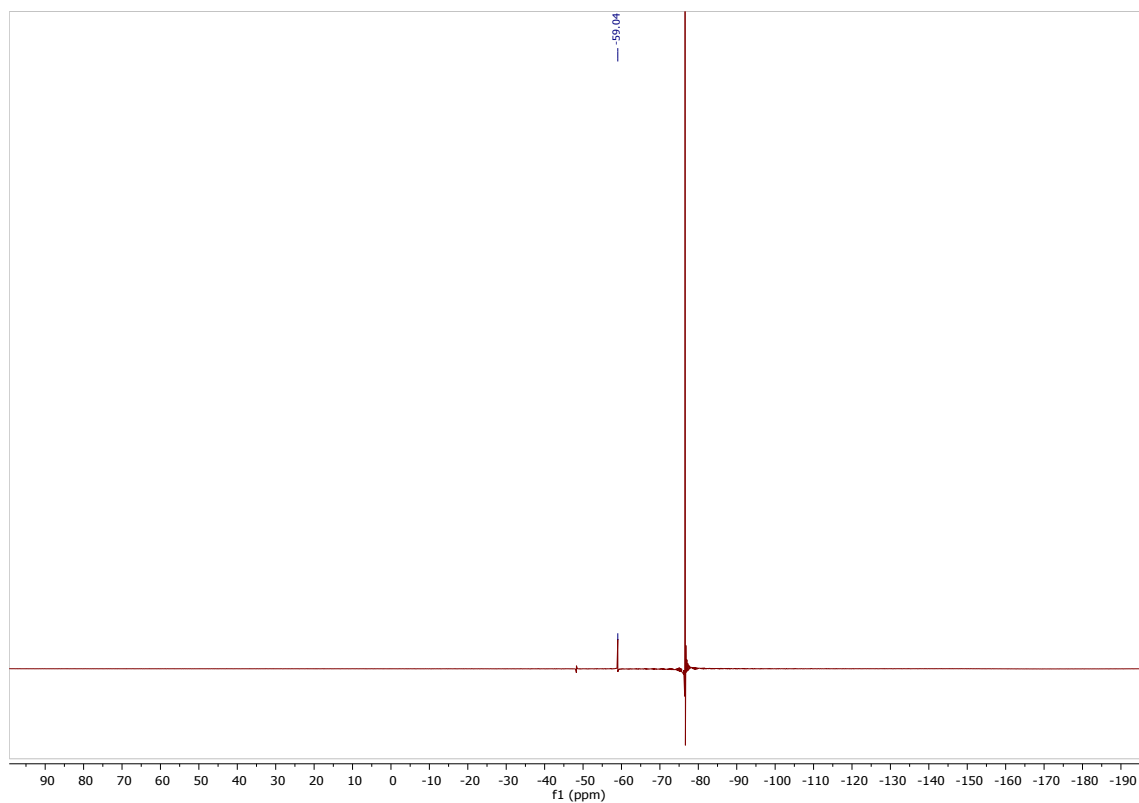


Figure 52 ^{19}F NMR of 1b (470 MHz, $\text{DMSO-}d_6$).

Acquisition Parameter

Source Type	ESI	Ion Polarity	Negative	Set Nebulizer	2.0 Bar
Focus	Not active	Set Capillary	3500 V	Set Dry Heater	240 °C
Scan Begin	50 m/z	Set End Plate Offset	-500 V	Set Dry Gas	10.0 l/min
Scan End	1000 m/z	Set Collision Cell RF	100.0 Vpp	Set Divert Valve	Waste

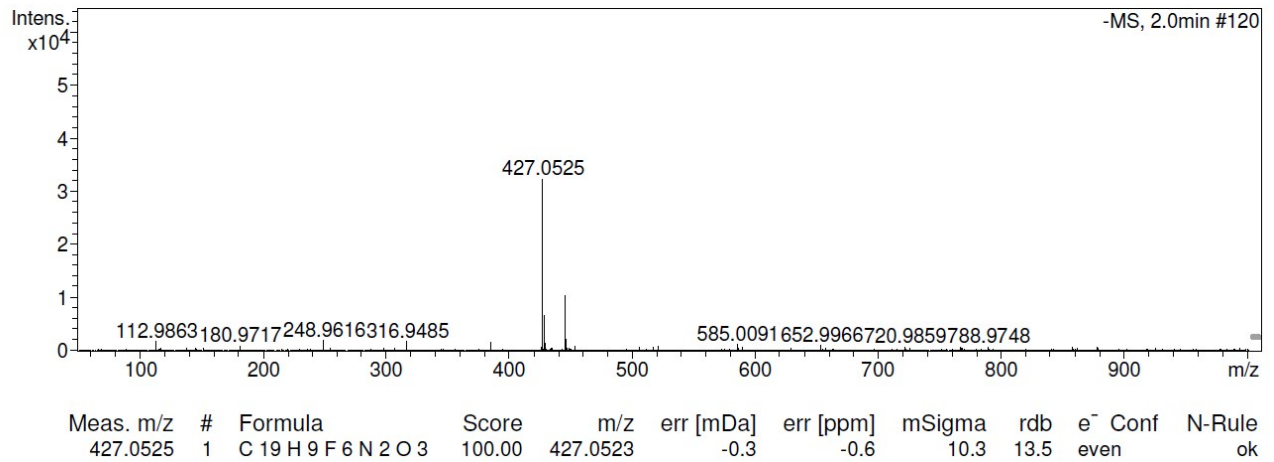
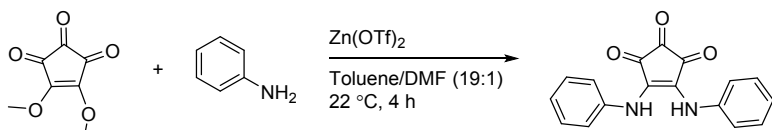


Figure 53 LC-HRMS (ESI) of 1b.

4,5-Bis(phenylamino)cyclopent-4-ene-1,2,3-trione (**1c**)



Dimethylcroconate (200 mg, 1.18 mmol) and $\text{Zn}(\text{OTf})_2$ (85 mg, 0.236 mmol) was suspended in toluene/DMF (19:1, 10 ml) and aniline (230 mg, 225 μl , 2.47 mmol) was added. The flask was fitted with a stopper and the reaction was stirred at room temperature for four hours. Hereafter, dichloromethane (20 ml) was added and the precipitate was centrifuged down and washed several times with ethyl acetate (7×40 ml) to yield **1c** as a dark red solid (194 mg, 56 %), decompose above 240°C. ^1H NMR (500 MHz, $\text{DMSO}-d_6$) δ 10.07 (s, 2H), 7.01 (t, $J = 7.8$ Hz, 2H), 6.88 (t, $J = 7.4$ Hz, 2H), 6.75 (d, $J = 7.6$ Hz, 4H). ^{13}C NMR (126 MHz, $\text{DMSO}-d_6$) δ 186.04, 180.20, 145.26, 137.51, 127.84, 124.07, 122.06. LC-HRMS: $m/z = 291.0778$ [$\text{M}-\text{H}^+$] (Calculated 291.0775).

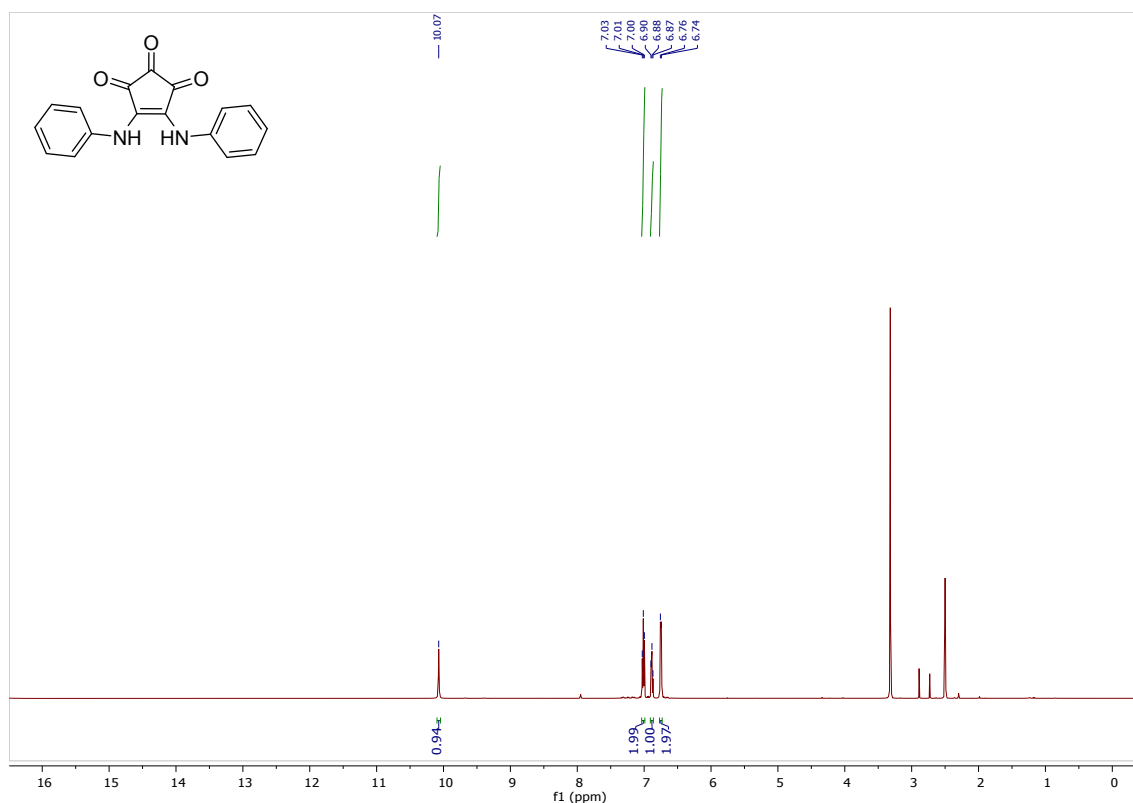


Figure 54 ^1H NMR of **1c** (500 MHz, $\text{DMSO}-d_6$).

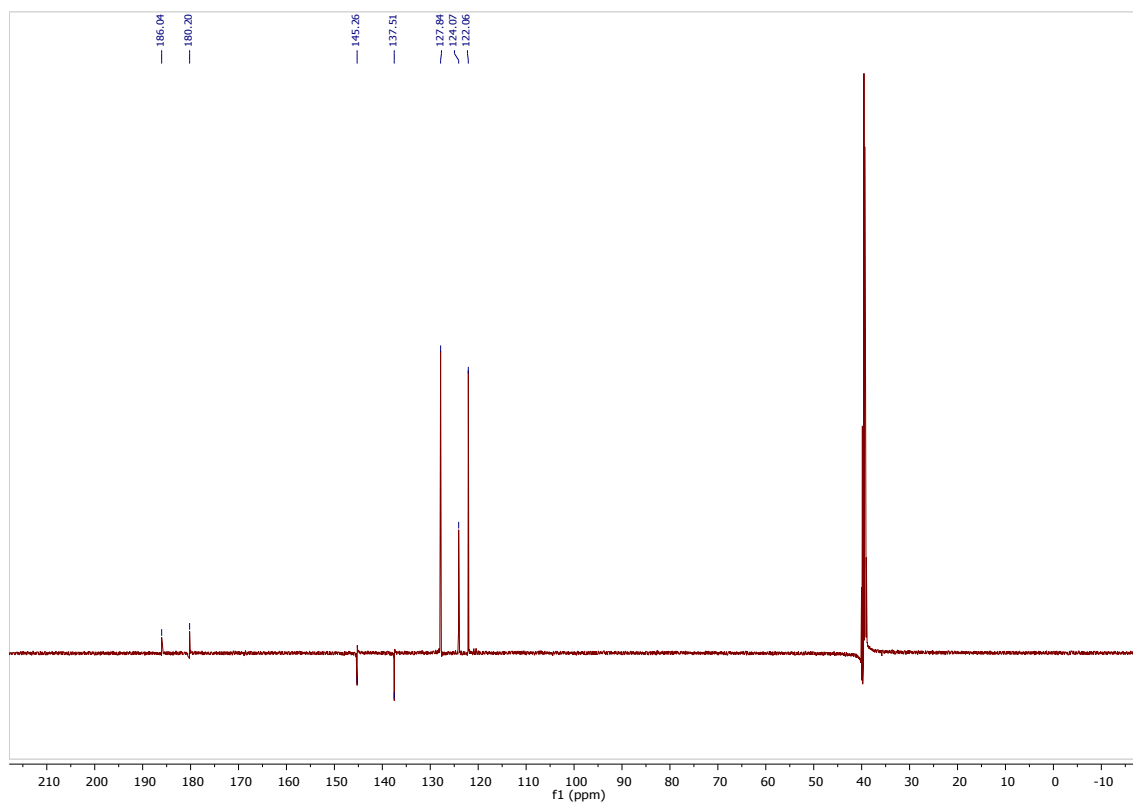
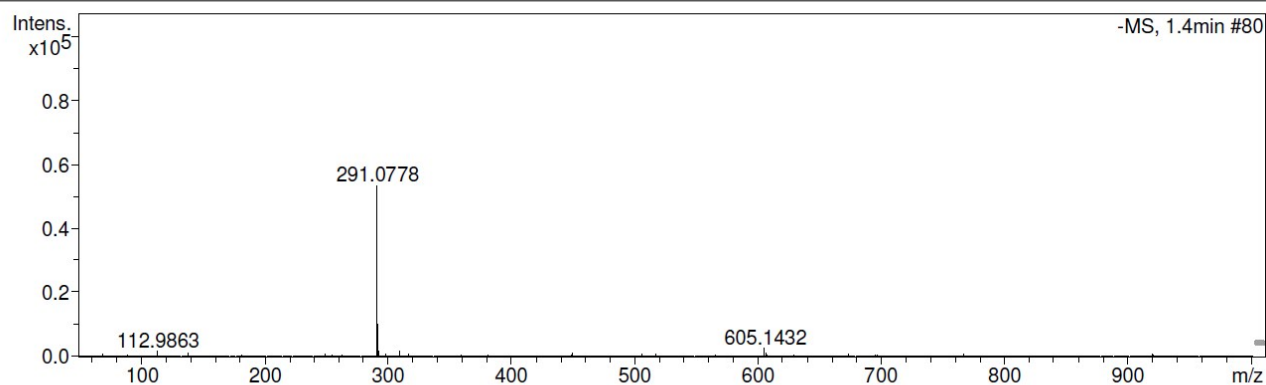


Figure 55 ^{13}C NMR (APT) of **1c** (126 MHz, $\text{DMSO-}d_6$).

Acquisition Parameter

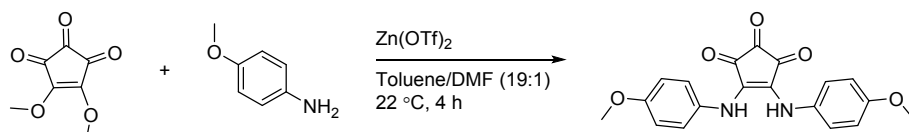
Source Type	ESI	Ion Polarity	Negative	Set Nebulizer	2.0 Bar
Focus	Not active	Set Capillary	3500 V	Set Dry Heater	240 °C
Scan Begin	50 m/z	Set End Plate Offset	-500 V	Set Dry Gas	10.0 l/min
Scan End	1000 m/z	Set Collision Cell RF	100.0 Vpp	Set Divert Valve	Waste



Meas. m/z	#	Formula	Score	m/z	err [mDa]	err [ppm]	mSigma	rdb	e ⁻	Conf	N-Rule
291.0778	1	C ₁₇ H ₁₁ N ₂ O ₃	100.00	291.0775	-0.3	-0.9	2.8	13.5	even		ok

Figure 56 LC-HRMS (ESI) of **1c**.

4,5-bis((4-methoxyphenyl)amino)cyclopent-4-ene-1,2,3-trione (**1d**)



Dimethylcroconate (200 mg, 1.18 mmol) and $\text{Zn}(\text{OTf})_2$ (85 mg, 0.236 mmol) was suspended in toluene/DMF (19:1, 10 ml) and *p*-anisidine (304 mg, 2.47 mmol) was added. The flask was fitted with a stopper and the reaction was stirred at room temperature for four hours. The mixture was evaporated to dryness, and the resulting crude was dissolved in methanol (30 ml) to which was added diethyl ether (50 ml). The precipitate was centrifuged down and washed several times with diethyl ether (4×15 ml) to yield compound **1d** (337 mg, 81 %) as a dark red solid, decompose above 250°C. ^1H NMR (500 MHz, $\text{DMSO}-d_6$) δ 9.94 (s, 2H), 6.69 (d, $J = 8.9$ Hz, 4H), 6.60 (d, $J = 8.9$ Hz, 4H), 3.67 (s, 6H). ^{13}C NMR (126 MHz, $\text{DMSO}-d_6$) δ 185.47, 179.99, 156.51, 145.72, 130.65, 123.80, 113.28, 55.32. LC-HRMS: $m/z = 351.0989$ [$\text{M}-\text{H}^+$] (Calculated 351.0986).

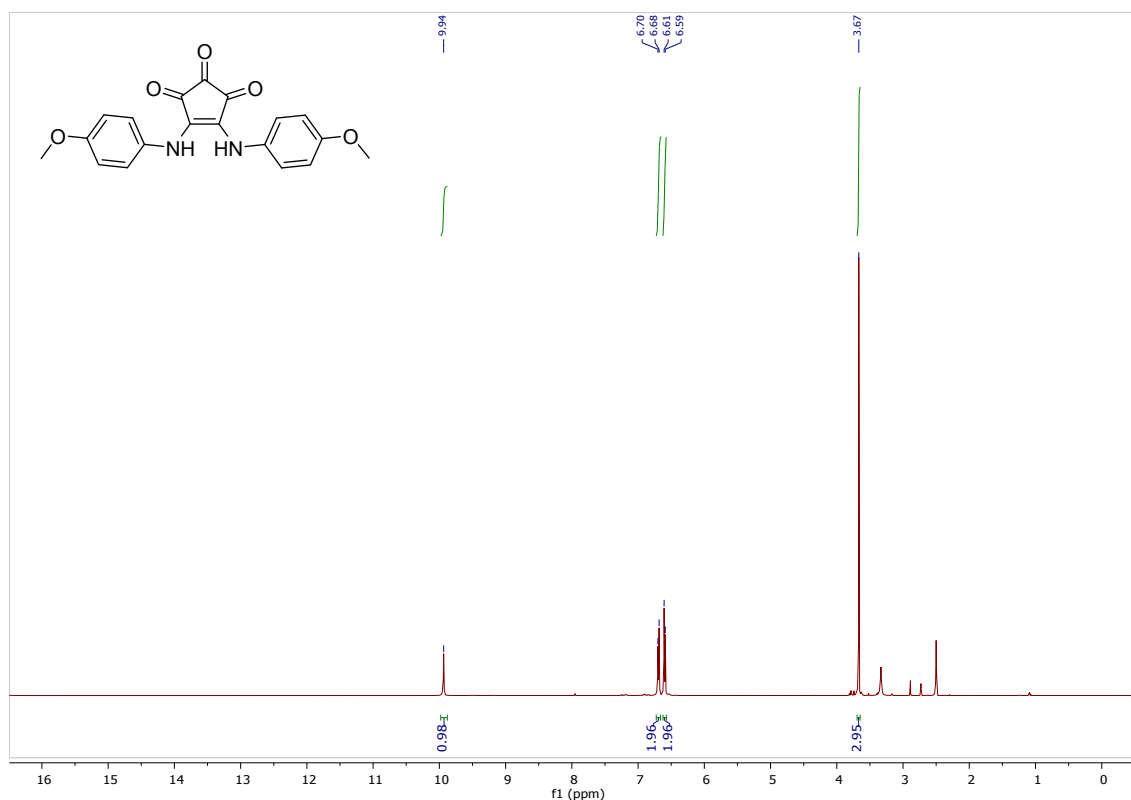


Figure 57 ^1H NMR of **1d** (500 MHz, $\text{DMSO}-d_6$).

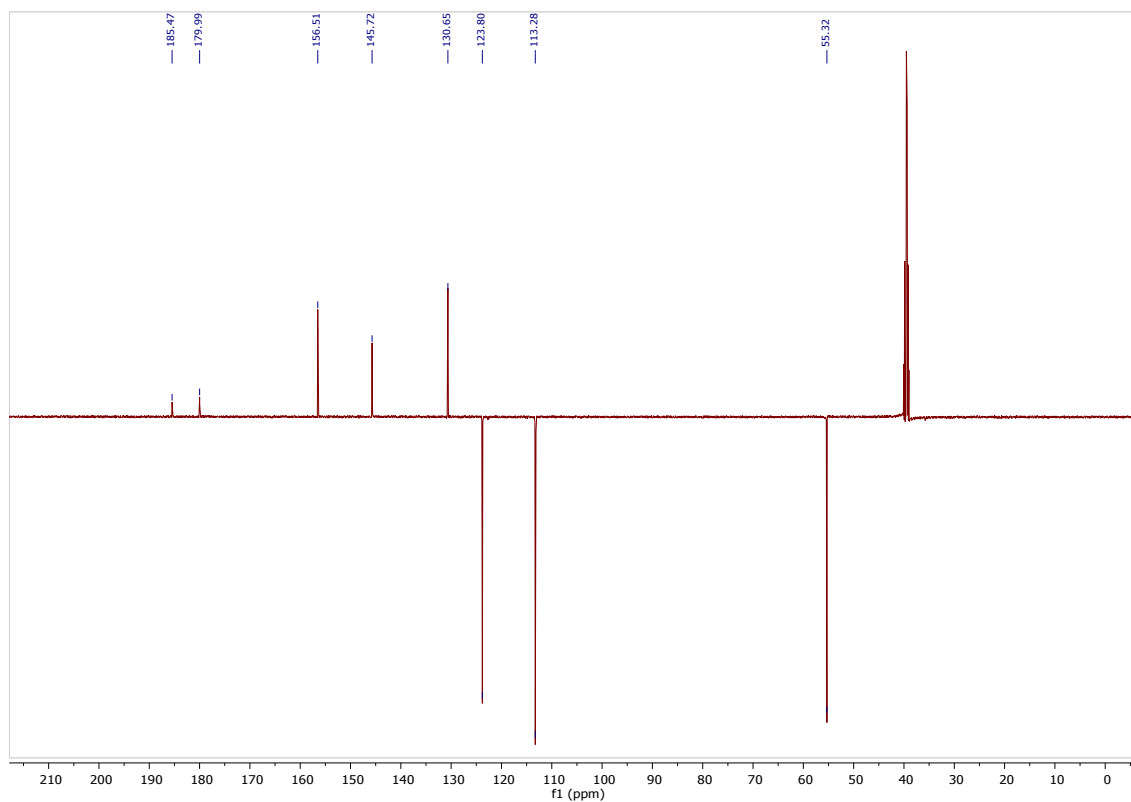
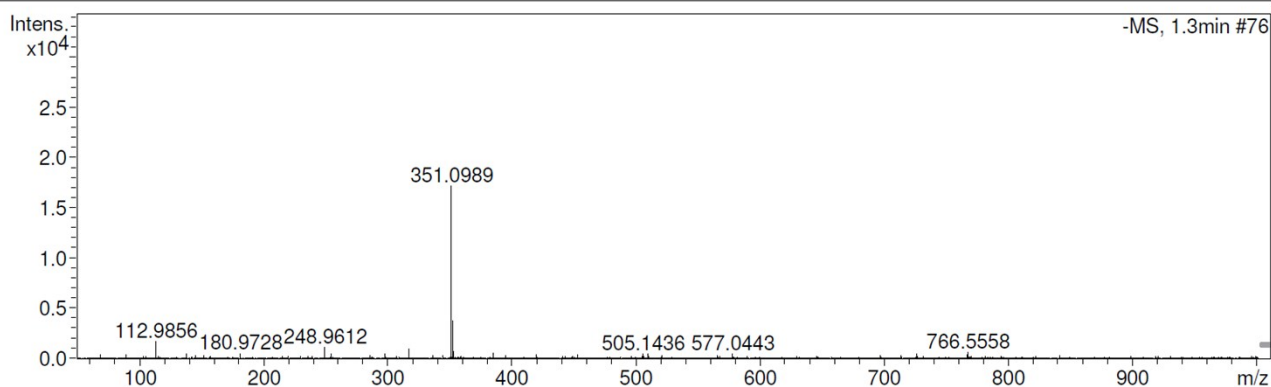


Figure 58 ^{13}C NMR (APT) of **1d** (126 MHz, $\text{DMSO-}d_6$).

Acquisition Parameter

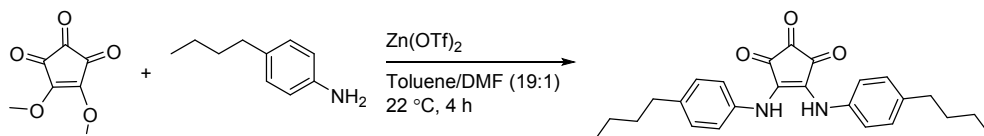
Source Type	ESI	Ion Polarity	Negative	Set Nebulizer	2.0 Bar
Focus	Not active	Set Capillary	3500 V	Set Dry Heater	240 °C
Scan Begin	50 m/z	Set End Plate Offset	-500 V	Set Dry Gas	10.0 l/min
Scan End	1000 m/z	Set Collision Cell RF	100.0 Vpp	Set Divert Valve	Waste



Meas. m/z	#	Formula	Score	m/z	err [mDa]	err [ppm]	mSigma	rdb	e ⁻ Conf	N-Rule
351.0989	1	C ₁₉ H ₁₅ N ₂ O ₅	100.00	351.0986	-0.2	-0.6	5.4	13.5	even	ok

Figure 59 LC-HRMS (ESI) of **1d**.

4,5-bis((4-butylphenyl)amino)cyclopent-4-ene-1,2,3-trione (**1e**)



Dimethylcroconate (200 mg, 1.18 mmol) and $\text{Zn}(\text{OTf})_2$ (85 mg, 0.236 mmol) was suspended in toluene/DMF (19:1, 10 ml) and 4-butylaniline (0.37 ml, 2.5 mmol) was added. The flask was fitted with a stopper and the reaction was stirred at room temperature for four hours. The mixture was evaporated to dryness, and the resulting crude dissolved in methanol (40 ml) to which was added diethyl ether (50 ml). The precipitate was centrifuged down and washed several times with diethyl ether (4×15 ml) to yield **1e** (220 mg, 46 %) as a dark solid, mp. 233 – 234 °C. ^1H NMR (500 MHz, $\text{DMSO}-d_6$) δ 10.06 (s, 2H), 6.77 (d, $J = 8.3$ Hz, 4H), 6.60 (d, $J = 8.3$ Hz, 4H), 2.39 (t, $J = 7.6$ Hz, 4H), 1.49 – 1.40 (m, 4H), 1.23 – 1.30 (m, 4H), 0.91 (t, $J = 7.3$ Hz, 6H). ^{13}C NMR (126 MHz, $\text{DMSO}-d_6$) δ 185.56, 180.42, 145.27, 138.27, 135.19, 127.60, 122.04, 34.26, 33.15, 21.63, 13.82. LC-HRMS: $m/z = 405.2171$ [$\text{M}-\text{H}^+$] (Calculated 405.2173).

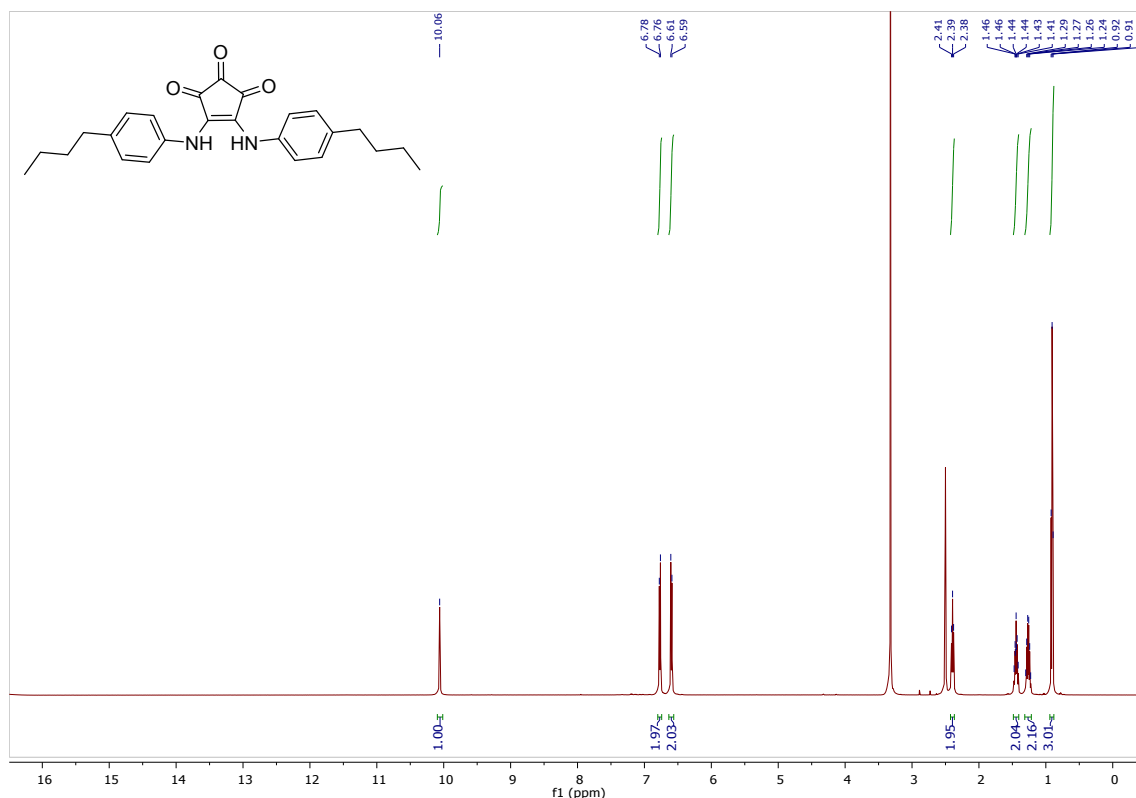


Figure 60 ^1H NMR of **1e** (500 MHz, $\text{DMSO}-d_6$).

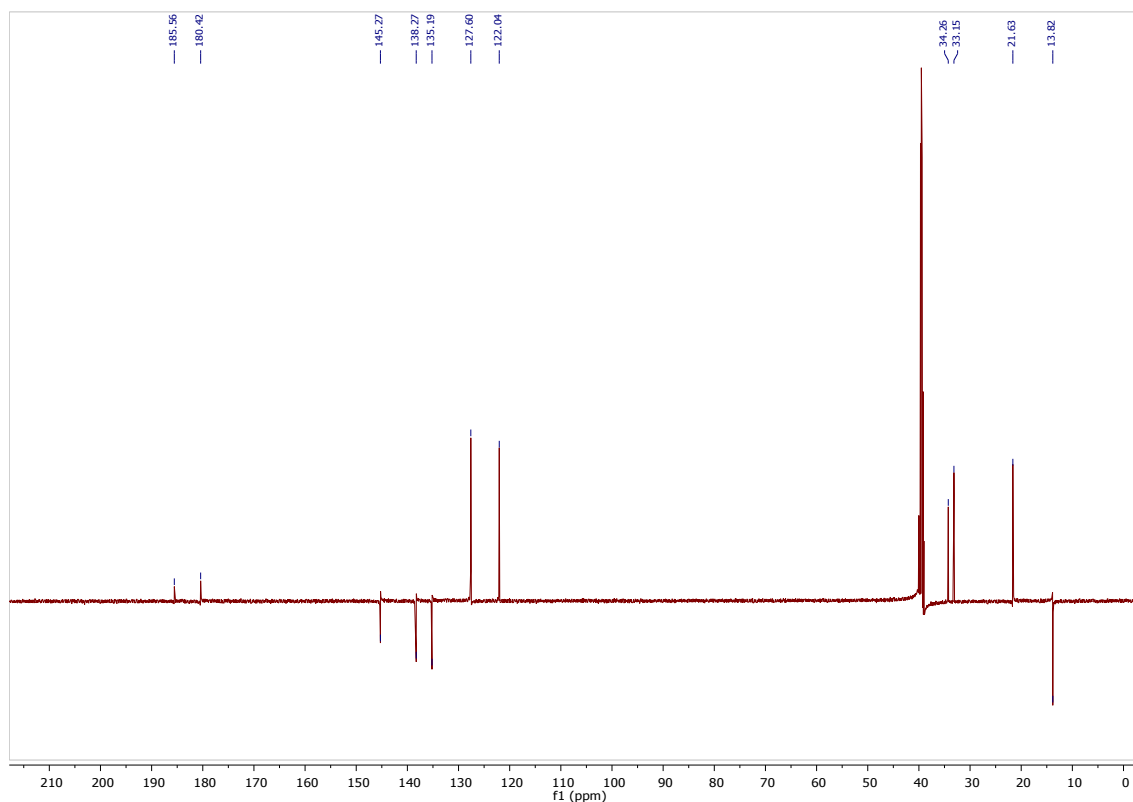


Figure 61 ^{13}C NMR (APT) of **1e** (126 MHz, $\text{DMSO}-d_6$).

Acquisition Parameter

Source Type	ESI	Ion Polarity	Positive	Set Nebulizer	2.0 Bar
Focus	Not active	Set Capillary	4500 V	Set Dry Heater	240 °C
Scan Begin	50 m/z	Set End Plate Offset	-500 V	Set Dry Gas	10.0 l/min
Scan End	1000 m/z	Set Collision Cell RF	100.0 Vpp	Set Divert Valve	Waste

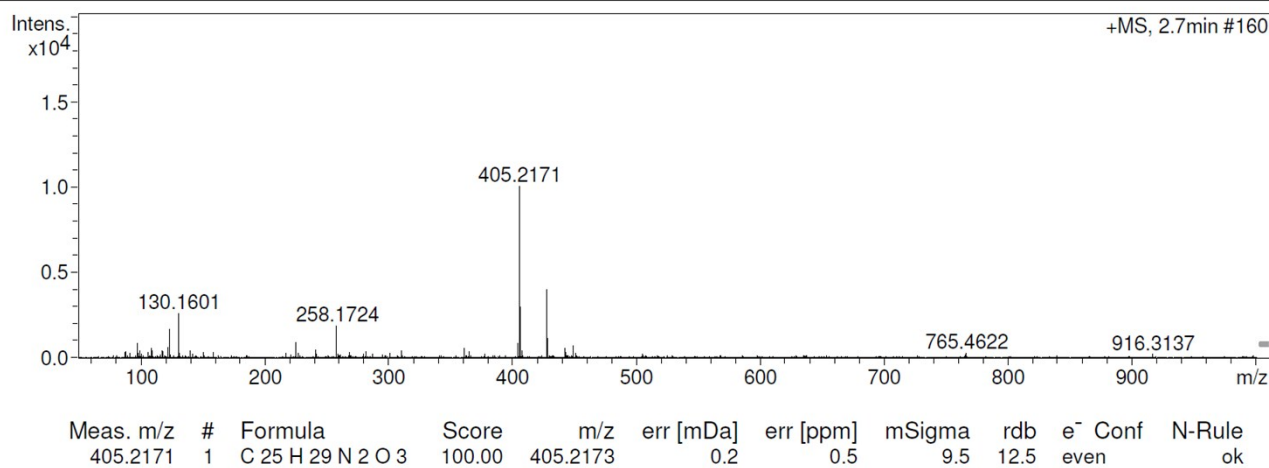
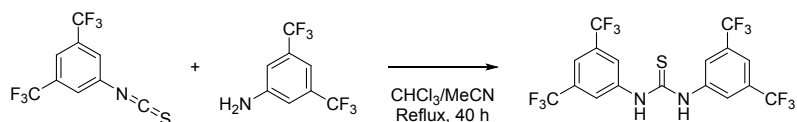


Figure 62 LC-HRMS (ESI) of **1e**.

Bis(3,5-bis[trifluoromethyl]phenyl) Thiourea (Schreiner's catalyst)¹¹

¹¹ Huang, Y.-B. & Cai, C. Direct reductive amination of aldehydes and ketones mediated by a thiourea derivative as an organocatalyst. *J. Chem. Res.* **2009**, 686-688 (2009).



3,5-Bis(trifluoromethyl)aniline (165 mg, 0.718 mmol, 1.2 eq.) was dissolved in CHCl_3 (5.0 mL) and 3,5-bis(trifluoromethyl)phenyl isothiocyanate (163 mg, 0.601 mmol, 1.0 eq.) was added. Acetonitrile (2.0 mL) was added and the resulting clear solution was heated under reflux for 40 hours after which all of the solvent was removed under reduced pressure. The white residue was recrystallized from boiling chloroform (9 mL) to yield the title compound as white needles (292 mg, 97 %), mp. 174 – 175 °C. ^1H NMR (500 MHz, $\text{DMSO-}d_6$) δ = 10.64 (s, 2H), 8.20 (s, 4H), 7.87 (s, 2H). ^{13}C NMR (126 MHz, $\text{DMSO-}d_6$) δ = 180.59, 141.15, 130.34 (q, $J=32.7$), 124.16, 123.16 (q, $J=272.3$), 117.79. ^{19}F NMR (282 MHz, $\text{DMSO-}d_6$) δ = -59.77. Elemental analysis for $\text{C}_{17}\text{H}_8\text{F}_{12}\text{N}_2\text{S}$: Found (calculated) 41.15 % C (40.81), 1.48 % H (1.61), 5.60 % N (5.60). LC-HRMS: 501.0292 [$\text{M}+\text{H}^+$] (Calculated 501.0289).

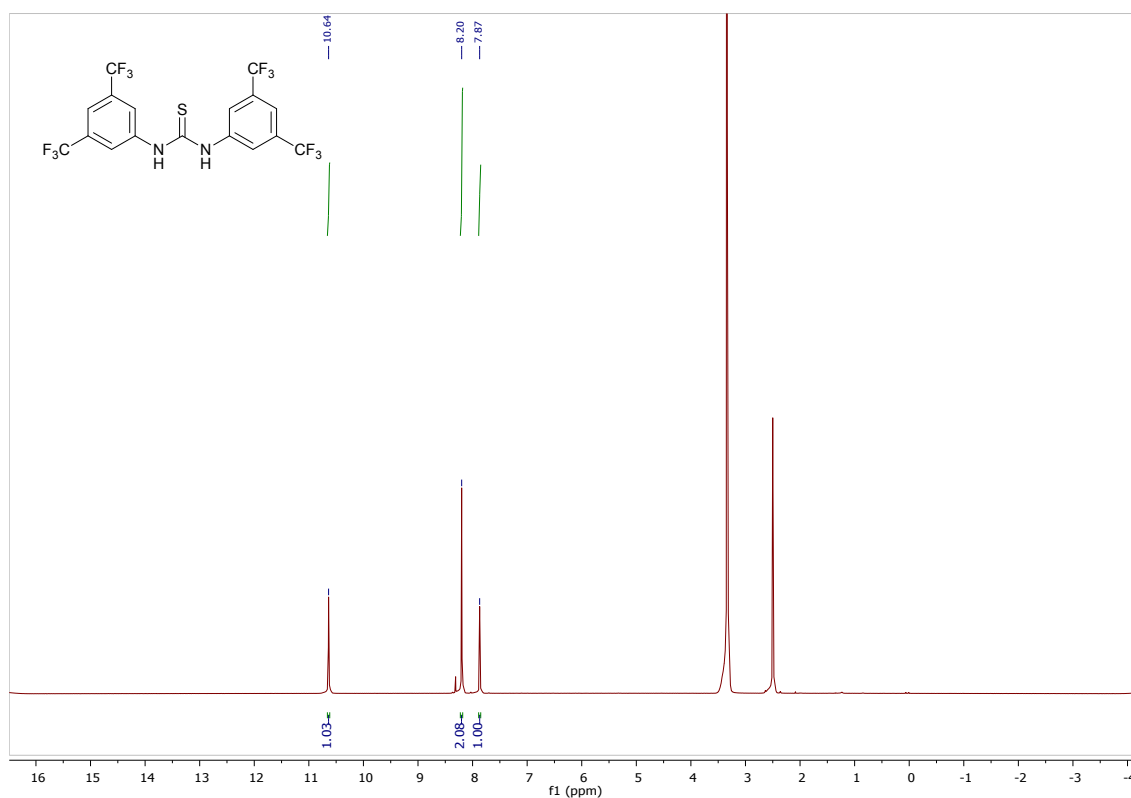


Figure 63 ^1H NMR of Bis(3,5-bis[trifluoromethyl]phenyl) Thiourea (500 MHz, $\text{DMSO-}d_6$).

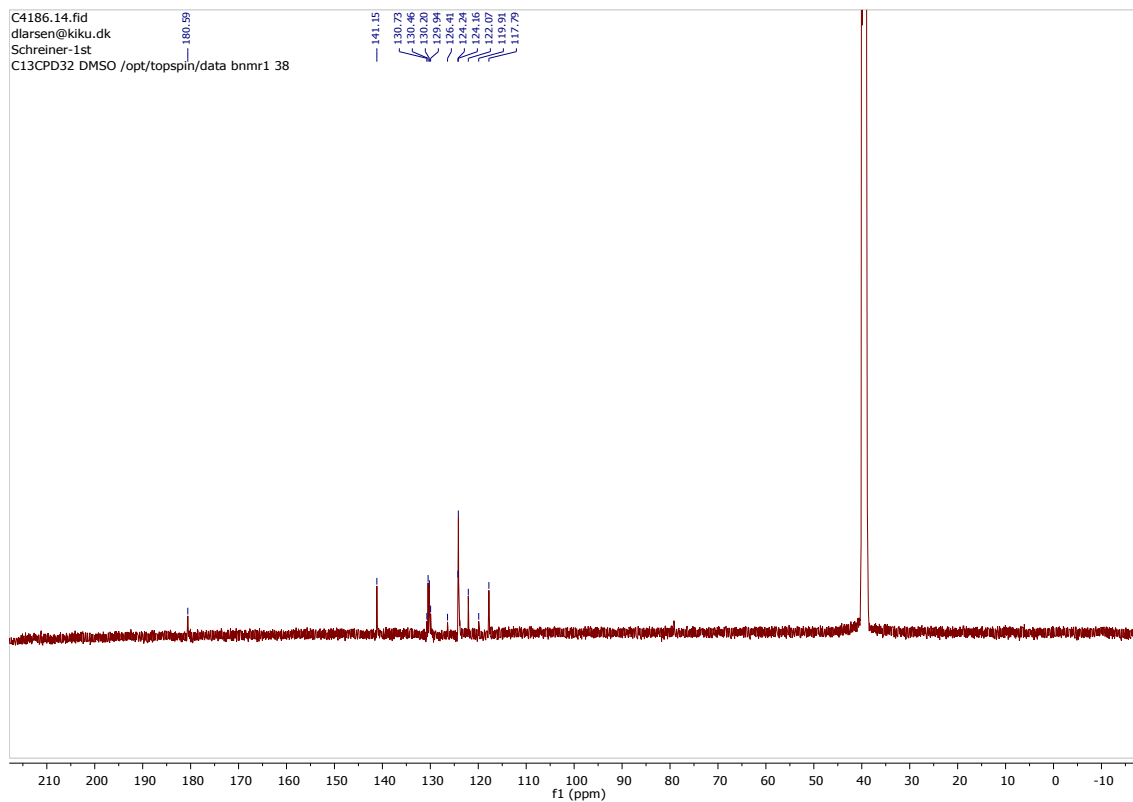


Figure 64 ^{13}C NMR (APT) of Bis(3,5-bis(trifluoromethyl)phenyl) (126 MHz, $\text{DMSO-}d_6$).

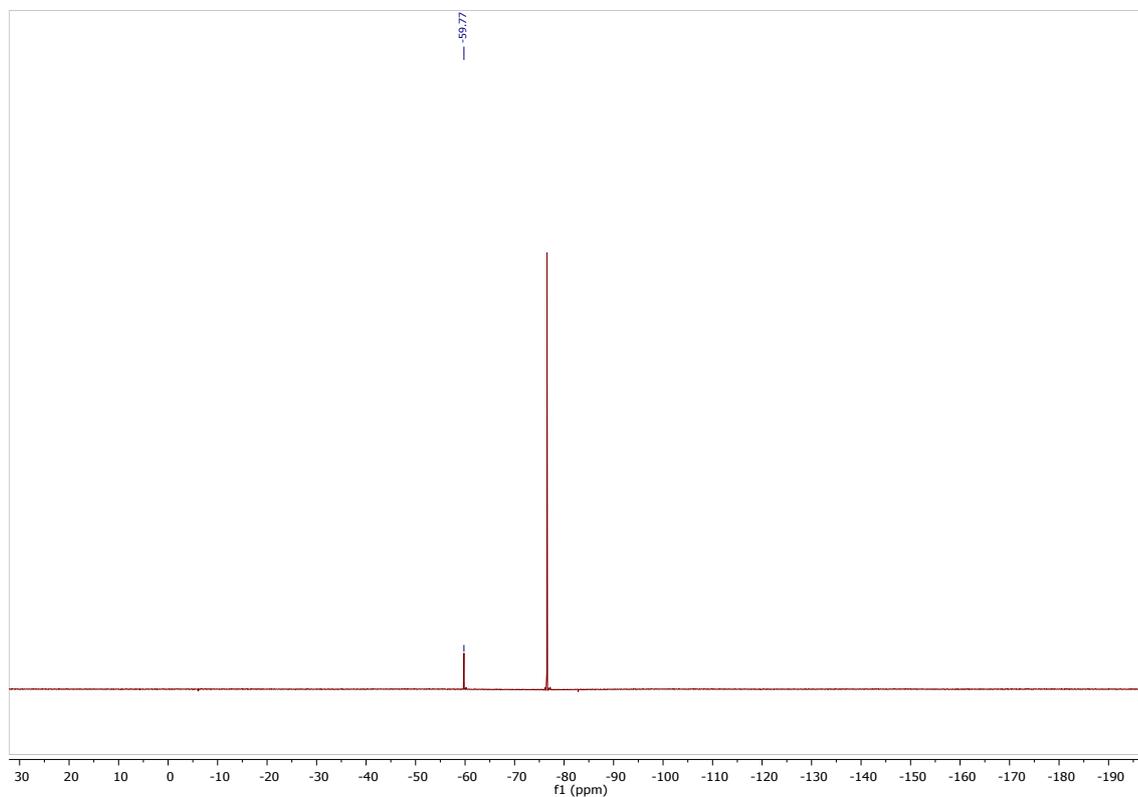


Figure 65 ^{19}F NMR of Bis(3,5-bis(trifluoromethyl)phenyl) (470 MHz, $\text{DMSO-}d_6$).

Acquisition Parameter

Source Type	ESI	Ion Polarity	Positive	Set Nebulizer	1.2 Bar
Focus	Not active	Set Capillary	4500 V	Set Dry Heater	200 °C
Scan Begin	50 m/z	Set End Plate Offset	-500 V	Set Dry Gas	8.0 l/min
Scan End	1000 m/z	Set Collision Cell RF	100.0 Vpp	Set Divert Valve	Waste

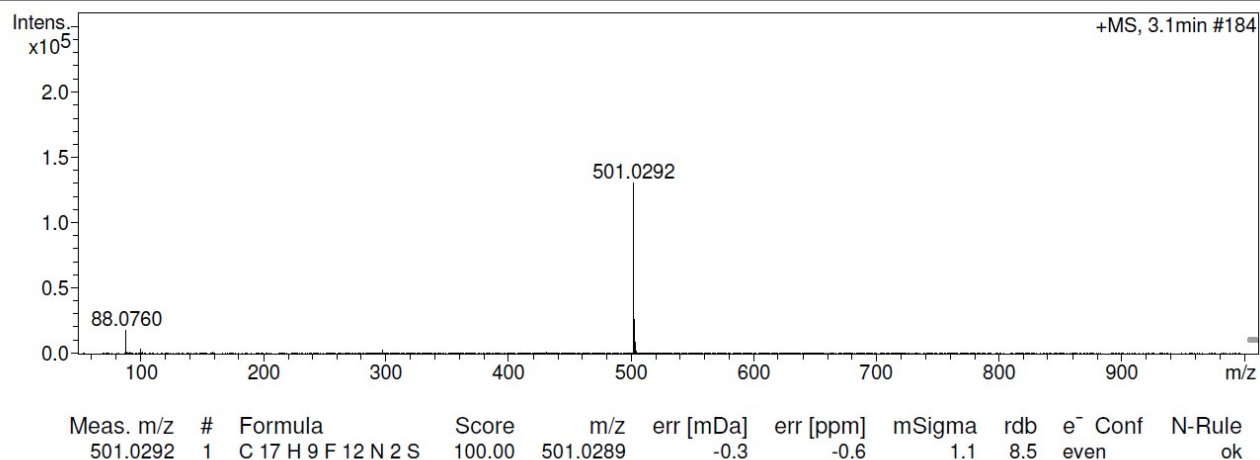


Figure 66 LC-HRMS (ESI) of Bis(3,5-bis[trifluoromethyl]phenyl).